Higher-order Boussinesq systems: Modeling, numerics and applications

Master Thesis in Applied and Computational Mathematics

Sondre Dahle Hatland

University of Bergen
Department of Mathematics

June 3, 2019

Acknowledgements

I would like to thank my supervisor Professor Henrik Kalisch for his guidance in writing this thesis. I truly appreciate his helpful comments, and I am thankful for his patience and expert knowledge on the subjects at hand.

Contents

Chapter 1

Introduction

1.1 Basic theory of fluid mechanics

In this section we begin by introducing some basic theory of fluid mechanics. We will only present what is most relevant for the current text. The following theory is based mainly on [1], with some details from [4], and [2].

Consider an inviscid, incompressible fluid occupying a time – dependent domain Ω_t in $\mathbb{R}^3$, with the variable t denoting time. Using a Cartesian coordinate system (x, y, z) with the z-axis pointing vertically upwards, we let $\mathbf{i}$, $\mathbf{j}$ and $\mathbf{k}$ denote the unit vectors in the positive x –, y – and z – directions, respectively. The fluid velocity field $\mathbf{u}(x, y, z, t) = u\mathbf{i} + v\mathbf{j} + w\mathbf{k}$ (where u, v and w each depend on (x, y, z, t)) and the pressure field $p(x, y, z, t)$ then obey the Euler equations

$$\frac{\partial \mathbf{u}}{\partial t} + (\mathbf{u} \cdot \nabla)\,\mathbf{u} + \nabla p = -g\mathbf{k}, \quad \text{in} \quad \Omega_t, \tag{1.1}$$

$$\nabla \cdot \mathbf{u} = 0, \quad \text{in} \quad \Omega_t, \tag{1.2}$$

as they are stated in [1], where g denotes the gravitational acceleration, and $\nabla = \left(\frac{\partial}{\partial x}, \frac{\partial}{\partial y}, \frac{\partial}{\partial z}\right)^T$. Equation (1.1) follows from the Navier Stokes equation when the fluid is incompressible and inviscid, and equation (1.2) is derived from the equation for conservation of mass when the assumption of incompressibility is used.

Next, we introduce the vorticity $\boldsymbol{\omega}$ of the flow, defined as the curl of the velocity field $\mathbf{u}$

$$\boldsymbol{\omega} = \nabla \times \mathbf{u}.$$

It can be shown that $\boldsymbol{\omega}$ represents twice the rotation rate of a fluid element, see e.g. [2], p. 91.

A fluid flow is said to be irrotational if $\boldsymbol{\omega} = \mathbf{0}$. As will be discussed shortly, Helmholtz' vorticity principle states that if a flow is initially irrotational, then it remains so for all time.

By assuming that the flow is irrotational, then $\mathbf{u}$ can be written as the gradient of a velocity potential function $\phi(x, y, z, t)$, i.e.,

$$\mathbf{u} = \nabla\phi. \tag{1.3}$$

This follows from the fact that

$$\nabla \times \mathbf{u} = (w_y - v_z, u_z - w_x, v_x - u_y)^T = (0, 0, 0)^T$$

is identically satisfied when $(u, v, w)^T = (\phi_x, \phi_y, \phi_z)^T$.

From the incompressible continuity equation (1.2) it then follows that ϕ satisfies the Laplace equation

$$\Delta\phi = \phi_{xx} + \phi_{yy} + \phi_{zz} = 0, \tag{1.4}$$

where $\Delta = \nabla^2 = \frac{\partial^2}{\partial x^2} + \frac{\partial^2}{\partial y^2} + \frac{\partial^2}{\partial z^2}$ is the Laplace operator.

Assume now that the fluid occupying Ω_t is water, bounded below by a fixed surface at $z = -h(x, y)$, and bounded above by the interface $z = \eta(x, y, t)$ separating water from air above it. The interface $\eta(x, y, t)$ will be referred to as a free surface. The coordinate system is chosen such that the x and y axes are aligned with the undisturbed free surface of the water, i.e., $z = 0$ describes the undisturbed free surface. Assume in addition that Ω_t is unbounded in the x and y direction, that is,

$$\Omega_t = \left\{(x, y, z)^T \in \mathbb{R}^3 |\ x \in \mathbb{R},\ y \in \mathbb{R},\ -h(x, y) < z < \eta(x, y, t),\ t \geq 0\right\}.$$

The bottom boundary $z = -h(x, y)$ is assumed to be impermeable, so that no fluid can cross it. This means, from the principle of conservation of mass, that the component of the fluid velocity normal to the bottom must equal the velocity of the bottom normal to itself. Since the bottom boundary is stationary, we must then have $\mathbf{n} \cdot \mathbf{u} = 0$ at $z = -h(x, y)$, where $\mathbf{n}$ is a unit vector normal to the boundary, pointing inward into Ω_t.

Since $\nabla(z + h(x, y)) = (h_x, h_y, 1)^T$ is normal to the surface $z + h(x, y) = 0$, pointing inward into Ω_t, we can take $\mathbf{n} = \frac{1}{\sqrt{h_x^2 + h_y^2 + 1}}(h_x, h_y, 1)^T$, which means from (1.3) and $\mathbf{n} \cdot \mathbf{u} = 0$, that

$$\phi_x h_x + \phi_y h_y + \phi_z = 0, \qquad \text{on} \quad z = -h(x, y). \tag{1.5}$$

This ensures that no fluid can flow through the fixed boundary at the bottom.

The interface between two fluids is defined by the property that fluid does not cross it. Thus, at the free surface, separating air and water in this case, a kinematic boundary condition must apply. The kinematic boundary condition states that the fluid velocity normal to the free surface must equal the velocity of the free surface normal to itself. Letting $\mathbf{u}_s$ be the velocity of the free surface, and $\mathbf{n}_s$ be a unit vector normal to the free surface, this is equivalent with requiring that

$$(\mathbf{n}_s \cdot \mathbf{u})\,|_{z=\eta} = \mathbf{n}_s \cdot \mathbf{u}_s. \tag{1.6}$$

The free surface $\eta(x,y,t)$ is described by the equation $f(x,y,z,t) \coloneqq z - \eta(x,y,t) = 0$, and a unit vector normal to this surface, pointing out of the liquid, is $\mathbf{n}_s = \nabla f/|\nabla f| = (-\eta_x, -\eta_y, 1)/|\nabla f|$. The normal velocity of the fluid is then $\mathbf{n}_s \cdot \nabla\phi = \frac{1}{|\nabla f|}(-\phi_x\eta_x - \phi_y\eta_y + \phi_z)$. It is assumed that the velocity of the free surface is purely vertical everywhere, so we can write $\mathbf{u}_s = \eta_t \mathbf{k}$. Thus, the normal velocity of the free surface is $\mathbf{n}_s \cdot \mathbf{u}_s = \frac{1}{|\nabla f|}\eta_t$, and according to (1.6), the kinematic boundary condition at the free surface is

$$\eta_t + \phi_x\eta_x + \phi_y\eta_y - \phi_z = 0, \qquad \text{on} \quad z = \eta(x,y,t). \tag{1.7}$$

The second boundary condition at the free surface is obtained from (1.1). Making use of the vector identity

$$\nabla\left(|\mathbf{u}|^2\right) = \nabla(\mathbf{u}\cdot\mathbf{u}) = 2\mathbf{u}\times(\nabla\times\mathbf{u}) + 2(\mathbf{u}\cdot\nabla)\mathbf{u} = 2\mathbf{u}\times\boldsymbol{\omega} + 2(\mathbf{u}\cdot\nabla)\mathbf{u},$$

and the anti-commutativity of the cross product, equation (1.1) can be rewritten as

$$\frac{\partial\mathbf{u}}{\partial t} + \nabla\left(\frac{1}{2}|\mathbf{u}|^2\right) + \boldsymbol{\omega}\times\mathbf{u} + \nabla p = -g\mathbf{k}. \tag{1.8}$$

Since the curl of a gradient vector is the zero vector, we can take the curl of equation (1.8) to obtain Helmholtz' equation

$$\frac{\partial\boldsymbol{\omega}}{\partial t} + \nabla\times(\boldsymbol{\omega}\times\mathbf{u}) = \mathbf{0}, \tag{1.9}$$

where we also used the fact that the order in which the curl operator and the t – derivative is applied can be interchanged.

Now, using $\nabla\cdot\mathbf{u} = 0$ from (1.2), the fact that the divergence of the curl is zero, and the vector identity

$$\begin{aligned}\nabla\times(\boldsymbol{\omega}\times\mathbf{u}) &= \boldsymbol{\omega}(\nabla\cdot\mathbf{u}) - \mathbf{u}(\nabla\cdot\boldsymbol{\omega}) + (\mathbf{u}\cdot\nabla)\boldsymbol{\omega} - (\boldsymbol{\omega}\cdot\nabla)\mathbf{u}\\ &= (\mathbf{u}\cdot\nabla)\boldsymbol{\omega} - (\boldsymbol{\omega}\cdot\nabla)\mathbf{u},\end{aligned}$$

we can rewrite (1.9) as

$$\frac{D\boldsymbol{\omega}}{Dt} \equiv \frac{\partial\boldsymbol{\omega}}{\partial t} + (\mathbf{u}\cdot\nabla)\boldsymbol{\omega} = (\boldsymbol{\omega}\cdot\nabla)\mathbf{u}. \tag{1.10}$$

Here $\frac{D}{Dt} = \frac{\partial}{\partial t} + (\mathbf{u}\cdot\nabla)$ is the material derivative operator, which when applied to a physical quantity, such as the vorticity of the fluid, measures the change in that quantity with time as we follow a specific fluid particle. Obviously, $\boldsymbol{\omega} = \mathbf{0}$ is a possible solution of (1.10). This solution is unique as long as each component $\frac{\partial u_i}{\partial x_j}$ of $\nabla\mathbf{u}$ stays bounded, which means that if the initial flow is irrotational, then the flow will remain irrotational for all time. This is referred to as the Helmholtz vorticity principle.

Returning to (1.8), by assuming irrotational flow and substituting $\mathbf{u} = \nabla\phi$, we integrate the third equation (i.e., the z component) in (1.8) with respect to z to obtain

$$\phi_t + \frac{1}{2}|\nabla\phi|^2 + (p - p_0) + gz = C(t). \tag{1.11}$$

Here the constant p_0, which we separated from the integration constant $C(t)$, denotes the ambient pressure. Defining a new velocity potential by $\phi' = \phi - \int C(t)dt$, substituting it into (1.11), and assuming that the pressure on the free surface, $p|_{z=\eta}$, equals the ambient pressure, we thus obtain the second boundary condition at the free surface

$$\phi_t + \tfrac{1}{2}|\nabla\phi|^2 + gz = 0, \qquad \text{on} \quad z = \eta(x, y, t), \tag{1.12}$$

where the prime over the new velocity potential has been dropped.

As discussed in [1], the system of equations (1.4), (1.5), (1.7), and (1.12) in the unknowns η and ϕ is difficult to treat numerically and analytically due to the nonlinear nature of the free surface boundary conditions, and the fact that Ω_t depends on time.

From here on, we will only consider fluid flow which is assumed to be uniform in the y – direction, i.e., the velocity field (and thus the velocity potential) and the free surface do not depend on y. Additionally, we always assume that the flow is irrotational and inviscid. The bottom is assumed to be flat and located at $z = -h_0$. The Cartesian coordinate system can then be considered two dimensional in x and z, with the x – axis aligned with the undisturbed free surface, and the z – axis pointing vertically upwards, so that the undisturbed free surface is located at $z = 0$.

Then equations (1.4), (1.5), (1.7), and (1.12) simplify to

$$\phi_{xx} + \phi_{zz} = 0, \qquad \text{in} \quad -h_0 < z < \eta(x, t), \tag{1.13}$$

$$\phi_z = 0, \qquad \text{on} \quad z = -h_0, \tag{1.14}$$

$$\left.\begin{aligned} \eta_t + \phi_x\eta_x - \phi_z &= 0, \\ \phi_t + \frac{1}{2}\left(\phi_x^2 + \phi_z^2\right) + gz &= 0, \end{aligned}\right\} \quad \text{on} \quad z = \eta(x, t). \tag{1.15}$$

where $x \in \mathbb{R}$, $t \geq 0$. Suitable boundary conditions must be chosen for $x \to \pm\infty$, and an initial condition must be specified at $t = 0$.

1.2 Linearized theory of water waves

Next, we introduce some basic theory of gravity waves in water, which will be needed later. The content in this section is based on [2] and [3].

We start by linearizing the free surface boundary conditions in (1.15). The first equation in (1.15) may be linearized by noting that the factor η_x in the $\phi_x\eta_x$ term is small compared to the other terms, presuming that the slope of the waves is small. It then becomes

$$\eta_t \cong \phi_z\Big|_{z=\eta}. \tag{1.16}$$

We may linearize further by Taylor expanding the right hand side around $z = 0$.
This yields

$$\eta_t \cong \phi_z\Big|_{z=\eta} = \phi_z\Big|_{z=0} + \eta\phi_{zz}\Big|_{z=0} + ... \tag{1.17}$$

Since both ϕ_z and η are assumed small, we may neglect quadratic and higher order terms in ϕ_z (and its higher order derivatives) and η on the right hand side to obtain the following approximation

$$\eta_t \cong \phi_z\Big|_{z=0}, \tag{1.18}$$

valid for $a_0/\lambda \ll 1$, where λ is a typical wavelength, as argued in [2].
The second equation in (1.15) linearizes to

$$\phi_t\Big|_{z=\eta} \cong -g\eta$$

after neglecting the terms quadratic in ϕ_z and ϕ_x, both assumed small.
Using the same reasoning as above, we Taylor expand the left hand side around $z = 0$ and neglect terms of quadratic order in η and ϕ_z (and its higher order derivatives) to obtain

$$\phi_t\Big|_{z=0} \cong -g\eta, \tag{1.19}$$

again valid for $a_0/\lambda \ll 1$.
The linearized water wave problem is then

$$\phi_{xx} + \phi_{zz} = 0, \quad \text{in} \quad -h_0 < z < \eta(x,t), \tag{1.20}$$

$$\phi_z = 0, \quad \text{on} \quad z = -h_0, \tag{1.21}$$

$$\eta_t - \phi_z = 0, \quad \text{on} \quad z = 0 \tag{1.22}$$

$$\phi_t + g\eta = 0, \quad \text{on} \quad z = 0. \tag{1.23}$$

Before we can apply the boundary conditions above, we also need an initial condition for the shape of the free surface η. Since small amplitude water waves tend to become sinusoidal some time after their generation [3], it is expedient to assume that the free surface takes the form of a simple travelling wave

$$\eta(x,t) = a\cos(kx - \omega t), \tag{1.24}$$

so that the intitial condition becomes $\eta(x,0) = a\cos(kx)$.

Here $k = 2\pi/\lambda$ is the wave number (spatial wave frequency), and ω is the wave's radian frequency.

From (1.22) and (1.23) it then follows that ϕ must be a sine function in $kx - \omega t$, so we can write

$$\phi = f(z)\sin(kx - \omega t), \tag{1.25}$$

where $f(z)$ and $\omega(k)$ are functions to be determined.

Now substitute the ansatz (1.25) into the Laplace equation (1.20) to obtain the second order ODE

$$\frac{d^2 f}{dz^2} - k^2 f = 0,$$

with general solution

$$f(z) = Ae^{kz} + Be^{-kz},$$

where A and B are constants.

Thus the velocity potential becomes

$$\phi = \left(Ae^{kz} + Be^{-kz}\right)\sin(kx - \omega t). \tag{1.26}$$

To find the constants A and B, first substitute (1.26) into the boundary condition on the bottom, (1.21), to get

$$k\left(Ae^{-kh_0} - Be^{kh_0}\right)\sin(kx - \omega t) = 0,$$

which holds true for all $kx - \omega t$ if

$$B = Ae^{-2kh_0}. \tag{1.27}$$

Now substitute the ansatz for η from (1.24), and (1.26) into (1.22) to obtain

$$k(A - B)\sin(kx - \omega t) = \omega a \sin(kx - \omega t),$$

which is true for all $kx - \omega t$ if

$$k(A - B) = \omega a \tag{1.28}$$

The two equations (1.27) and (1.28) can now be solved for A and B, and we obtain

$$A = \frac{a\omega}{k\left(1 - e^{-2kh_0}\right)}, \qquad \text{and} \qquad B = \frac{a\omega e^{-2kh_0}}{k\left(1 - e^{-2kh_0}\right)}.$$

Finally, the velocity potential then becomes

$$\phi = \frac{a\omega}{k}\frac{\cosh(k(z + h_0))}{\sinh(kh_0)}\sin(kx - \omega t). \tag{1.29}$$

Now the horizontal and vertical velocity components u and w are readily obtained by differentiating (1.29) with respect to x and z, respectively.

They are

$$u = a\omega \frac{\cosh(k(z+h_0))}{\sinh(kh_0)} \cos(kx - \omega t)$$

and

$$w = a\omega \frac{\sinh(k(z+h_0))}{\sinh(kh_0)} \sin(kx - \omega t).$$

To find a relation between k and ω, substitute (1.24) and (1.29) into (1.23) to get

$$-\frac{a\omega^2}{k} \frac{\cosh(kh_0)}{\sinh(kh_0)} \cos(kx - \omega t) = -ag \cos(kx - \omega t),$$

which simplifies to

$$\omega^2 = gk \tanh(kh_0). \tag{1.30}$$

Relation (1.30) is the dispersion relation for the linearized water wave problem. Assuming that the waves are right-travelling, it may be rewritten as

$$c = \frac{\omega}{k} = \sqrt{\frac{g}{k} \tanh(kh_0)}, \tag{1.31}$$

where c is the phase speed of the surface waves. This shows how the phase speed depends on the wave number k. Because of this, surface waves are called dispersive waves.

From (1.31) we can derive an important approximation for the phase speed for surface waves of long wavelength in shallow water, that is, for $kh_0 \ll 1$.

Since $\tanh(x) \approx x$ as $x \to 0$, we can write $\tanh(kh_0) \approx kh_0$ as $kh_0 \to 0$, and so (1.31) can be approximated as

$$c = \sqrt{gh_0} \tag{1.32}$$

for $kh_0 \to 0$.

It is important that the wavelength is significantly longer measured *relative* to the undisturbed water depth in order for (1.32) to be valid. As noted in [2], it yields better than 3% accuracy if $h_0 < 0.07\lambda$. From (1.32) we note that shallow water waves of long wavelength are non-dispersive.

1.3 Higher order Boussinesq equations

Most of the discussion in this text will be centered around the specific fluid flow regime where the water waves are of small amplitude and long wavelength, both measured relative to the undisturbed depth h_0. Therefore, it is convenient to introduce the standard parameters $\alpha = a_0/h_0$ and $\beta = h_0^2/\ell^2$, where a_0 denotes a typical wave amplitude, ℓ is a typical wavelength, and h_0 is the undisturbed depth as always. The parameters α and β

measure the relative strength of the nonlinear and dispersive effects in the flow. Assuming that these effects are nearly balanced, the Stokes number $S = \alpha/\beta$ must be of order one.

The goal now is to obtain approximations to equations (1.13), (1.14) and (1.15) by employing an ansatz for the velocity potential in the form of a Taylor series, as is done in [1]. Since our assumptions on the flow imply that $\alpha \ll 1$, $\beta \ll 1$ and $S = \alpha/\beta = \mathcal{O}(1)$, it is expedient to expand the series in terms of the small parameters α and β. Following [1], we choose to expand in terms of β as the primary parameter. Then higher order terms in α and β can be neglected in the series expansions of equations (1.13), (1.14) and (1.15) in order to approximate the full equations to order of accuracy β^n. For the equations to be expanded in terms of β, it is best to scale the variables such that all dependent quantities and the initial data are of order one, and the assumptions of small wavelength appear explicitly connected with small parameters appearing in the equations of motion.

The dimensionless variables to be used are as follows

$$x = \ell\tilde{x},\ z = h_0(\tilde{z} - 1),\ \eta = a_0\tilde{\eta},\ t = \ell\tilde{t}/c_0,\ \phi = ga_0\ell\tilde{\phi}/c_0, \tag{1.33}$$

where $c_0 = \sqrt{gh_0}$ is the linear phase speed approximation for surface waves of long wavelength relative to the undisturbed depth.

This scaling implies from the chain rule that the derivatives are scaled as $\frac{\partial}{\partial x} = \frac{\partial}{\partial \tilde{x}}\frac{d\tilde{x}}{dx} = \frac{1}{\ell}\frac{\partial}{\partial \tilde{x}}$, $\frac{\partial}{\partial t} = \frac{\partial}{\partial \tilde{t}}\frac{d\tilde{t}}{dt} = \frac{c_0}{\ell}\frac{\partial}{\partial \tilde{t}}$ and $\frac{\partial}{\partial z} = \frac{\partial}{\partial \tilde{z}}\frac{d\tilde{z}}{dz} = \frac{1}{h_0}\frac{\partial}{\partial \tilde{z}}$. In particular, this implies that the horizontal fluid velocity component $u(x, z, t)$ is scaled as $u = \phi_x = \frac{gA\ell}{c_0}\frac{1}{\ell}\tilde{\phi}_{\tilde{x}} = \frac{gA}{c_0}\tilde{\phi}_{\tilde{x}} \coloneqq \frac{gA}{c_0}\tilde{u}$.

In the new variables, the equations are

$$\beta\tilde{\phi}_{\tilde{x}\tilde{x}} + \tilde{\phi}_{\tilde{z}\tilde{z}} = 0, \qquad \text{in } 0 < \tilde{z} < 1 + \alpha\tilde{\eta}(\tilde{x}, \tilde{t}), \tag{1.34}$$

$$\tilde{\phi}_{\tilde{z}} = 0, \qquad \text{on } \tilde{z} = 0, \tag{1.35}$$

$$\left.\begin{aligned} \tilde{\eta}_{\tilde{t}} + \alpha\tilde{\phi}_{\tilde{x}}\tilde{\eta}_{\tilde{x}} - \frac{1}{\beta}\tilde{\phi}_{\tilde{z}} = 0, \\ \tilde{\eta} + \tilde{\phi}_{\tilde{t}} + \frac{1}{2}\alpha\tilde{\phi}_{\tilde{x}}^2 + \frac{1}{2}\frac{\alpha}{\beta}\tilde{\phi}_{\tilde{z}}^2 = 0, \end{aligned}\right\} \text{ on } \tilde{z} = 1 + \alpha\tilde{\eta}(\tilde{x}, \tilde{t}), \tag{1.36}$$

for $\tilde{x} \in \mathbb{R}$, $\tilde{t} > 0$.

To simplify the notation, we drop the tilde over the dimensionless variables in further calculations unless otherwise is stated. The following calculations are all done in the non-dimensional variables.

Proceeding as in [1], the standard approach is to use an ansatz of the form

$$\phi(x, z, t) = \sum_{m=0}^{\infty} f_m(x, t) z^m \tag{1.37}$$

for the velocity potential. Substituting this into the non-dimensional Laplace equation (1.34) we get

$$\beta \sum_{m=0}^{\infty} \frac{\partial^2 f_m}{\partial x^2} z^m + \sum_{m=0}^{\infty} (m+2)(m+1) f_{m+2} z^m = 0. \tag{1.38}$$

Using the boundary condition at the bottom, $\phi_z(x,z,t)\big|_{z=0} = 0$, it follows from (1.37) that $f_1(x,t) = 0$.

Since equation (1.38) must hold for all $z \in (0, 1+\alpha\eta)$, we get the following recurrence relation by requiring that the coefficients of terms of order z^m for each $m = 0, 1, 2, ...$ on the left hand side are equal to zero

$$\beta \frac{\partial^2 f_m}{\partial x^2} + (m+2)(m+1) f_{m+2} = 0,$$

or

$$f_{m+2} = -\frac{1}{(m+2)(m+1)} \frac{\partial^2 f_m}{\partial x^2} \beta, \tag{1.39}$$

for $m = 0, 1, 2, ...$

Now let $F(x,t) = f_0(x,t)$, which, from (1.37), is the velocity potential at the bottom $z = 0$. Using (1.39) repeatedly, keeping in mind that $f_1 = 0$, we see that $f_2 = -\frac{1}{2!}\frac{\partial^2 F}{\partial x^2}\beta$, $f_3 = 0$, $f_4 = -\frac{1}{4\times 3}\frac{\partial^2 f_2}{\partial x^2}\beta = \frac{1}{4!}\frac{\partial^4 F}{\partial x^4}\beta^2$, $f_5 = 0$, $f_6 = -\frac{1}{6\times 5}\frac{\partial^2 f_4}{\partial x^2}\beta = -\frac{1}{6!}\frac{\partial^6 F}{\partial x^6}\beta^3$, $f_7 = 0, ...$

Then, formally, we get by induction that

$$f_{2k}(x,t) = \frac{(-1)^k}{(2k)!} \frac{\partial^{2k} F(x,t)}{\partial x^{2k}} \beta^k, \qquad k = 0, 1, 2, ...,$$

and

$$f_{2k+1}(x,t) = 0, \qquad k = 0, 1, 2, ...$$

Inserting this into the ansatz (1.37) we get the following expression for the velocity potential

$$\phi(x,z,t) = \sum_{k=0}^{\infty} \frac{(-1)^k}{(2k)!} \frac{\partial^{2k} F(x,t)}{\partial x^{2k}} z^{2k} \beta^k.$$

Now insert this series into the non-dimensional free surface boundary conditions (1.36) and evaluate at $z = 1 + \alpha\eta(x,t)$ to obtain the following system of equations

$$\eta_t + \alpha\eta_x \sum_{k=0}^{\infty} \frac{(-1)^k}{(2k)!} \frac{\partial^{2k+1} F}{\partial x^{2k+1}} (1+\alpha\eta)^{2k} \beta^k + \sum_{k=0}^{\infty} \frac{(-1)^k}{(2k+1)!} \frac{\partial^{2k+2} F}{\partial x^{2k+2}} (1+\alpha\eta)^{2k+1} \beta^k = 0 \tag{1.40}$$

$$\begin{aligned} &\eta + \sum_{k=0}^{\infty} \frac{(-1)^k}{(2k)!} \frac{\partial^{2k+1} F}{\partial x^{2k} \partial t} (1+\alpha\eta)^{2k} \beta^k + \frac{1}{2}\alpha \left\{ \sum_{k=0}^{\infty} \frac{(-1)^k}{(2k)!} \frac{\partial^{2k+1} F}{\partial x^{2k+1}} (1+\alpha\eta)^{2k} \beta^k \right\}^2 \\ &+ \frac{1}{2}\alpha\beta \left\{ \sum_{k=0}^{\infty} \frac{(-1)^k}{(2k+1)!} \frac{\partial^{2k+2} F}{\partial x^{2k+2}} (1+\alpha\eta)^{2k+1} \beta^k \right\}^2 = 0. \end{aligned} \tag{1.41}$$

The series in (1.40) and (1.41) may be truncated at terms of order β^n, $n = 0, 1, 2, ...$, to obtain approximate equations for the free surface $\eta(x,t)$ and the horizontal fluid velocity at the bottom, $F_x(x,t)$. In [1], systems of $\mathcal{O}(\alpha,\beta)$, $\mathcal{O}(\alpha\beta,\beta^2)$ and $\mathcal{O}(\alpha^2\beta,\alpha\beta^2,\beta^3)$ are derived in this way. By introducing a parameter $\theta \in [0,1]$, equations (1.40) and (1.41) can be transformed into a system of equations instead modelling the horizontal fluid velocity $w \coloneqq \phi_x(x,z,t)|_{z=\theta}$ at an arbitrary non-dimensional height $z = \theta$, as well as the free surface $\eta(x,t)$, as shown in [1].

Before we proceed, we must clarify some notation. By "n –th order equation" we always mean that the highest order derivative appearing in the equation is an n–th order derivative, not that the equation is to n–th order in β. If the equation is to order n in β, it will be explicitly specified, e.g. by writing $\mathcal{O}(\beta^n)$.

As will be shown shortly, a certain equivalent version of the fifth order system to $\mathcal{O}(\alpha^2\beta,\alpha\beta^2,\beta^3)$ for $w(x,t)$ and $\eta(x,t)$ derived in [1] has an unbounded dispersion relation for all $\theta \in [0,1] \setminus \left\{1/\sqrt{5}\right\}$, which is not physically correct, and may lead to instability if the equations are solved numerically. If the value $\theta = 1/\sqrt{5}$ is chosen in the equations, the fifth order system reduces to a third order system.

In Chapter 2 we will derive a seventh order Boussinesq-type system to $\mathcal{O}(\alpha^3\beta,\alpha^2\beta^2,\alpha\beta^3,\beta^4)$ and investigate whether this system has a better dispersion relation than this particular fifth order system to $\mathcal{O}(\alpha^2\beta,\alpha\beta^2,\beta^3)$ derived in [1].

Going to a higher order also yields a more accurate approximation of the full equations, as the neglected terms are of smaller magnitude, assuming long wavelength and small wave amplitude compared to the undisturbed depth. As far as we can tell, there exists no literature on the seventh order Boussinesq-type system, its derivation, nor on any of its properties.

The derivation procedure is the same as in [1], except that we keep the terms of $\mathcal{O}(\alpha^2\beta,\alpha\beta^2,\beta^3)$ as well. The lower order systems may be derived from the 7th order Boussinesq system by neglecting higher order terms. As shown in [1] the fifth order Boussinesq system modelling the fluid velocity w at the non-dimensional height $z = \theta$, where $0 \leq \theta \leq 1$, can be derived from equations (1.40) and (1.41). Since the procedure is the same as for the seventh order system, which we derive in Chapter 2, we refer to that chapter (or [1]) for the details. The fifth order system is then obtained by collecting all terms of order $\alpha^2\beta$, $\alpha\beta^2$ and β^3 in system (2.10), (2.12) and writing $\mathcal{O}(\alpha^2\beta,\alpha\beta^2,\beta^3)$ in place of those terms.

The fifth order system is then

$$\begin{aligned}&\eta_t + w_x + \alpha\left(\eta w\right)_x + \frac{1}{2}\left(\theta^2 - \frac{1}{3}\right)\beta w_{xxx} + \frac{1}{2}\left(\theta^2 - 1\right)\alpha\beta\left(\eta w_{xx}\right)_x \\ &+\frac{5}{24}\left(\theta^2 - \frac{1}{5}\right)^2 \beta^2 w_{xxxxx} = \mathcal{O}(\alpha^2\beta,\alpha\beta^2,\beta^3)\end{aligned} \tag{1.42}$$

$$\eta_x + w_t + \frac{1}{2}\left(\theta^2 - 1\right)\beta w_{xxt} + \alpha w w_x - \alpha\beta\left(\eta w_{xt}\right)_x + \frac{1}{2}\left(\theta^2 + 1\right)\alpha\beta w_x w_{xx} + \frac{1}{2}\left(\theta^2 - 1\right)\alpha\beta w w_{xxx} + \frac{5}{24}\left(\theta^2 - 1\right)\left(\theta^2 - \frac{1}{5}\right)\beta^2 w_{xxxxt} = \mathcal{O}(\alpha^2\beta, \alpha\beta^2, \beta^3). \tag{1.43}$$

We now want to investigate whether this system has a bounded and positive dispersion relation. The linear well-posedness of the system (1.42), (1.43) and many of its variants is extensively studied in [1], but the particular fifth order BBM-type system we investigate below is not studied explicitly, except for a short note on BBM systems which describes sufficient conditions for well-posedness for systems of BBM-type. BBM-type systems (named after Benjamin, Bona and Mahony) may be defined for our purposes as any Boussinesq-type system obtained from (1.40) and (1.41) (such as system (1.42), (1.43)) where *at least* the highest order derivative in both the truncated equations obtained from (1.40) and (1.41) is of the form $\frac{\partial^n}{\partial x^{n-1}\partial t}$, where n is the order of the highest order derivative. It is well known that systems of BBM-type are well behaved numerically, in the sense that they are more amenable to numerical integration [12].

To investigate the dispersion relation for the linearized version of equations (1.42) and (1.43), we linearize these equations around the rest state $\eta = 0$ and $w = 0$ by substituting $w = \epsilon\bar{w}$ and $\eta = \epsilon\bar{\eta}$ into these equations. Here $\epsilon\bar{w}$ and $\epsilon\bar{\eta}$, where $|\epsilon| \ll 1$, are small perturbations of w and η around their rest states. We neglect terms of $\mathcal{O}(\epsilon^2)$. It is easy to see that when these are substituted into the equations, all non-linear terms drop out as they contain factors of $\mathcal{O}(\epsilon^2)$, but the rest of the equations remain as before.

The linearized form of (1.42), (1.43) is then

$$\eta_t + w_x + \frac{1}{2}\left(\theta^2 - \frac{1}{3}\right)\beta w_{xxx} + \frac{5}{24}\left(\theta^2 - \frac{1}{5}\right)^2 \beta^2 w_{xxxxx} = \mathcal{O}(\beta^3) \tag{1.44}$$

$$\eta_x + w_t + \frac{1}{2}\left(\theta^2 - 1\right)\beta w_{xxt} + \frac{5}{24}\left(\theta^2 - 1\right)\left(\theta^2 - \frac{1}{5}\right)\beta^2 w_{xxxxt} = \mathcal{O}(\beta^3), \tag{1.45}$$

where we have dropped the 'bar' over the new variables.

As shown in [1], equations (1.42) and (1.43) can be altered further by manipulating lower order terms and inserting these into the equations. Since we are mostly interested in systems that behave well numerically, BBM-type systems are of particular interest in the present text.

Following [1], by multiplying (1.42) with β^2 and differentiating both sides four times with respect to x, it follows that

$$\beta^2 w_{xxxxx} = -\beta^2 \eta_{xxxxt} + \mathcal{O}(\alpha\beta^2, \beta^3). \tag{1.46}$$

Replacing the last term on the left hand side of equation (1.44) with this, and converting to dimensional variables gives the following BBM-type system to $\mathcal{O}(\alpha^2\beta, \alpha\beta^2, \beta^3)$

$$\eta_t + h_0 w_x + \frac{1}{2}\left(\theta^2 - \frac{1}{3}\right) h_0^3 w_{xxx} - \frac{5}{24}\left(\theta^2 - \frac{1}{5}\right)^2 h_0^4 \eta_{xxxxt} = 0 \tag{1.47}$$

$$w_t + g\eta_x - \frac{1}{2}\left(1-\theta^2\right) h_0^2 w_{xxt} + \frac{5}{24}\left(\theta^2 - 1\right)\left(\theta^2 - \frac{1}{5}\right) h_0^4 w_{xxxxt} = 0. \tag{1.48}$$

Seeking a solution of equations (1.47) and (1.48) of the form $\eta = Ae^{ikx-i\omega t}, w = Be^{ikx-i\omega t}$, where $A, B \in \mathbb{R} \setminus \{0\}$, we obtain

$$-\omega\left[1 - \tfrac{5}{24}\left(\theta^2 - \tfrac{1}{5}\right)^2 h_0^4 k^4\right] A + k\left[h_0 - \tfrac{1}{2}\left(\theta^2 - \tfrac{1}{3}\right) h_0^3 k^2\right] B = 0, \tag{1.49}$$

and

$$gkA - \omega\left[1 + \tfrac{1}{2}\left(1-\theta^2\right) h_0^2 k^2 + \tfrac{5}{24}\left(\theta^2 - 1\right)\left(\theta^2 - \tfrac{1}{5}\right) h_0^4 k^4\right] B = 0. \tag{1.50}$$

This is equivalent with the matrix equation

$$\begin{pmatrix} -\omega\left[1 - \frac{5}{24}\left(\theta^2 - \frac{1}{5}\right)^2 h_0^4 k^4\right] & k\left[h_0 - \frac{1}{2}\left(\theta^2 - \frac{1}{3}\right) h_0^3 k^2\right] \\ gk & -\omega\left[1 + \frac{1}{2}\left(1-\theta^2\right) h_0^2 k^2 + \frac{5}{24}\left(\theta^2 - 1\right)\left(\theta^2 - \frac{1}{5}\right) h_0^4 k^4\right] \end{pmatrix} \begin{pmatrix} A \\ B \end{pmatrix} = \begin{pmatrix} 0 \\ 0 \end{pmatrix}$$

and since $A, B \neq 0$ by assumption, the determinant of the matrix above must be zero. This yields the following dispersion relation

$$\frac{\omega^2}{k^2} = \frac{gh_0\left(1 - \frac{1}{2}\left(\theta^2 - \frac{1}{3}\right) h_0^2 k^2\right)}{\left(1 - \frac{5}{24}\left(\theta^2 - \frac{1}{5}\right)^2 h_0^4 k^4\right)\left(1 + \frac{1}{2}\left(1-\theta^2\right) h_0^2 k^2 + \frac{5}{24}\left(\theta^2 - 1\right)\left(\theta^2 - \frac{1}{5}\right) h_0^4 k^4\right)}. \tag{1.51}$$

Note that when $\theta^2 = 1/5$, equation (1.51) becomes $\frac{\omega^2}{k^2} = gh_0 \frac{k^2 h_0^2 + 15}{3\left(2k^2 h_0^2 + 5\right)}$ which is bounded above (by its maximum value gh_0 at $kh_0 = 0$), and is clearly non-negative for all k. Thus the linearized version of system (1.42), (1.43) has a bounded and positive dispersion relation for $\theta^2 = 1/5$.

Since the first two roots of the polynomial $1 - \frac{5}{24}\left(\theta^2 - \frac{1}{5}\right)^2 h_0^4 k^4$ are $k_{1,2} = \pm\sqrt[4]{\frac{24}{5h_0^4(\theta^2 - 1/5)^2}}$ when $\theta^2 \neq 1/5$, which are real for all values of θ, the dispersion relation (1.51) may become unbounded (in the limiting sense) for any fixed $\theta \in [0,1] \setminus \left\{\frac{1}{\sqrt{5}}\right\}$. Plotting the dispersion relation for such θ suggests that it is always unbounded for these values of θ.

As will be shown in Chapter 3, when the Fourier transform is taken of the fifth order system for the purpose of numerically solving the equations, we are dividing by the functions appearing in the denominator of dispersion relation, hence, if $\theta \in [0,1] \setminus \left\{1/\sqrt{5}\right\}$ we are dividing by zero for some values of k.

It is also important that the dispersion relation stays bounded, positive and approaches zero for large kh_0 like the dispersion relation for the full water wave problem (1.30), because an unbounded dispersion relation is physically incorrect. The dispersion relation should

tend to zero as the wavenumbers k become large, such that both the phase velocity ω/k and the group velocity $d\omega/dk$ tend to zero as well for large k, as was argued in [12]. This implies that fine scale features of the solution do not propagate, which in turn means that the system responds weakly to artificial short wave components that may be generated during a numerical computation, as argued in [12]. The phase velocity and the group velocity should also be bounded above over all wavenumbers, hence the importance of the bounded dispersion relation.

Note also that the fifth order system (1.42) (with the w_{xxxxx} term replaced by $-\eta_{xxxxt}$), (1.43) reduces to a third order system and is no longer a BBM–type system when $\theta = \sqrt{1/5}$. Therefore the fifth order BBM-type system (1.42), (1.43) is not so interesting for our purposes, and we will derive a seventh order system instead. This is done in Chapter 2.

In order to investigate whether the linearized system (1.42), (1.43) has a bounded and positive dispersion relation for a larger range of θ-values, one can also replace the βw_{xxx} term in (1.42) by a t-derivative, in a similar way as was done above. We will obtain a system that is formally equivalent up to the same order of α and β as the standard fifth order system (1.42), (1.43). We will nevertheless first derive a general seventh order Boussinesq system and investigate whether this system has a better dispersion relation. Then all other formally equivalent fifth order systems can be easily obtained by neglecting higher order terms in the various seventh order systems we derive in Chapter 2.

We can replace terms in the equations by manipulating lower order terms, and inserting these into the original equations, still keeping the formal order of approximation. Solving (1.42) for w_x, differentiating both sides $n-1$ times with respect to x, and multiplying both sides by β^m ($m \geq 1$) gives

$$\begin{aligned}\beta^m \partial_x^n w = -\beta^m \partial_x^{n-1}\eta_t - \alpha\beta^m \partial_x^n (\eta w) - \frac{1}{2}\left(\theta^2 - \frac{1}{3}\right)\beta^{m+1}\partial_x^{n+2} w - \frac{1}{2}\left(\theta^2 - 1\right)\alpha\beta^{m+1}\partial_x^n (\eta w_{xx}) \\ -\frac{5}{24}\left(\theta^2 - \frac{1}{5}\right)^2 \beta^{m+2}\partial_x^{n+4} w + \mathcal{O}(\alpha^2\beta^{m+1}, \alpha\beta^{m+2}, \beta^{m+3}).\end{aligned} \tag{1.52}$$

(Higher order terms are included here for use in later equations).

Thus we can write

$$\begin{aligned}\beta w_{xxx} = -\beta\eta_{xxt} - \alpha\beta (\eta w)_{xxx} - \frac{1}{2}\left(\theta^2 - \frac{1}{3}\right)\beta^2 w_{xxxxx} - \frac{1}{2}\left(\theta^2 - 1\right)\alpha\beta^2 (\eta w_{xx})_{xxx} \\ -\frac{5}{24}\left(\theta^2 - \frac{1}{5}\right)^2 \beta^3 w_{xxxxxxx} + \mathcal{O}(\alpha^2\beta^2, \alpha\beta^3, \beta^4),\end{aligned} \tag{1.53}$$

$$\beta^2 w_{xxxxx} = -\beta^2\eta_{xxxxt} - \alpha\beta^2 (\eta w)_{xxxxx} - \frac{1}{2}\left(\theta^2 - \frac{1}{3}\right)\beta^3 w_{xxxxxxx} + \mathcal{O}(\alpha\beta^3, \beta^4), \tag{1.54}$$

and

$$\beta^3 w_{xxxxxxx} = -\beta^3 \eta_{xxxxxxt} + \mathcal{O}(\alpha\beta^3, \beta^4). \tag{1.55}$$

Inserting (1.55) into (1.54) yields

$$\beta^2 w_{xxxxx} = -\beta^2 \eta_{xxxxt} - \alpha\beta^2 (\eta w)_{xxxxx} + \frac{1}{2}\left(\theta^2 - \frac{1}{3}\right)\beta^3 \eta_{xxxxxxt} + \mathcal{O}(\alpha\beta^3, \beta^4), \tag{1.56}$$

and inserting (1.56), (1.55) into (1.53) we obtain

$$\begin{aligned}\beta w_{xxx} = &-\beta\eta_{xxt} - \alpha\beta (\eta w)_{xxx} + \frac{1}{2}\left(\theta^2 - \frac{1}{3}\right)\beta^2 \eta_{xxxxt} - \frac{1}{2}\left(\theta^2 - 1\right)\alpha\beta^2 (\eta w_{xx})_{xxx} \\ &+\frac{1}{2}\left(\theta^2 - \frac{1}{3}\right)\alpha\beta^2 (\eta w)_{xxxxx} - \frac{1}{360}\left(15\theta^4 - 30\theta^2 + 7\right)\beta^3 \eta_{xxxxxxt} + \mathcal{O}(\alpha^2\beta^2, \alpha\beta^3, \beta^4),\end{aligned} \tag{1.57}$$

after simplifying.

These relations can be used to transform the Boussinesq equations into a formally equivalent system where all the $\frac{\partial^n}{\partial x^n}$ derivatives on the linear terms are replaced by $\frac{\partial^n}{\partial x^{n-1}\partial t}$ terms. The purpose of this is to obtain a system that is more well behaved numerically.

In order to remove t-derivatives on the nonlinear terms appearing in the equations, some other relations are needed. This is useful for easily taking the Fourier transform of the equations later. Solving (1.43) for w_t and differentiating both sides three times with respect to x, we obtain

$$w_{xxxt} = -\eta_{xxxx} + \mathcal{O}(\alpha, \beta). \tag{1.58}$$

Likewise, solving (1.43) for w_t and differentiating once with respect to x yields

$$w_{xt} = -\eta_{xx} - \alpha (w w_x)_x - \frac{1}{2}\left(\theta^2 - 1\right)\beta w_{xxxt} + \mathcal{O}(\alpha\beta, \beta^2). \tag{1.59}$$

Now insert (1.58) into (1.59) to obtain

$$w_{xt} = -\eta_{xx} - \alpha (w w_x)_x + \frac{1}{2}\left(\theta^2 - 1\right)\beta \eta_{xxxx} + \mathcal{O}(\alpha\beta, \beta^2). \tag{1.60}$$

Relations (1.58) and (1.60) will be made use of later when the equations are solved numerically.

Chapter 2

Seventh order Boussinesq systems and their properties

In this chapter, we derive multiple equivalent seventh order Boussinesq systems of equations modelling the horizontal fluid velocity $w(x,t)$ at a non-dimensional height $z = \theta$ in the fluid column, where $0 \leq \theta \leq 1$, as well as the free surface $\eta(x,t)$. We derive dispersion relations for linearized versions of the seventh order systems, and discuss requirements on the parameter θ which make the systems well behaved numerically, in the sense that the dispersion relations remain bounded and non-negative for all wavenumbers k. The results presented in this chapter, including the seventh order systems and all their properties, have, to our knowledge, not been derived or discussed before in other literature.

2.1 Derivation of the seventh order Boussinesq system

In the derivation of the general seventh order system, we use the notation $\frac{\partial^n f(x,t)}{\partial x^m \partial t^p} = f_{x^m t^p}$ where $m+p=n$. The procedure is the same as in [1], the only difference is that we include terms of one higher order in α and β and their products. Expanding (1.40), (1.41) and keeping terms of order $\beta^3, \alpha\beta^2$ and $\alpha^2\beta$ we get from (1.40)

$$
\begin{aligned}
&\eta_t + \alpha\eta_x \left[F_x - \frac{1}{2}F_{x^3}\left(1+\alpha\eta\right)^2\beta + \frac{1}{4!}F_{x^5}\left(1+\alpha\eta\right)^4\beta^2 + \mathcal{O}(\beta^3)\right] \\
&+\left[F_{x^2}\left(1+\alpha\eta\right) - \frac{1}{3!}F_{x^4}\left(1+\alpha\eta\right)^3\beta + \frac{1}{5!}F_{x^6}\left(1+\alpha\eta\right)^5\beta^2 - \frac{1}{7!}F_{x^8}\left(1+\alpha\eta\right)^7\beta^3 + \mathcal{O}(\beta^4)\right] = \\
&\eta_t + \alpha\eta_x \left[F_x - \frac{1}{2}F_{x^3}\left(1+2\alpha\eta\right)\beta + \frac{1}{4!}F_{x^5}\left(1\right)\beta^2\right] \\
&+\left[F_{x^2}\left(1+\alpha\eta\right) - \frac{1}{3!}F_{x^4}\left(1+3\alpha\eta+3\alpha^2\eta^2\right)\beta + \frac{1}{5!}F_{x^6}\left(1+5\alpha\eta\right)\beta^2 - \frac{1}{7!}F_{x^8}(1)\beta^3\right] \\
&+\mathcal{O}(\alpha^3\beta, \alpha^2\beta^2, \alpha\beta^3, \beta^4) \\
&= \eta_t + \eta_x F_x\alpha - \frac{1}{2}F_{x^3}\eta_x\left(1+2\alpha\eta\right)\alpha\beta + \frac{1}{24}F_{x^5}\eta_x\alpha\beta^2 \\
&+F_{x^2}\left(1+\alpha\eta\right) - \frac{1}{6}F_{x^4}\left(1+3\alpha\eta+3\alpha^2\eta^2\right)\beta + \frac{1}{120}F_{x^6}\left(1+5\alpha\eta\right)\beta^2 \\
&-\frac{1}{5040}F_{x^8}\beta^3 + \mathcal{O}(\alpha^3\beta, \alpha^2\beta^2, \alpha\beta^3, \beta^4) = 0.
\end{aligned}
\tag{2.1}
$$

Let $u = F_x$ as in [1], and insert this into the last equation of (2.1) to get

$$
\begin{aligned}
&\eta_t + \eta_x u\alpha - \frac{1}{2}u_{x^2}\eta_x\left(1+2\alpha\eta\right)\alpha\beta + \frac{1}{24}u_{x^4}\eta_x\alpha\beta^2 \\
&+u_x\left(1+\alpha\eta\right) - \frac{1}{6}u_{x^3}\left(1+3\alpha\eta+3\alpha^2\eta^2\right)\beta + \frac{1}{120}u_{x^5}\left(1+5\alpha\eta\right)\beta^2 \\
&-\frac{1}{5040}u_{x^7}\beta^3 + \mathcal{O}(\alpha^3\beta, \alpha^2\beta^2, \alpha\beta^3, \beta^4) = 0.
\end{aligned}
\tag{2.2}
$$

From (1.41) we get

$$\eta+\left[F_t-\frac{1}{2}F_{tx^2}\left(1+\alpha\eta\right)^2\beta+\frac{1}{4!}F_{tx^4}\left(1+\alpha\eta\right)^4\beta^2-\frac{1}{6!}F_{tx^6}\left(1+\alpha\eta\right)^6\beta^3+\mathcal{O}(\beta^4)\right]$$
$$+\frac{1}{2}\alpha\Big\{\left[F_x-\frac{1}{2}F_{x^3}\left(1+\alpha\eta\right)^2\beta+\frac{1}{4!}F_{x^5}\left(1+\alpha\eta\right)^4\beta^2+\mathcal{O}(\beta^3)\right]\times$$
$$\times\left[F_x-\frac{1}{2}F_{x^3}\left(1+\alpha\eta\right)^2\beta+\frac{1}{4!}F_{x^5}\left(1+\alpha\eta\right)^4\beta^2+\mathcal{O}(\beta^3)\right]\Big\}$$
$$+\frac{1}{2}\alpha\beta\left\{\left[F_{x^2}\left(1+\alpha\eta\right)-\frac{1}{3!}F_{x^4}\left(1+\alpha\eta\right)^3\beta+\mathcal{O}(\beta^2)\right]\left[F_{x^2}\left(1+\alpha\eta\right)-\frac{1}{3!}F_{x^4}\left(1+\alpha\eta\right)^3\beta+\mathcal{O}(\beta^2)\right]\right\}$$
$$+\mathcal{O}(\alpha^3\beta,\alpha^2\beta^2,\alpha\beta^3,\beta^4)=\eta+\left[F_t-\frac{1}{2}F_{tx^2}\left(1+\alpha\eta\right)^2\beta+\frac{1}{4!}F_{tx^4}\left(1+4\alpha\eta\right)\beta^2-\frac{1}{6!}F_{tx^6}(1)\beta^3\right]$$
$$+\frac{1}{2}\alpha\Big\{\ F_x\left[F_x-\frac{1}{2}F_{x^3}\left(1+\alpha\eta\right)^2\beta+\frac{1}{4!}F_{x^5}\left(1+\alpha\eta\right)^4\beta^2+\mathcal{O}(\beta^3)\right]$$
$$-\frac{1}{2}F_{x^3}\left[F_x\left(1+\alpha\eta\right)^2\beta-\frac{1}{2}F_{x^3}\left(1+\alpha\eta\right)^4\beta^2+\mathcal{O}(\beta^3)\right]+\frac{1}{4!}F_{x^5}\left[F_x\left(1+\alpha\eta\right)^4\beta^2+\mathcal{O}(\beta^3)\right]+\mathcal{O}(\beta^3)\Big\}$$
$$+\frac{1}{2}\Big\{F_{x^2}\left[F_{x^2}(1+\alpha\eta)^2\alpha\beta-\frac{1}{3!}F_{x^4}(1+\alpha\eta)^4\alpha\beta^2+\mathcal{O}(\alpha\beta^3,\beta^4)\right]$$
$$-\frac{1}{3!}F_{x^4}\left[F_{x^2}(1+\alpha\eta)^4\alpha\beta^2+\mathcal{O}(\alpha\beta^3,\beta^4)\right]+\mathcal{O}(\alpha\beta^3,\beta^4)\Big\}+\mathcal{O}(\alpha^3\beta,\alpha^2\beta^2,\alpha\beta^3,\beta^4)$$
$$=\eta+\left[F_t-\frac{1}{2}F_{tx^2}\left(1+\alpha\eta\right)^2\beta+\frac{1}{4!}F_{tx^4}\left(1+4\alpha\eta\right)\beta^2-\frac{1}{6!}F_{tx^6}\beta^3\right]$$
$$+\frac{1}{2}\alpha\Big\{\ F_x\left[F_x-\frac{1}{2}F_{x^3}\left(1+2\alpha\eta\right)\beta+\frac{1}{4!}F_{x^5}(1)\beta^2\right]$$
$$-\frac{1}{2}F_{x^3}\left[F_x\left(1+2\alpha\eta\right)\beta-\frac{1}{2}F_{x^3}\left(1\right)\beta^2\right]+\frac{1}{4!}F_{x^5}F_x\left(1\right)\beta^2\Big\}$$
$$+\frac{1}{2}\Big\{F_{x^2}\left[F_{x^2}(1+2\alpha\eta)\alpha\beta-\frac{1}{3!}F_{x^4}(1)\alpha\beta^2\right]$$
$$-\frac{1}{3!}F_{x^4}F_{x^2}(1)\alpha\beta^2\Big\}+\mathcal{O}(\alpha^3\beta,\alpha^2\beta^2,\alpha\beta^3,\beta^4)$$
$$=\eta+F_t-\frac{1}{2}F_{tx^2}\left(1+\alpha\eta\right)^2\beta+\frac{1}{24}F_{tx^4}\left(1+4\alpha\eta\right)\beta^2-\frac{1}{720}F_{tx^6}\beta^3$$
$$+\frac{1}{2}\alpha\left\{\ \left(F_x\right)^2-F_{x^3}F_x\left(1+2\alpha\eta\right)\beta+\frac{1}{12}F_{x^5}F_x\beta^2+\frac{1}{4}\left(F_{x^3}\right)^2\beta^2\right\}$$
$$+\frac{1}{2}\left(F_{x^2}\right)^2(1+2\alpha\eta)\alpha\beta-\frac{1}{6}F_{x^4}F_{x^2}\alpha\beta^2+\mathcal{O}(\alpha^3\beta,\alpha^2\beta^2,\alpha\beta^3,\beta^4)$$
$$=\eta+F_t-\frac{1}{2}F_{tx^2}\left(1+\alpha\eta\right)^2\beta+\frac{1}{24}F_{tx^4}\left(1+4\alpha\eta\right)\beta^2$$
$$+\frac{1}{2}\alpha\left(F_x\right)^2-\frac{1}{2}F_{x^3}F_x\left(1+2\alpha\eta\right)\alpha\beta+\frac{1}{24}F_{x^5}F_x\alpha\beta^2+\frac{1}{8}\left(F_{x^3}\right)^2\alpha\beta^2$$
$$+\frac{1}{2}\left(F_{x^2}\right)^2(1+2\alpha\eta)\alpha\beta-\frac{1}{6}F_{x^4}F_{x^2}\alpha\beta^2-\frac{1}{720}F_{tx^6}\beta^3+\mathcal{O}(\alpha^3\beta,\alpha^2\beta^2,\alpha\beta^3,\beta^4)=0. \tag{2.3}$$

Next, differentiate the last equation in (2.3) with respect to x and substitute $u = F_x$ as above to get

$$\begin{aligned}
&\eta_x + F_{xt} - \frac{1}{2}F_{tx^3}\left(1+\alpha\eta\right)^2\beta - F_{tx^2}\left(1+\alpha\eta\right)\eta_x\alpha\beta + \left[\frac{1}{24}F_{tx^5}\left(1+4\alpha\eta\right)\beta^2 + \frac{1}{24}F_{tx^4}\left(4\alpha\eta_x\right)\beta^2\right]\\
&+\alpha F_xF_{x^2} - \frac{1}{2}\alpha\beta\left[\left(F_{x^4}F_x + F_{x^3}F_{x^2}\right)\left(1+2\alpha\eta\right) + 2F_{x^3}F_x\alpha\eta_x\right] + \left[\frac{1}{24}F_{x^6}F_x\alpha\beta^2 + \frac{1}{24}F_{x^5}F_{x^2}\alpha\beta^2\right]\\
&+\frac{1}{4}F_{x^3}F_{x^4}\alpha\beta^2 + \frac{1}{2}\alpha\beta\left[2F_{x^2}F_{x^3}(1+2\alpha\eta) + 2\left(F_{x^2}\right)^2\alpha\eta_x\right] - \frac{1}{6}F_{x^5}F_{x^2}\alpha\beta^2 - \frac{1}{6}F_{x^4}F_{x^3}\alpha\beta^2\\
&-\frac{1}{720}F_{tx^7}\beta^3 + \mathcal{O}(\alpha^3\beta, \alpha^2\beta^2, \alpha\beta^3, \beta^4) =\\
&\eta_x + u_t - \frac{1}{2}u_{tx^2}\left(1+\alpha\eta\right)^2\beta - u_{tx}\left(1+\alpha\eta\right)\eta_x\alpha\beta + \frac{1}{24}u_{tx^4}\left(1+4\alpha\eta\right)\beta^2 + \frac{1}{24}u_{tx^3}\left(4\alpha\eta_x\right)\beta^2\\
&+\alpha uu_x - \frac{1}{2}\alpha\beta\left[\left(u_{x^3}u + u_{x^2}u_x\right)\left(1+2\alpha\eta\right) + 2u_{x^2}u\alpha\eta_x\right] + \frac{1}{24}u_{x^5}u\alpha\beta^2 + \frac{1}{24}u_{x^4}u_x\alpha\beta^2\\
&+\frac{1}{4}u_{x^2}u_{x^3}\alpha\beta^2 + \frac{1}{2}\alpha\beta\left[2u_xu_{x^2}(1+2\alpha\eta) + 2\left(u_x\right)^2\alpha\eta_x\right] - \frac{1}{6}u_{x^4}u_x\alpha\beta^2 - \frac{1}{6}u_{x^3}u_{x^2}\alpha\beta^2\\
&-\frac{1}{720}u_{tx^6}\beta^3 + \mathcal{O}(\alpha^3\beta, \alpha^2\beta^2, \alpha\beta^3, \beta^4) =\\
&\eta_x + u_t + \alpha uu_x - \frac{1}{2}u_{tx^2}\left(1+\alpha\eta\right)^2\beta - u_{tx}\eta_x\left(1+\alpha\eta\right)\alpha\beta + \frac{1}{24}u_{tx^4}\left(1+4\alpha\eta\right)\beta^2 + \frac{1}{6}u_{tx^3}\left(\alpha\eta_x\right)\beta^2\\
&-\frac{1}{2}\alpha\beta\left[\left(u_{x^3}u + u_{x^2}u_x\right)\left(1+2\alpha\eta\right) + 2u_{x^2}u\alpha\eta_x\right] + \frac{1}{24}\left[u_{x^5}u + u_{x^4}u_x + 6u_{x^2}u_{x^3}\right]\alpha\beta^2\\
&+\alpha\beta\left[u_xu_{x^2}(1+2\alpha\eta) + \left(u_x\right)^2\alpha\eta_x\right] - \frac{1}{6}u_{x^4}u_x\alpha\beta^2 - \frac{1}{6}u_{x^3}u_{x^2}\alpha\beta^2\\
&-\frac{1}{720}u_{tx^6}\beta^3 + \mathcal{O}(\alpha^3\beta, \alpha^2\beta^2, \alpha\beta^3, \beta^4) = 0
\end{aligned} \tag{2.4}$$

Proceding as in [1], we define $w = \phi_x|_{z=\theta}$ as the horizontal velocity at the dimensional *height* $z = (\theta-1)h_0$, with $0 \le \theta \le 1$, and a formal use of Taylor's formula with remainder gives

$$\begin{aligned}
w = \phi_x|_{z=\theta} &= F_x - \tfrac{1}{2}\beta\theta^2F_{x^3} + \tfrac{1}{4!}\beta^2\theta^4F_{x^5} - \tfrac{1}{6!}\beta^3\theta^6F_{x^7} + \mathcal{O}(\beta^4)\\
&= u - \tfrac{1}{2}\beta\theta^2u_{x^2} + \tfrac{1}{4!}\beta^2\theta^4u_{x^4} - \tfrac{1}{6!}\beta^3\theta^6u_{x^6} + \mathcal{O}(\beta^4)
\end{aligned} \tag{2.5}$$

as $\beta \to 0$ (see the expression for the velocity potential $\phi(x,z,t)$ derived in Section 1.3).

Recalling the definition of the Fourier transform in the spatial variable x of a function f, given by

$$\hat{f}(k) = \int_{-\infty}^{+\infty} e^{-ikx}f(x)dx$$

and using the standard result $\widehat{\frac{\partial^n}{\partial x^n}f(x,t)} = (ik)^n\hat{f}(k,t)$,

we get

$$\hat{w} = \left[1 + \frac{1}{2}\beta\theta^2k^2 + \frac{1}{4!}\beta^2\theta^4k^4 + \frac{1}{6!}\beta^3\theta^6k^6\right]\hat{u} + \mathcal{O}(\beta^4)$$

after taking the Fourier transform of (2.5).
Next, invert the positive Fourier multiplier to get

$$\begin{aligned}
\hat{u} &= \left[1 + \frac{1}{2}\beta\theta^2k^2 + \frac{1}{4!}\beta^2\theta^4k^4 + \frac{1}{6!}\beta^3\theta^6k^6\right]^{-1}\hat{w} + \mathcal{O}(\beta^4)\\
&= \left[1 - \left(-\frac{1}{2}\beta\theta^2k^2 - \frac{1}{4!}\beta^2\theta^4k^4 - \frac{1}{6!}\beta^3\theta^6k^6\right)\right]^{-1}\hat{w} + \mathcal{O}(\beta^4)\\
&= \Big[1 + \left(-\frac{1}{2}\beta\theta^2k^2 - \frac{1}{4!}\beta^2\theta^4k^4 - \frac{1}{6!}\beta^3\theta^6k^6\right) + \left(-\frac{1}{2}\beta\theta^2k^2 - \frac{1}{4!}\beta^2\theta^4k^4 - \frac{1}{6!}\beta^3\theta^6k^6\right)^2\\
&+ \left(-\frac{1}{2}\beta\theta^2k^2 - \frac{1}{4!}\beta^2\theta^4k^4 - \frac{1}{6!}\beta^3\theta^6k^6\right)^3 + \mathcal{O}(\beta^4)\Big]\hat{w} + \mathcal{O}(\beta^4)\\
&= \Big[1 - \frac{1}{2}\beta\theta^2k^2 - \frac{1}{4!}\beta^2\theta^4k^4 - \frac{1}{6!}\beta^3\theta^6k^6 + \left(\frac{1}{4}\beta^2\theta^4k^4 + \frac{1}{24}\beta^3\theta^6k^6 + \mathcal{O}(\beta^4)\right)\\
&+ \left(-\frac{1}{8}\beta^3\theta^6k^6 + \mathcal{O}(\beta^4)\right) + \mathcal{O}(\beta^4)\Big]\hat{w} + \mathcal{O}(\beta^4)\\
&= \left[1 - \frac{1}{2}\beta\theta^2k^2 + \frac{5}{24}\beta^2\theta^4k^4 - \frac{61}{720}\beta^3\theta^6k^6\right]\hat{w} + \mathcal{O}(\beta^4).
\end{aligned} \tag{2.6}$$

This is equivalent with

$$\begin{aligned}
\hat{u} &= \hat{w} + \frac{1}{2}\beta\theta^2(ik)^2\hat{w} + \frac{5}{24}\beta^2\theta^4(ik)^4\hat{w} + \frac{61}{720}\beta^3\theta^6(ik)^6\hat{w} + \mathcal{O}(\beta^4)\\
&= \hat{w} + \frac{1}{2}\beta\theta^2\widehat{w_{x^2}} + \frac{5}{24}\beta^2\theta^4\widehat{w_{x^4}} + \frac{61}{720}\beta^3\theta^6\widehat{w_{x^6}} + \mathcal{O}(\beta^4).
\end{aligned} \tag{2.7}$$

Finally, taking the inverse Fourier transform of (2.7) yields

$$u = w + \frac{1}{2}\beta\theta^2w_{x^2} + \frac{5}{24}\beta^2\theta^4w_{x^4} + \frac{61}{720}\beta^3\theta^6w_{x^6} + \mathcal{O}(\beta^4). \tag{2.8}$$

Inserting (2.8) into (2.2) and neglecting terms of $\mathcal{O}(\alpha^3\beta, \alpha^2\beta^2, \alpha\beta^3, \beta^4)$ gives

$$
\begin{aligned}
&\eta_t + \left[w + \frac{1}{2}\beta\theta^2 w_{x^2} + \frac{5}{24}\beta^2\theta^4 w_{x^4} + \mathcal{O}(\beta^3)\right]\eta_x\alpha - \frac{1}{2}\eta_x(1+2\alpha\eta)\alpha\beta\left[w_{x^2} + \frac{1}{2}\beta\theta^2 w_{x^4} + \mathcal{O}(\beta^2)\right]\\
&+\frac{1}{24}\eta_x\alpha\beta^2\left[w_{x^4} + \mathcal{O}(\beta)\right] + (1+\alpha\eta)\left[w_x + \frac{1}{2}\beta\theta^2 w_{x^3} + \frac{5}{24}\beta^2\theta^4 w_{x^5} + \frac{61}{720}\beta^3\theta^6 w_{x^7} + \mathcal{O}(\beta^4)\right]\\
&-\frac{1}{6}(1+3\alpha\eta+3\alpha^2\eta^2)\beta\left[w_{x^3} + \frac{1}{2}\beta\theta^2 w_{x^5} + \frac{5}{24}\beta^2\theta^4 w_{x^7} + \mathcal{O}(\beta^3)\right]\\
&+\frac{1}{120}(1+5\alpha\eta)\beta^2\left[w_{x^5} + \frac{1}{2}\beta\theta^2 w_{x^7} + \mathcal{O}(\beta^2)\right] - \frac{1}{5040}\beta^3\left[w_{x^7} + \mathcal{O}(\beta)\right]\\
&+\mathcal{O}(\alpha^3\beta, \alpha^2\beta^2, \alpha\beta^3, \beta^4)\\
&= \eta_t + \left[w + \frac{1}{2}\beta\theta^2 w_{x^2} + \frac{5}{24}\beta^2\theta^4 w_{x^4}\right]\eta_x\alpha - \frac{1}{2}\eta_x\alpha\beta\left[w_{x^2} + \frac{1}{2}\beta\theta^2 w_{x^4}\right] - \eta_x\eta w_{x^2}\alpha^2\beta + \frac{1}{24}\eta_x\alpha\beta^2 w_{x^4}\\
&+\left[w_x + \frac{1}{2}\beta\theta^2 w_{x^3} + \frac{5}{24}\beta^2\theta^4 w_{x^5} + \frac{61}{720}\beta^3\theta^6 w_{x^7}\right] + \alpha\eta\left[w_x + \frac{1}{2}\beta\theta^2 w_{x^3} + \frac{5}{24}\beta^2\theta^4 w_{x^5}\right]\\
&-\frac{1}{6}\beta\left[w_{x^3} + \frac{1}{2}\beta\theta^2 w_{x^5} + \frac{5}{24}\beta^2\theta^4 w_{x^7}\right] - \frac{1}{2}\eta\ \alpha\beta\left[w_{x^3} + \frac{1}{2}\beta\theta^2 w_{x^5}\right] - \frac{1}{2}\eta^2\alpha^2\beta w_{x^3}\\
&+\frac{1}{120}\beta^2\left[w_{x^5} + \frac{1}{2}\beta\theta^2 w_{x^7}\right] + \frac{1}{24}\eta w_{x^5}\alpha\beta^2 - \frac{1}{5040}\beta^3 w_{x^7} + \mathcal{O}(\alpha^3\beta, \alpha^2\beta^2, \alpha\beta^3, \beta^4) = 0.
\end{aligned}
\tag{2.9}
$$

Collecting terms in the last equation above, we end up with the first equation of the desired system to $\mathcal{O}(\alpha^3\beta, \alpha^2\beta^2, \alpha\beta^3, \beta^4)$

$$
\begin{aligned}
&\eta_t + w_x + \alpha\left(\eta w\right)_x + \frac{1}{2}\left(\theta^2 - \tfrac{1}{3}\right)\beta w_{xxx} + \frac{1}{2}\left(\theta^2 - 1\right)\alpha\beta(\eta w_{xx})_x\\
&+\frac{5}{24}\left(\theta^2 - \tfrac{1}{5}\right)^2\beta^2 w_{xxxxx} - \frac{1}{2}\alpha^2\beta\left(\eta^2 w_{xx}\right)_x + \frac{5}{24}\left(\theta^2 - \tfrac{1}{5}\right)\left(\theta^2 - 1\right)\alpha\beta^2\left(\eta w_{xxxx}\right)_x\\
&+\frac{1}{5040}\left(7\theta^2\left(61\theta^4 - 25\theta^2 + 3\right) - 1\right)\beta^3 w_{xxxxxxx} + \mathcal{O}(\alpha^3\beta, \alpha^2\beta^2, \alpha\beta^3, \beta^4) = 0.
\end{aligned}
\tag{2.10}
$$

Similarly, inserting (2.8) into the last equation in (2.4) and neglecting terms of $\mathcal{O}(\alpha^3\beta, \alpha^2\beta^2, \alpha\beta^3, \beta^4)$ yields

$$
\begin{aligned}
&\eta_x + \left[w_t + \frac{1}{2}\beta\theta^2 w_{x^2t} + \frac{5}{24}\beta^2\theta^4 w_{x^4t} + \frac{61}{720}\beta^3\theta^6 w_{x^6t} + \mathcal{O}(\beta^4)\right] \\
&+\alpha\left[w + \frac{1}{2}\beta\theta^2 w_{x^2} + \frac{5}{24}\beta^2\theta^4 w_{x^4} + \mathcal{O}(\beta^3)\right]\left[w_x + \frac{1}{2}\beta\theta^2 w_{x^3} + \frac{5}{24}\beta^2\theta^4 w_{x^5} + \mathcal{O}(\beta^3)\right] \\
&-\frac{1}{2}(1+\alpha\eta)^2\beta\left[w_{x^2t} + \frac{1}{2}\beta\theta^2 w_{x^4t} + \frac{5}{24}\beta^2\theta^4 w_{x^6t} + \mathcal{O}(\beta^3)\right] - \eta_x(1+\alpha\eta)\alpha\beta\left[w_{xt} + \frac{1}{2}\beta\theta^2 w_{x^3t} + \mathcal{O}(\beta^2)\right] \\
&+\frac{1}{24}(1+4\alpha\eta)\beta^2\left[w_{x^4t} + \frac{1}{2}\beta\theta^2 w_{x^6t} + \mathcal{O}(\beta^2)\right] + \frac{1}{6}\eta_x\alpha\beta^2\left[w_{x^3t} + \mathcal{O}(\beta)\right] \\
&-\frac{1}{2}\alpha\beta(1+2\alpha\eta)\Big\{\left[w + \frac{1}{2}\beta\theta^2 w_{x^2} + \mathcal{O}(\beta^2)\right]\left[w_{x^3} + \frac{1}{2}\beta\theta^2 w_{x^5} + \mathcal{O}(\beta^2)\right] \\
&+\left[w_x + \frac{1}{2}\beta\theta^2 w_{x^3} + \mathcal{O}(\beta^2)\right]\left[w_{x^2} + \frac{1}{2}\beta\theta^2 w_{x^4} + \mathcal{O}(\beta^2)\right]\Big\} - \alpha^2\beta\eta_x\left[w + \mathcal{O}(\beta)\right]\left[w_{x^2} + \mathcal{O}(\beta)\right] \\
&+\frac{1}{24}\alpha\beta^2\left\{\left[w + \mathcal{O}(\beta)\right]\left[w_{x^5} + \mathcal{O}(\beta)\right] + \left[w_x + \mathcal{O}(\beta)\right]\left[w_{x^4} + \mathcal{O}(\beta)\right] + 6\left[w_{x^2} + \mathcal{O}(\beta)\right]\left[w_{x^3} + \mathcal{O}(\beta)\right]\right\} \\
&+\alpha\beta(1+2\alpha\eta)\left[w_x + \frac{1}{2}\beta\theta^2 w_{x^3} + \mathcal{O}(\beta^2)\right]\left[w_{x^2} + \frac{1}{2}\beta\theta^2 w_{x^4} + \mathcal{O}(\beta^2)\right] + \eta_x\alpha^2\beta\left[w_x + \mathcal{O}(\beta)\right]\left[w_x + \mathcal{O}(\beta)\right] \\
&-\frac{1}{6}\alpha\beta^2\left[w_x + \mathcal{O}(\beta)\right]\left[w_{x^4} + \mathcal{O}(\beta)\right] - \frac{1}{6}\alpha\beta^2\left[w_{x^2} + \mathcal{O}(\beta)\right]\left[w_{x^3} + \mathcal{O}(\beta)\right] - \frac{1}{720}\beta^3\left[w_{x^6t} + \mathcal{O}(\beta)\right] \\
&+\mathcal{O}(\alpha^3\beta, \alpha^2\beta^2, \alpha\beta^3, \beta^4) \\
&= \eta_x + w_t + \frac{1}{2}\beta\theta^2 w_{x^2t} + \frac{5}{24}\beta^2\theta^4 w_{x^4t} + \frac{61}{720}\beta^3\theta^6 w_{x^6t} \\
&+\left\{\alpha w\left[w_x + \frac{1}{2}\beta\theta^2 w_{x^3} + \frac{5}{24}\beta^2\theta^4 w_{x^5}\right] + \frac{1}{2}\alpha\beta\theta^2 w_{x^2}\left[w_x + \frac{1}{2}\beta\theta^2 w_{x^3}\right] + \frac{5}{24}\alpha\beta^2\theta^4 w_{x^4}w_x\right\} \\
&+\left\{\left[-\frac{1}{2}\beta w_{x^2t} - \frac{1}{4}\beta^2\theta^2 w_{x^4t} - \frac{5}{48}\beta^3\theta^4 w_{x^6t}\right] + \left[-\alpha\beta\eta w_{x^2t} - \frac{1}{2}\alpha\beta^2\theta^2\eta w_{x^4t}\right] - \frac{1}{2}\alpha^2\beta\eta^2 w_{x^2t}\right\} \\
&+\left\{\left[-\alpha\beta\eta_x w_{xt} - \frac{1}{2}\alpha\beta^2\theta^2\eta_x w_{x^3t}\right] - \alpha^2\beta\eta\eta_x w_{xt}\right\} + \left\{\left[\frac{1}{24}\beta^2 w_{x^4t} + \frac{1}{48}\beta^3\theta^2 w_{x^6t}\right] + \frac{1}{6}\alpha\beta^2\eta w_{x^4t}\right\} \\
&+\frac{1}{6}\alpha\beta^2\eta_x w_{x^3t} \\
&-\frac{1}{2}\alpha\beta\left\{\left[ww_{x^3} + \frac{1}{2}\beta\theta^2 ww_{x^5} + \frac{1}{2}\beta\theta^2 w_{x^2}w_{x^3} + \mathcal{O}(\beta^2)\right] + \left[w_xw_{x^2} + \frac{1}{2}\beta\theta^2 w_xw_{x^4} + \frac{1}{2}\beta\theta^2 w_{x^2}w_{x^3} + \mathcal{O}(\beta^2)\right]\right\} \\
&-\eta\alpha^2\beta\left\{\left[ww_{x^3} + \mathcal{O}(\beta)\right] + \left[w_xw_{x^2} + \mathcal{O}(\beta)\right]\right\} - \alpha^2\beta\eta_x ww_{x^2} + \frac{1}{24}\alpha\beta^2\left[ww_{x^5} + w_xw_{x^4} + 6w_{x^2}w_{x^3}\right] \\
&+\alpha\beta\left[w_xw_{x^2} + \frac{1}{2}\beta\theta^2 w_xw_{x^4} + \frac{1}{2}\beta\theta^2 w_{x^2}w_{x^3} + \mathcal{O}(\beta^2)\right] + 2\eta\alpha^2\beta\left[w_xw_{x^2} + \mathcal{O}(\beta)\right] \\
&+\eta_x\alpha^2\beta\left(w_x\right)^2 - \frac{1}{6}\alpha\beta^2 w_xw_{x^4} - \frac{1}{6}\alpha\beta^2 w_{x^2}w_{x^3} - \frac{1}{720}\beta^3 w_{x^6t} + \mathcal{O}(\alpha^3\beta, \alpha^2\beta^2, \alpha\beta^3, \beta^4) =
\end{aligned}
$$

$$
\begin{aligned}
&= \eta_x + w_t + \frac{1}{2}\beta\theta^2 w_{x^2t} + \frac{5}{24}\beta^2\theta^4 w_{x^4t} + \frac{61}{720}\beta^3\theta^6 w_{x^6t} \\
&+\alpha w w_x + \frac{1}{2}\alpha\beta\theta^2 w w_{x^3} + \frac{5}{24}\alpha\beta^2\theta^4 w w_{x^5} + \frac{1}{2}\alpha\beta\theta^2 w_x w_{x^2} + \frac{1}{4}\alpha\beta^2\theta^4 w_{x^2} w_{x^3} + \frac{5}{24}\alpha\beta^2\theta^4 w_x w_{x^4} \\
&-\frac{1}{2}\beta w_{x^2t} - \frac{1}{4}\beta^2\theta^2 w_{x^4t} - \frac{5}{48}\beta^3\theta^4 w_{x^6t} - \alpha\beta\eta w_{x^2t} - \frac{1}{2}\alpha\beta^2\theta^2\eta w_{x^4t} - \frac{1}{2}\alpha^2\beta\eta^2 w_{x^2t} \\
&-\alpha\beta\eta_x w_{xt} - \frac{1}{2}\alpha\beta^2\theta^2\eta_x w_{x^3t} - \alpha^2\beta\eta\eta_x w_{xt} + \frac{1}{24}\beta^2 w_{x^4t} + \frac{1}{48}\beta^3\theta^2 w_{x^6t} + \frac{1}{6}\alpha\beta^2\eta w_{x^4t} + \frac{1}{6}\alpha\beta^2\eta_x w_{x^3t} \\
&-\frac{1}{2}\alpha\beta w w_{x^3} - \frac{1}{4}\alpha\beta^2\theta^2 w w_{x^5} - \frac{1}{4}\alpha\beta^2\theta^2 w_{x^2} w_{x^3} - \frac{1}{2}\alpha\beta w_x w_{x^2} - \frac{1}{4}\alpha\beta^2\theta^2 w_x w_{x^4} - \frac{1}{4}\alpha\beta^2\theta^2 w_{x^2} w_{x^3} \\
&-\eta\alpha^2\beta\left\{w w_{x^3} + w_x w_{x^2}\right\} - \alpha^2\beta\eta_x w w_{x^2} + \frac{1}{24}\alpha\beta^2\left[w w_{x^5} + w_x w_{x^4} + 6 w_{x^2} w_{x^3}\right] \\
&+\alpha\beta\left[w_x w_{x^2} + \frac{1}{2}\beta\theta^2 w_x w_{x^4} + \frac{1}{2}\beta\theta^2 w_{x^2} w_{x^3}\right] + 2\eta\alpha^2\beta w_x w_{x^2} + \eta_x\alpha^2\beta\left(w_x\right)^2 - \frac{1}{6}\alpha\beta^2 w_x w_{x^4} \\
&-\frac{1}{6}\alpha\beta^2 w_{x^2} w_{x^3} - \frac{1}{720}\beta^3 w_{x^6t} + \mathcal{O}(\alpha^3\beta, \alpha^2\beta^2, \alpha\beta^3, \beta^4) = 0
\end{aligned}
\tag{2.11}
$$

Finally, collecting terms in the last equation in (2.11), we end up with the second equation of the desired system

$$
\begin{aligned}
&\eta_x + w_t + \alpha w w_x + \frac{1}{2}\left(\theta^2 - 1\right)\beta w_{xxt} - \alpha\beta(\eta w_{xt})_x + \frac{1}{2}\left(\theta^2 - 1\right)\alpha\beta w w_{xxx} \\
&+\frac{1}{2}\left(1 + \theta^2\right)\alpha\beta w_x w_{xx} + \frac{5}{24}\left(\theta^2 - \tfrac{1}{5}\right)\left(\theta^2 - 1\right)\beta^2 w_{xxxxt} - \frac{1}{2}\alpha^2\beta\left(\eta^2 w_{xt}\right)_x - \alpha^2\beta w(\eta w_{xx})_x \\
&+\alpha^2\beta w_x(\eta w_x)_x - \frac{1}{2}\left(\theta^2 - \tfrac{1}{3}\right)\alpha\beta^2(\eta w_{xxxt})_x + \frac{5}{24}\left(\theta^2 - \tfrac{1}{5}\right)\left(\theta^2 - 1\right)\alpha\beta^2 w w_{xxxxx} \\
&+\left(\frac{5}{24}\left(\theta^2 + \tfrac{3}{5}\right)^2 - \frac{1}{5}\right)\alpha\beta^2 w_x w_{xxxx} + \frac{1}{4}\left(\theta^4 + \tfrac{1}{3}\right)\alpha\beta^2 w_{xx} w_{xxx} \\
&+\frac{1}{720}\left(\theta^2 - 1\right)\left(61\theta^4 - 14\theta^2 + 1\right)\beta^3 w_{xxxxxxt} + \mathcal{O}(\alpha^3\beta, \alpha^2\beta^2, \alpha\beta^3, \beta^4) = 0.
\end{aligned}
\tag{2.12}
$$

Note that when $\theta = 0$ in equations (2.12) and (2.10), they reduce to (2.2) and the last equation in (2.4), as expected, since $z = \theta = 0$ gives the horizontal fluid velocity $u(x,t)$ at the bottom $z = -h_0$ (in dimensional variables).

We now want to investigate which values of $\theta \in [0,1]$ give a bounded and positive dispersion relation for the linearized version of system (2.10), (2.12).

Since systems of BBM type are more amenable to numerical integration, we substitute the relation $\beta^3 w_{x^7} = -\beta^3\eta_{x^6t} + \mathcal{O}(\alpha\beta^3, \beta^4)$ in the last term of (2.10) in order to obtain a BBM-type system. (More general systems can be derived from (2.10), (2.12) by introducing other parameters, such as is done for the fifth order system in [1], but since we are mostly

interested in solving these equations numerically, only BBM-type systems are considered here.) The linearized versions of equation (2.10) with the last term replaced, and equation (2.12) in dimensional variables are

$$\eta_t+h_0w_x+\frac{1}{2}\left(\theta^2-\frac{1}{3}\right)h_0^3w_{x^3}+\frac{5}{24}\left(\theta^2-\frac{1}{5}\right)^2h_0^5w_{x^5}-\frac{1}{5040}\left(7\theta^2\left(61\theta^4-25\theta^2+3\right)-1\right)h_0^6\eta_{x^6t}=0 \tag{2.13}$$

$$g\eta_x+w_t+\frac{1}{2}\left(\theta^2-1\right)h_0^2w_{x^2t}+\frac{5}{24}\left(\theta^2-\frac{1}{5}\right)\left(\theta^2-1\right)h_0^4w_{x^4t}+\frac{1}{720}\left(\theta^2-1\right)\left(61\theta^4-14\theta^2+1\right)h_0^6w_{x^6t}=0 \tag{2.14}$$

to order β^4.

Proceeding as with the fifth order system, we seek a solution of the form $\eta = Ae^{ikx-i\omega t}, w = Be^{ikx-i\omega t}$, which gives

$$-\omega\left[1+\tfrac{1}{5040}\left(7\theta^2\left(61\theta^4-25\theta^2+3\right)-1\right)h_0^6k^6\right]A+kh_0\left[1-\tfrac{1}{2}\left(\theta^2-\tfrac{1}{3}\right)k^2h_0^2+\tfrac{5}{24}\left(\theta^2-\tfrac{1}{5}\right)^2k^4h_0^4\right]B=0,$$
$$gkA-\omega\left[1-\tfrac{1}{2}\left(\theta^2-1\right)h_0^2k^2+\tfrac{5}{24}\left(\theta^2-\tfrac{1}{5}\right)\left(\theta^2-1\right)h_0^4k^4-\tfrac{1}{720}\left(\theta^2-1\right)\left(61\theta^4-14\theta^2+1\right)h_0^6k^6\right]B=0.$$

Rewriting this as a matrix equation and requiring that the determinant of the coefficient matrix is zero gives the following dispersion relation

$$\frac{\omega^2}{k^2}=gh_0\frac{f_0(k,\theta)}{f_1(k,\theta)f_2(k,\theta)} \tag{2.15}$$

where

$$f_0(k,\theta)=1-\frac{1}{2}\left(\theta^2-\frac{1}{3}\right)k^2h_0^2+\frac{5}{24}\left(\theta^2-\frac{1}{5}\right)^2h_0^4k^4,$$

$$\begin{aligned}f_1(k,\theta)=&1+\frac{1}{5040}\left(7\theta^2\left(61\theta^4-25\theta^2+3\right)-1\right)h_0^6k^6\\=&1+\frac{1}{5040}\left(427\theta^6-175\theta^4+21\theta^2-1\right)h_0^6k^6,\end{aligned}$$

and

$$f_2(k,\theta)=1-\frac{1}{2}\left(\theta^2-1\right)h_0^2k^2+\frac{5}{24}\left(\theta^2-\frac{1}{5}\right)\left(\theta^2-1\right)h_0^4k^4-\frac{1}{720}\left(\theta^2-1\right)\left(61\theta^4-14\theta^2+1\right)h_0^6k^6.$$

First, note in particular that this dispersion relation becomes singular when $\theta = 0$. Indeed, when $\theta = 0$, eq. (2.15) reduces to

$$\frac{\omega^2}{k^2}=-\frac{30240((kh_0)^4+20(kh_0)^2+120)}{((kh_0)^6-5040)((kh_0)^6+30(kh_0)^4+360(kh_0)^2+720)}. \tag{2.16}$$

One of the real roots of the sixth degree polynomial $(kh_0)^6 - 5040$ in k is $k_1 = \frac{1}{h_0}\sqrt[6]{5040}$. It is easy to check that the limits of the right hand side of (2.16) as $k \to k_1$ from the left and right side are $+\infty$ and $-\infty$, respectively. Hence the dispersion relation (2.16) becomes unbounded for these values of k. This shows why we needed to introduce θ in (2.2) and the last equation in (2.4), since these equations, which model the horizontal fluid velocity $u(x,t)$ at the bottom $z = -h_0$ (in dimensional variables), are not well behaved numerically.

It turns out that the dispersion relation (2.15) is bounded above and positive for all wavenumbers k when $s_0 \leq \theta^2 \leq 1$, where

$$s_0 = \frac{1}{1281}\left(175 + \sqrt[3]{759304 - 71736\sqrt{102}} + 2\sqrt[3]{94913 + 8967\sqrt{102}}\right) \approx 0.2511.$$

To prove this, we first show that $f_1(k,\theta) \geq 1$ for all $\theta^2 \in [s_0, 1], k \in \mathbb{R}$, $h_0 > 0$.

Let $s = \theta^2$ and consider the function

$$p(k,s) = \frac{1}{5040}\left(427s^3 - 175s^2 + 21s - 1\right)k^6h_0^6. \tag{2.17}$$

The discriminant of the cubic polynomial $p_0(s) \coloneqq 427s^3 - 175s^2 + 21s - 1$ appearing in (2.17) is $\Delta_s = -426496 < 0$, so $p_0(s)$ has one real root and two non-real, complex conjugate roots. Its real root can be found from the cubic formula, and it is

$$\theta^2 = s = s_0 = \frac{1}{1281}\left(175 + \sqrt[3]{759304 - 71736\sqrt{102}} + 2\sqrt[3]{94913 + 8967\sqrt{102}}\right) \approx 0.2511.$$

Since $p_0(s=0) = -1 < 0$, and $p_0(s=1) = 272 > 0$, we conclude that $p_0(s) \geq 0$ for $s = \theta^2 \geq s_0$, and $p_0(s) < 0$ for $s = \theta^2 < s_0$. It follows that

$$p(k,s) = \frac{1}{5040}\left(427s^3 - 175s^2 + 21s - 1\right)k^6h_0^6 \geq 0 \tag{2.18}$$

for any $s = \theta^2 \in [s_0, 1]$ and any $k \in \mathbb{R}$, $h_0 > 0$. Now add 1 to both sides of inequality (2.18) to conclude that $f_1(k,\theta) \geq 1$ for any $\theta^2 \in [s_0, 1]$, $k \in \mathbb{R}$, $h_0 > 0$.

Note that if $\theta^2 < s_0$, then $p_0 < 0$ and there exists some $k \in \mathbb{R}$ such that

$$\frac{1}{5040}\left(427\theta^6 - 175\theta^4 + 21\theta^2 - 1\right)k^6h_0^6 = -1$$

and hence $f_1 = 0$. Thus the dispersion relation (2.15) *may* become unbounded for $\theta^2 \in (0, s_0)$.

Next, we show that $f_2(k,\theta) \geq 1$ for all $\theta^2 \in [0,1], k \in \mathbb{R}$. Let $r = h_0^2k^2$. We begin by looking at the sign of the polynomial

$$p_1(r,\theta) = 1 - \frac{5}{12}\left(\theta^2 - \frac{1}{5}\right)r + \frac{1}{360}\left(61\theta^4 - 14\theta^2 + 1\right)r^2. \tag{2.19}$$

Treating p_1 as a quadratic polynomial in r, with coefficients depending on θ, its discriminant is

$$\Delta_r(\theta) = \frac{1}{720}(-363\theta^4 + 62\theta^2 - 3).$$

Note that $61\theta^4 - 14\theta^2 + 1$ has no real roots, so p_1 is always a quadratic polynomial in r. Since $\Delta_r < 0$ for all $\theta \in \mathbb{R}$, it follows that the polynomial (2.19) has no real roots r, for any fixed value of $\theta \in \mathbb{R}$. Moreover, we have $p_1(r,\theta)|_{r=0} = 1 > 0$ for any fixed $\theta \in \mathbb{R}$. Thus the following inequality is true for any fixed $\theta \in \mathbb{R}$ and all $r = (kh_0)^2 \geq 0$

$$p_1(r,\theta) = 1 - \frac{5}{12}\left(\theta^2 - \frac{1}{5}\right) r + \frac{1}{360}\left(61\theta^4 - 14\theta^2 + 1\right) r^2 > 0. \tag{2.20}$$

Now assume $0 \leq \theta^2 < 1$ and $r = (kh_0)^2 > 0$, and multiply both sides of inequality (2.20) by $-\frac{1}{2}(\theta^2 - 1)r > 0$. Then add 1 to both sides to obtain

$$1 - \frac{1}{2}\left(\theta^2 - 1\right) r + \frac{5}{24}\left(\theta^2 - \frac{1}{5}\right)\left(\theta^2 - 1\right) r^2 - \frac{1}{720}\left(\theta^2 - 1\right)\left(61\theta^4 - 14\theta^2 + 1\right) r^3 > 1. \tag{2.21}$$

Inequality (2.21) is true for any fixed $\theta^2 \in [0,1)$ and all $r > 0$. Since $r = (kh_0)^2$, the expression on the left hand side of inequality (2.21) is equal to $f_2(k,\theta)$, and we have shown that $f_2(k,\theta) > 1$ for any fixed $\theta^2 \in [0,1)$ and all $kh_0 \neq 0$. Looking at the expression for $f_2(k,\theta)$, we have $f_2 = 1$ when $kh_0 = 0$ or when $\theta = 1$. Thus, we have shown that $f_2(k,\theta) \geq 1$ for all $k \in \mathbb{R}$, $h_0 > 0$, for any fixed $\theta^2 \in [0,1]$.

In order to prove that the dispersion relation (2.15) is always positive for $\theta^2 \in [s_0, 1]$, $k \in \mathbb{R}$, we need to show that $f_0(k,\theta) > 0$ for such θ, k. Again letting $r = (kh_0)^2$, we have

$$f_0(r,\theta) = 1 - \frac{1}{2}\left(\theta^2 - \frac{1}{3}\right) r + \frac{5}{24}\left(\theta^2 - \frac{1}{5}\right)^2 r^2.$$

The discriminant of the quadratic polynomial $f_0(r,\theta)$ in r is

$$\Delta_r = \frac{1}{180}(-105\theta^4 + 30\theta^2 - 1).$$

Since $\Delta_r < 0$ for $\theta^2 > \frac{1}{105}\left(15 + 2\sqrt{30}\right) \approx 0.2472$, and $\frac{1}{105}\left(15 + 2\sqrt{30}\right) < s_0$, it follows that $f_0(r,\theta)$ has no real roots r for any fixed $\theta^2 \in [s_0, 1]$ (it is obviously also always a quadratic polynomial in r for such θ). Since $f_0(r,\theta)|_{r=0} = 1 > 0$ for any $\theta \in \mathbb{R}$, we have $f_0(k,\theta) > 0$ for any fixed $\theta^2 \in [s_0, 1]$, $k \in \mathbb{R}$, $h_0 > 0$. From the discussion above, we conclude that the dispersion relation (2.15) is positive for any $\theta^2 \in [s_0, 1]$, $k \in \mathbb{R}$ $h_0 > 0$.

Since we have shown that $f_1(k,\theta) \geq 1$ and $f_2(k,\theta) \geq 1$ for all $k \in \mathbb{R}$, $h_0 > 0$ when $\theta^2 \in [s_0, 1]$, the dispersion relation (2.15) has no singularities for these values of θ, k and h_0.

Now fix any $\theta^2 \in [s_0, 1]$. Note that since $1/5 < s_0$, the polynomial in the numerator of (2.15) is always of degree 4 in kh_0, while the expanded polynomial in the denominator of (2.15) is of degree 12 in kh_0, provided $s_0 < \theta^2 < 1$ (it is easy to check that $61\theta^4 - 14\theta^2 + 1$ has no real roots). If $\theta^2 = s_0$ or $\theta^2 = 1$, the expanded polynomial in the denominator is of degree 6 in kh_0. In either case, the polynomial in the denominator is of higher degree in kh_0 than the polynomial in the numerator of (2.15). Thus, for any fixed $\theta^2 \in [s_0, 1]$ the dispersion relation (2.15) remains bounded above as $kh_0 \to \pm\infty$, since the denominator

dominates the numerator for large k, h_0. Hence we have proved the fact that the dispersion relation (2.15) is bounded above and positive for $\theta^2 \in [s_0, 1]$, $k \in \mathbb{R}$ and $h_0 > 0$.

Note that there may exist values of $\theta^2 \in (0, s_0)$ for which the dispersion relation (2.15) is bounded above and positive for all $k \in \mathbb{R}$ as well, but there is no guarantee for this, as there always exist $k \in \mathbb{R}$ such that $f_1 = 0$ for these values of θ. Plotting the dispersion relation for $\theta^2 \in (0, s_0)$ suggests that the dispersion relation is always unbounded for some $k \in \mathbb{R}$ for such θ.

If both sides of the dispersion relation is multiplied by k^2, so that ω^2 is a function of k, the numerator on the right hand side is a polynomial of degree 6 in k, for any $\theta^2 \in [s_0, 1]$. Since the polynomial in the numerator is of degree 12 in kh_0 when $\theta^2 \in (s_0, 1)$, ω^2 will stay bounded for any $\theta^2 \in (s_0, 1)$.

A plot of the dispersion relation (2.15) for $\sqrt{s_0} \leq \theta \leq 1$ is shown in Figure (2.1).

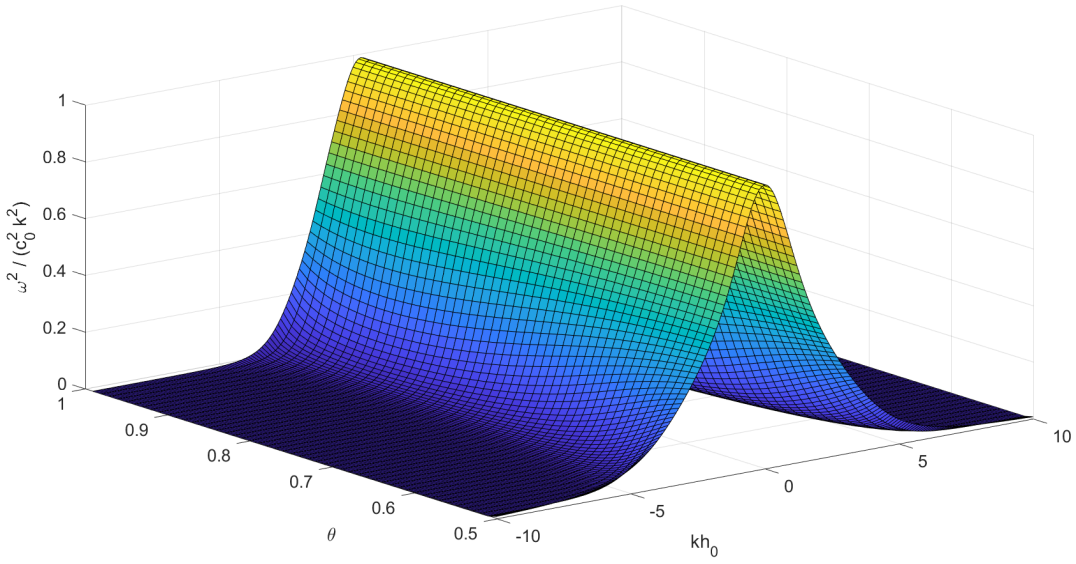

Figure 2.1: Plot of the dispersion relation (2.15) for the linearized seventh order BBM system (2.13), (2.14) for $\sqrt{s_0} \leq \theta \leq 1$

2.2 Seventh order system of pure BBM type

Another interesting equivalent system to consider is when $\frac{\partial^n}{\partial x^n}$ derivatives in the linear terms are replaced by $\frac{\partial^n}{\partial x^{n-1}\partial t}$ derivatives in (2.10), for all $n \geq 3$.

Inserting relations (1.55),(1.56) and (1.57) into (2.10) we obtain

$$\begin{aligned}
&\eta_t + w_x + \alpha\left(\eta w\right)_x - \frac{1}{2}\left(\theta^2 - \frac{1}{3}\right)\beta\eta_{xxt} + \frac{1}{2}\left(\theta^2 - 1\right)\alpha\beta\left(\eta w_{xx}\right)_x \\
&-\frac{1}{2}\left(\theta^2 - \frac{1}{3}\right)\alpha\beta\left(\eta w\right)_{xxx} + \frac{1}{360}\left(15\theta^4 - 30\theta^2 + 7\right)\beta^2\eta_{xxxxt} \\
&-\frac{1}{4}\left(\theta^2 - \frac{1}{3}\right)\left(\theta^2 - 1\right)\alpha\beta^2\left(\eta w_{xx}\right)_{xxx} + \frac{1}{360}\left(15\theta^4 - 30\theta^2 + 7\right)\alpha\beta^2\left(\eta w\right)_{xxxxx} \\
&+\frac{5}{24}\left(\theta^2 - \frac{1}{5}\right)\left(\theta^2 - 1\right)\alpha\beta^2\left(\eta w_{xxxx}\right)_x - \frac{1}{2}\alpha^2\beta\left(\eta^2 w_{xx}\right)_x \\
&-\frac{1}{15120}\left(21\theta^6 - 105\theta^4 + 147\theta^2 - 31\right)\beta^3\eta_{xxxxxxt} + \mathcal{O}(\alpha^3\beta, \alpha^2\beta^2, \alpha\beta^3, \beta^4) = 0
\end{aligned} \tag{2.22}$$

after simplifying.

The system (2.22), (2.12) will be referred to as the seventh order system of pure BBM type.

The linearized version of (2.22) is

$$\begin{aligned}
&\eta_t + w_x - \frac{1}{2}\left(\theta^2 - \frac{1}{3}\right)\beta\eta_{x^2t} + \frac{1}{360}\left(15\theta^4 - 30\theta^2 + 7\right)\beta^2\eta_{x^4t} \\
&-\frac{1}{15120}\left(21\theta^6 - 105\theta^4 + 147\theta^2 - 31\right)\beta^3\eta_{x^6t} + \mathcal{O}(\beta^4) = 0.
\end{aligned} \tag{2.23}$$

The linear system (2.23), (2.14) in dimensional variables leads to the dispersion relation

$$\frac{\omega^2}{k^2} = gh_0\frac{1}{f_2(k,\theta)f_3(k,\theta)} \tag{2.24}$$

where

$$f_3(k,\theta) = 1 + \frac{1}{2}\left(\theta^2 - \frac{1}{3}\right)h_0^2k^2 + \frac{1}{360}\left(15\theta^4 - 30\theta^2 + 7\right)h_0^4k^4 + \frac{1}{15120}\left(21\theta^6 - 105\theta^4 + 147\theta^2 - 31\right)h_0^6k^6 \tag{2.25}$$

and $f_2(k,\theta)$ is as defined in (2.15).

We now investigate which $\theta \in [0,1]$ make the dispersion relation (2.24) bounded and positive. Let $r \in \mathbb{R}$, and consider the polynomial

$$F(r,\theta) = 1 + \frac{1}{2}\left(\theta^2 - \frac{1}{3}\right)r + \frac{1}{360}\left(15\theta^4 - 30\theta^2 + 7\right)r^2 + \frac{1}{15120}\left(21\theta^6 - 105\theta^4 + 147\theta^2 - 31\right)r^3. \tag{2.26}$$

Note that $f_3(k,\theta)$ is equal to $F(r,\theta)$ when r is evaluated at $(kh_0)^2 \geq 0$.

A general cubic polynomial ax^3+bx^2+cx+d has discriminant $\Delta = 18abcd - 4b^3d + b^2c^2 - 4ac^3 - 27a^2d^2$. If $\Delta > 0$, the equation has three distinct real roots. If $\Delta = 0$ then the equation has a multiple root and all its roots are real. If $\Delta < 0$, then the equation has two non-real complex conjugate roots and one real root. If the highest order coefficient a in the cubic polynomial is zero, the discriminant becomes $b^2c^2 - 4b^3d = b^2(c^2-4bd)$, i.e., b^2 times the discriminant of the quadratic polynomial bx^2+cx+d. Thus, if the leading coefficient of a cubic polynomial is zero, its discriminant computed from the formula for a cubic polynomial has the same sign as the discriminant computed from the formula for the discriminant of the quadratic polynomial bx^2+cx+d.

Treating $F(r,\theta)$ in eq. (2.26) as a cubic polynomial in r with coefficients depending on θ, its discriminant is found to be

$$\Delta_r(\theta) = \frac{1}{571536000}\left(-463056\theta^{12} + 3307506\theta^{10} - 4652556\theta^8 + 373806\theta^6 - 400576\theta^4 + 219876\theta^2 - 29017\right). \tag{2.27}$$

We look at the sign of the polynomial

$$\delta_r(\theta) \coloneqq -463056\theta^{12} + 3307506\theta^{10} - 4652556\theta^8 + 373806\theta^6 - 400576\theta^4 + 219876\theta^2 - 29017.$$

To analyze the sign of the 12th degree polynomial $\delta_r(\theta)$ for $\theta \in [0,1]$, we will use Sturm's theorem, which we state below.

Sturm's theorem

The Sturm sequence of a polynomial $P(x)$ of one real variable, with real coefficients is the sequence $S(x) = \{P_0(x), P_1(x), ...\}$ of polynomials $P_0(x), P_1(x), ...$, defined by

$$P_0 = P,\ P_1 = P',\ P_{i+1} = -\mathrm{Rem}(P_{i-1}, P_i)$$

for $i \geq 1$, where P' is the derivative of P and $\mathrm{Rem}(P_{i-1}, P_i)$ is the remainder of the Euclidean division of P_{i-1} by P_i, that is, P_{i+1} satisfies $P_{i-1} = P_iQ_i - P_{i+1}$, where Q_i is the quotient when P_{i-1} is divided by P_i, for $i \geq 1$. The length of the Sturm sequence is at most the degree of P.

The number of sign variations at x_0 of the Sturm sequence is the number of sign changes in the sequence $P_0(x_0), P_1(x_0), P_2(x_0)...$, ignoring zeros. We denote the number of sign variations by $N(x_0)$.

Sturm's theorem states that if P is a square-free polynomial, then the number of real roots of P in the half-open interval $(a,b]$ is $N(a) - N(b)$. Furthermore, if the polynomial P is not square-free, then $N(a) - N(b)$ is the number of real roots of P in $(a,b]$, if neither a nor b is a multiple root of P. Each multiple root of P in (a,b) is counted only once.

For more information on Sturm's theorem, see [13], [14], [15] or [16]. A proof of Sturm's theorem is given in [15], p. 220.

We will use Sturm's theorem to show that $\delta_r(\theta)$ has no real roots in the interval $(0, 1]$. It is easy to check that neither $\theta = 0$ nor $\theta = 1$ are roots of $\delta_r(\theta)$.

The Sturm sequence of $\delta_r(\theta)$ is

$$S(\theta) = \{P_0(\theta), P_1(\theta), ..., P_{12}(\theta)\}, \tag{2.28}$$

where

$$P_0(\theta) = \delta_r(\theta),$$

$$P_1(\theta) = \frac{d}{d\theta}\delta_r(\theta) = -5556660\theta^{11} + 33075000\theta^9 - 37220400\theta^7 + 2242800\theta^5 - 1602300\theta^3 + 439740\theta,$$

$$P_2(\theta) = -55125\theta^{10} + 155085\theta^8 - 18690\theta^6 + 267050\theta^4 - 183225\theta^2 + 29017$$

$$P_3(\theta) = -\frac{8721216\theta^9}{5} + \frac{17668224\theta^7}{5} + 2467584\theta^5 - 244608\theta^3 - \frac{3681216\theta}{25}$$

$$P_4(\theta) = -\frac{4471005\theta^8}{103} + \frac{9957570\theta^6}{103} - \frac{28302400\theta^4}{103} + \frac{18392850\theta^2}{103} - 29017$$

$$P_5(\theta) = \frac{3050496000\theta^7}{869} - \frac{1173932928000\theta^5}{869} + \frac{64480558080\theta^3}{869} - \frac{61969512960\theta}{6083}$$

$$P_6(\theta) = \frac{8334858273\theta^6}{5296} - \frac{851016971700\theta^4}{13240} - \frac{1392804231\theta^2}{26480} + 29017$$

$$P_7(\theta) = \frac{530479676813184000\theta^5}{396898013} - \frac{294967429288089600\theta^3}{396898013} + \frac{4069018121602560\theta}{396898013}$$

$$P_8(\theta) = -\frac{764188238132391170000\theta^4}{328918450405} + \frac{570068606645377420000\theta^2}{328918450405} - 29017$$

$$P_9(\theta) = -\frac{2771462966679627724492800\theta^3}{10916974830462731} + \frac{7031394280275830012992800\theta}{10916974830462731}$$

$$P_{10}(\theta) = -\frac{1474033591703930068482750000\theta^2}{1288812763522892357} + 29017$$

$$P_{11}(\theta) = \frac{1884213974328615096074240000\theta}{49134453056797668949425}$$

$$P_{12}(\theta) = -29017.$$

Note that the greatest common divisor of the polynomials $\delta_r(\theta)$ and $\frac{d}{d\theta}\delta_r(\theta)$ is equal to 1, so the polynomial $\delta_r(\theta)$ is square-free, i.e., it has no repeated roots (see [13]).

Evaluating the Sturm sequence (2.28) at $\theta = 0$ gives

$$\begin{aligned} S(0) =& \{P_0(0), P_1(0), ..., P_{12}(0)\} \\ =& \{-29017, 0, 29017, 0, -29017, 0, 29017, 0, -29017, 0, \\ & 29017, 0, -29017\} \end{aligned} \tag{2.29}$$

and evaluating (2.28) at $\theta = 1$ gives

$$\begin{aligned} S(1) =& \{P_0(1), P_1(1), ..., P_{12}(1)\} \\ =& \Big\{ -353152, -1908480, 194112, \frac{96628224}{25}, \\ & -\frac{7411736}{103}, -\frac{41100518400}{6083}, \frac{1201475893}{1324}, \frac{2762024287411200}{396898013}, \\ & -\frac{5791237964820652}{65783690081}, -\frac{20683235386520447232000}{10916974830462731}, \\ & -\frac{11000587921124923932520 6}{1288812763522892357}, \frac{18842139743286150960742 4}{49134453056797668949425}, -29017\Big\}. \end{aligned} \tag{2.30}$$

Going from left to right in the sequence (2.29), we see that there are six sign changes (ignoring zeros), hence $N(0) = 6$. Likewise, we see that there are six sign changes in (2.30), so $N(1) = 6$. Thus $N(0) - N(1) = 0$, and by Sturm's theorem the polynomial $\delta_r(\theta)$ has no real roots in $(0, 1]$. Moreover, when $\theta = 0$ we have $\delta_r = -29017 < 0$, and since $\Delta_r(\theta) = \frac{1}{571536000}\delta_r(\theta)$, we have shown that $\Delta_r(\theta)$ has no real roots in $[0, 1]$.

Since $\Delta_r(\theta = 0) = -\frac{29017}{571536000} < 0$, we conclude that the discriminant $\Delta_r(\theta) < 0$ for all $\theta \in [0, 1]$.

Note that if $\theta \in [0, 1]$ is chosen such that the coefficient $a(\theta) := \frac{1}{15120}\,(21\theta^6 - 105\theta^4 + 147\theta^2 - 31)$ in front of the cubic term r^3 in (2.26) is zero, then the discriminant $\Delta_r(\theta)$ (eq. (2.27)) computed from the formula for a cubic polynomial has the same sign as the discriminant computed from the formula for a quadratic polynomial. We will show later that $a(\theta)$ has exactly one real root θ in the interval $(0, 1)$, which we denote by $\sqrt{s_1}$. Thus, the quadratic polynomial $F(r, \theta)|_{\theta=\sqrt{s_1}}$ in (2.26) has no real roots r for $\theta = \sqrt{s_1}$, and the fourth degree polynomial $f_3(k, \theta)|_{\theta=\sqrt{s_1}}$ in (2.25) has four non-real roots, and it is positive for all $k \in \mathbb{R}, h_0 > 0$, since $f_3(k = 0, \theta = \sqrt{s_1}) = 1 > 0$.

The fact that $\Delta_r(\theta) < 0$ for all $\theta \in [0, 1]$, implies that the cubic polynomial $F(r, \theta)$ in r, where $r \in \mathbb{R}$, has two non-real roots (complex conjugates), call them r_1 and r_2, and one real root which we denote by r_3, for any fixed $\theta \in [0, 1] \setminus \{\sqrt{s_1}\}$.

The roots of the sixth degree polynomial $f_3(k, \theta)$ in kh_0 (eq. (2.25)), for the same fixed $\theta \in [0, 1] \setminus \{\sqrt{s_1}\}$, are then $k_{1,2} = \frac{1}{h_0}(r_1)^{\frac{1}{2}}$, $k_{3,4} = \frac{1}{h_0}(r_2)^{\frac{1}{2}}$, $k_{5,6} = \pm\frac{1}{h_0}\sqrt{r_3}$, where $(r_1)^{\frac{1}{2}}$ and $(r_2)^{\frac{1}{2}}$ both denote double valued square roots of the non-real numbers r_1 and r_2. Since the n-th root of a non-real number is always non-real, we always have

$k_{1,2,3,4} \in \mathbb{C} \setminus \mathbb{R}$. If $r_3 < 0$, then all 6 roots $k_{1,2,3,4,5,6}$ of $f_3(k,\theta)$ are non-real, and the dispersion relation has no singularities for any $k \in \mathbb{R}$, and it remains bounded above for all k. Since $f_2(k,\theta) \geq 1, f_3(k,\theta) > 0$ for all such θ and for all $k \in \mathbb{R}, h_0 > 0$, the dispersion relation is also positive for all such k, h_0, θ. If $r_3 \geq 0$, then $k_{5,6} \in \mathbb{R}$ and the dispersion relation becomes singular at these values of k.

Thus, in order to determine which values of θ give a bounded and positive dispersion relation (2.24), we need to investigate which choices of $\theta \in [0,1] \setminus \left\{\sqrt{s_1}\right\}$ give $r_3 < 0$. For this we will use *Descartes' rule of signs* on the cubic polynomial $F(r,\theta)$. (See $\star$ below for an alternative proof without using Descartes' rule of signs.)

Descartes' rule of signs states that if the terms of a single-variable polynomial $p(x)$ with real coefficients are ordered by descending variable exponent, then the number of positive roots of $p(x)$ is either equal to the number of sign differences between consecutive nonzero coefficients, or is less than it by a positive, even integer. Multiple roots are counted separately.

The number of negative roots of $p(x)$ can be found by substituting $x \mapsto -x$ in $p(x)$, and counting the number of positive roots using Descartes' rule of signs on the polynomial $p(-x)$.

For more information on Descartes' rule of signs, see [13], [16].

To apply Descartes' rule of signs on $F(r,\theta)$, where $r \in \mathbb{R}$, it will be treated as a single variable cubic polynomial in r, with coefficients depending on θ.

Write

$$F(r,\theta) = a(\theta)r^3 + b(\theta)r^2 + c(\theta)r + 1 \tag{2.31}$$

where $a(\theta) = \frac{1}{15120}\left(21\theta^6 - 105\theta^4 + 147\theta^2 - 31\right)$, $b(\theta) = \frac{1}{360}\left(15\theta^4 - 30\theta^2 + 7\right)$, $c(\theta) = \frac{1}{2}\left(\theta^2 - \frac{1}{3}\right)$, and $r \in \mathbb{R}$.

First note that $a(\theta)$ is a cubic polynomial in $s \coloneqq \theta^2$, and its roots can be found from the cubic formula. Its only real root is $s_1 = \theta^2 = \frac{1}{3}\left(5 - 2\sqrt[3]{\frac{1}{7}(11 - 6\sqrt{2})} - 2\sqrt[3]{\frac{1}{7}(11 + 6\sqrt{2})}\right) \approx 0.2549$ (the discriminant of $a(s)$ treated as a cubic polynomial in $s = \theta^2$ is $\Delta_s = -\frac{1}{19289340000} < 0$, by the same formula used above for calculating $\Delta_r(\theta)$, so it has only one real root, which must be s_1). Furthermore, we have $a(s=1) = \frac{2}{945} > 0$ and $a(s=0) = -\frac{31}{15120} < 0$, so $a(\theta) > 0$ for $\theta^2 > s_1$, and $a(\theta) < 0$ for $\theta^2 < s_1$.

Next, the roots of $b(s)$ are found to be $s_2 = \theta^2 = 1 - 2\sqrt{\frac{2}{15}} \approx 0.26970$, and $s_3 = \theta^2 = 1 + 2\sqrt{\frac{2}{15}} \approx 1.7303$, where $s = \theta^2$ as before. Since $b(s=1) = -\frac{1}{45} < 0$ and $b(s=0) = \frac{7}{360} > 0$, we have $b(\theta) > 0$ for $s = \theta^2 < s_2$ and $b(\theta) < 0$ for $s_2 < s = \theta^2 \leq 1$.

It is obvious that $r = 0$ is not a root of (2.31), so the only possibilities are $r > 0$ and $r < 0$.

First consider the case when $\frac{1}{3} < \theta^2 \leq 1$. Then $c(\theta) > 0$, $a(\theta) > 0$ and $b(\theta) < 0$, so we can write $F(r,\theta) = +a(\theta)r^3 - |b(\theta)|r^2 + c(\theta)r + 1$. Going from left to right in this polynomial, we see that there is a total of two sign changes between each coefficient. This

implies that $F(r,\theta)$ has either two positive, real roots r, or zero positive, real roots r, for any fixed $\theta^2 \in \left(\frac{1}{3}, 1\right]$. Since we already know that $F(r,\theta)$ has two non-real roots and one real root from the discussion above, we can conclude that $F(r,\theta)$ has zero real, positive roots, and one negative real root. (This can also be verified by substituting $r \mapsto -r$ and counting the number of positive roots of $F(-r,\theta)$, which shows that $F(r,\theta)$ has exactly one negative real root.) Thus, for any fixed $\theta^2 \in \left(\frac{1}{3}, 1\right]$, the sixth degree polynomial $f_3(k,\theta)$ has only non-real roots, and the dispersion relation is non-singular. The dispersion relation (2.24) is bounded above and positive for these values of θ.

Next, consider the case $s_2 < \theta^2 < \frac{1}{3}$. Then $b(\theta) < 0, a(\theta) > 0$, and $c(\theta) < 0$, so we can write $F(r,\theta) = +a(\theta)r^3 - |b(\theta)|r^2 - |c(\theta)|r + 1$. There are again two sign changes in this equation, so Descartes' rule of signs implies, by the same argument used above, that $F(r,\theta)$ has zero positive roots, and thus must have one negative root. Thus the dispersion relation (2.24) is bounded above and positive for $s_2 < \theta^2 < \frac{1}{3}$ as well.

The next case to consider is $s_1 < \theta^2 < s_2$. Then we have $b(\theta) > 0, a(\theta) > 0, c(\theta) < 0$, so $F(r,\theta) = +a(\theta)r^3 + b(\theta)r^2 - |c(\theta)|r + 1$. By Descartes' rule of signs and the same arguments as above, since there are two sign changes, we again conclude that the dispersion relation (2.24) is bounded above and positive $s_1 < \theta^2 < s_2$ as well.

The final interval to investigate is $0 \leq \theta^2 < s_1$. For such θ^2, we have $a(\theta) < 0, b(\theta) > 0$, and $c(\theta) < 0$. Thus we can write $F(r,\theta) = -|a(\theta)|r^3 + b(\theta)r^2 - |c(\theta)|r + 1$. Here there are three sign changes, which means that $F(r,\theta)$ has either three positive roots, or one positive root, by Descartes' rule of signs. Again, since we already know that $F(r,\theta)$ has two non-real roots and one real root, we can conclude that $F(r,\theta)$ has one positive real root r_3 for $0 \leq \theta^2 < s_1$. This means that the sixth degree polynomial $f_3(k,\theta)$ in kh_0 has two real roots $k_{5,6} = \pm\frac{1}{h_0}\sqrt{r_3}$ for such θ^2, and the dispersion relation becomes singular at these values of k. The dispersion relation (2.24) is thus not bounded for all k when $0 \leq \theta^2 < s_1$.

Finally, we look at the cases $\theta^2 = \frac{1}{3}$, and $\theta^2 = s_2$. When $\theta^2 = \frac{1}{3}$, we have $b(\theta) < 0$, $a(\theta) > 0$ and $c(\theta) = 0$, so $F(r,\theta) = +a(\theta)r^3 - |b(\theta)|r^2 + 1$. Here there are again two sign changes, so we conclude by the same arguments as above that the dispersion relation (2.24) is bounded above and positive for $\theta^2 = \frac{1}{3}$.

When $\theta^2 = s_2$, we have $b(\theta) = 0$, $a(\theta) > 0$ and $c(\theta) < 0$, and so $F(r,\theta) = +a(\theta)r^3 - |c(\theta)|r + 1$. Again, there are two sign changes, so the dispersion relation (2.24) is bounded above and positive for $\theta^2 = s_2$.

For the final case $\theta^2 = s_1$, we know from above that the fourth degree polynomial $f_3(k,\theta)|_{\theta^2=s_1}$ is always positive, hence (2.24) is bounded above and positive.

To summarize, we have shown that

- Given any fixed $\theta \in [0,1] \setminus \left\{\sqrt{s_1}\right\}$, the cubic polynomial $F(r,\theta)$ in $r \in \mathbb{R}$ (eq. (2.26)), with coefficients depending on θ, has two non-real roots r_1 and r_2, and one real root r_3 (by Sturm's theorem). If $\theta = \sqrt{s_1}$, the quadratic polynomial $F(r,\theta)|_{\theta=\sqrt{s_1}}$ has two non-real roots.

- Given any fixed $\theta^2 \in (s_1, 1]$, the cubic polynomial $F(r,\theta)$ in r has two non-real roots

$r_1 = |r_1|e^{i\phi_1}$ and $r_2 = |r_2|e^{i\phi_2}$, where $\phi_1, \phi_2 \neq j\pi$, $j \in \mathbb{Z}$ are the arguments of r_1 and r_2, and one negative real root $r_3 = -|r_3|$ (by Descartes' rule of signs).

For such a fixed $\theta^2 \in (s_1, 1]$, the sixth degree polynomial $f_3(k,\theta)$ (eq. (2.25)) in kh_0 has six non-real roots given by $k_{1,2} = \pm\frac{1}{h_0}\sqrt{|r_1|}e^{i\phi_1/2}$, $k_{3,4} = \pm\frac{1}{h_0}\sqrt{|r_2|}e^{i\phi_2/2}$ and $k_{5,6} = \pm\frac{1}{h_0}\sqrt{|r_3|}i$. When $\theta^2 = s_1$, the fourth degree polynomial $f_3(k,\theta)|_{\theta^2=s_1}$ in (2.25) is always positive, as discussed above.

- Since $f_3(k,\theta)|_{k=0} = 1 > 0$, for any fixed $\theta^2 \in [s_1, 1]$, and it has no real roots for such θ, we have $f_3(k,\theta) > 0$ for all $k \in \mathbb{R}$, $h_0 > 0$, for any fixed $\theta^2 \in [s_1, 1]$.

From the above discussion, and the fact that $f_2(k,\theta) \geq 1$ for all $\theta^2 \in [0,1]$ and all $k \in \mathbb{R}$, $h_0 > 0$, we conclude that the dispersion relation (2.24) for the linearized seventh order pure BBM system is bounded above and positive for

$$0.2549 \approx \frac{1}{3}\left(5 - 2\sqrt[3]{\frac{1}{7}(11-6\sqrt{2})} - 2\sqrt[3]{\frac{1}{7}(11+6\sqrt{2})}\right) = s_1 \leq \theta^2 \leq 1.$$

⋆ ALTERNATIVE PROOF:
For any polynomial $P(x)$ of odd degree we have

$$\lim_{x\to\infty} P(x) = \begin{cases} +\infty \text{ if } C > 0, \\ -\infty \text{ if } C < 0, \end{cases} \tag{2.32}$$

and

$$\lim_{x\to-\infty} P(x) = \begin{cases} -\infty \text{ if } C > 0, \\ +\infty \text{ if } C < 0, \end{cases} \tag{2.33}$$

where $C \in \mathbb{R}$ is the coefficient of the highest power in x of the polynomial $P(x)$. From (2.32), (2.33), the fact that the cubic polynomial $F(r,\theta)$ has exactly one real root r_3 for any fixed $\theta \in [0,1] \setminus \left\{\sqrt{s_1}\right\}$, and that $F(r,\theta)$ must pass through the point $F(r,\theta)|_{r=0} = 1$, it is clear that $F(r,\theta)$ has a negative root r_3 if and only if the highest order coefficient $a(\theta) = \frac{1}{15120}\left(21\theta^6 - 105\theta^4 + 147\theta^2 - 31\right) > 0$. (If $a(\theta) = 0$, i.e. $\theta = \sqrt{s_1}$, then $F(r,\theta)$ becomes a quadratic polynomial in r which has no real roots, so the fourth degree polynomial $f_3(k,\theta)|_{\theta=\sqrt{s_1}}$ in (2.25) is positive for all $k \in \mathbb{R}$ for $\theta = \sqrt{s_1}$ (see the discussion below eq. (2.30)).)

Note that $a(\theta)$ is a cubic polynomial in $s := \theta^2$, and its roots can be found from the cubic formula. Its only real root is $s_1 = \theta^2 = \frac{1}{3}\left(5 - 2\sqrt[3]{\frac{1}{7}(11-6\sqrt{2})} - 2\sqrt[3]{\frac{1}{7}(11+6\sqrt{2})}\right) \approx 0.2549$ (the discriminant of $a(s)$ treated as a cubic polynomial in $s = \theta^2$ is $\Delta_s = -\frac{1}{19289340000} < 0$, by the same formula used above for calculating $\Delta_r(\theta)$, so it has only one real root, which must be s_1). Furthermore, we have $a(s=1) = \frac{2}{945} > 0$ and $a(s=0) = -\frac{31}{15120} < 0$, so

$a(\theta) > 0$ for $\theta^2 > s_1$, and $a(\theta) < 0$ for $\theta^2 < s_1$. Hence, for any fixed $\theta^2 \in (s_1, 1]$, $F(r, \theta)$ has one negative real root $r_3 = -|r_3|$ and two non-real roots $r_1 = |r_1|e^{i\phi_1}$ and $r_2 = |r_2|e^{i\phi_2}$, where $\phi_1, \phi_2 \neq j\pi$, $j \in \mathbb{Z}$ are the arguments of r_1 and r_2.

For such a fixed $\theta^2 \in (s_1, 1]$, the sixth degree polynomial $f_3(k, \theta)$ (eq. (2.25)) in kh_0 has six non-real roots given by $k_{1,2} = \pm\frac{1}{h_0}\sqrt{|r_1|}e^{i\phi_1/2}$, $k_{3,4} = \pm\frac{1}{h_0}\sqrt{|r_2|}e^{i\phi_2/2}$ and $k_{5,6} = \pm\frac{1}{h_0}\sqrt{|r_3|}i$.

Since $f_3(k, \theta)|_{k=0} = 1 > 0$, for any fixed $\theta^2 \in [s_1, 1]$, and it has no real roots for such θ, we have $f_3(k, \theta) > 0$ for all $k \in \mathbb{R}$, $h_0 > 0$, for any fixed $\theta^2 \in [s_1, 1]$.

The alternative proof is obviously much less work, but we include both versions to illustrate the usefulness of Descartes' rule of signs, which can be employed to study more complicated dispersion relations, for example for even higher order systems.

The dispersion relation (2.24) for the linearized seventh order system of pure BBM-type is shown in Figure (2.2) below.

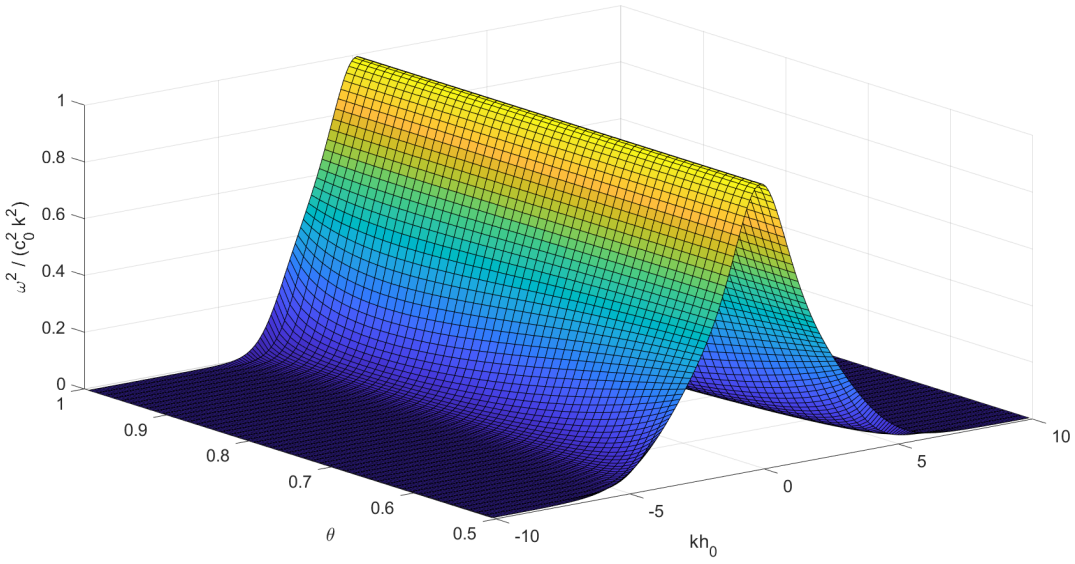

Figure 2.2: Plot of the dispersion relation (2.24) for the linearized seventh order system of pure BBM-type for $\sqrt{s_1} \leq \theta \leq 1$.

2.3 Comparison of dispersion relations

In this section, we compare dispersion relations for the third, fifth and seventh order BBM - type systems, for different values of θ, with the dispersion relation for the full water wave problem eq. (1.30).

First note that the dispersion relation for the full water wave problem (1.30) may be rewritten as

$$\frac{\omega^2}{k^2} = \frac{gh_0}{kh_0}\tanh(kh_0) = c_0^2\frac{\tanh(kh_0)}{kh_0}. \tag{2.34}$$

The lower order pure BBM type systems can be derived from the seventh order equations.

Collecting terms of order $\alpha\beta$ and order β^2 in (2.10) and (2.12) and writing $\mathcal{O}(\alpha\beta, \beta^2)$ in place of those terms, we obtain the widely studied third order Boussinesq system

$$\eta_t + w_x + \alpha\left(\eta w\right)_x + \frac{1}{2}\left(\theta^2 - \tfrac{1}{3}\right)\beta w_{xxx} + \mathcal{O}(\alpha\beta, \beta^2) = 0, \tag{2.35}$$

$$\eta_x + w_t + \alpha w w_x + \frac{1}{2}\left(\theta^2 - 1\right)\beta w_{xxt} + \mathcal{O}(\alpha\beta, \beta^2) = 0. \tag{2.36}$$

Now replace the βw_{xxx} term in (2.35) using relation (1.53) to obtain the well known 3rd order system of pure BBM - type

$$\eta_t + w_x + \alpha\left(\eta w\right)_x - \frac{1}{2}\left(\theta^2 - \tfrac{1}{3}\right)\beta\eta_{xxt} + \mathcal{O}(\alpha\beta, \beta^2) = 0, \tag{2.37}$$

$$\eta_x + w_t + \alpha w w_x + \frac{1}{2}\left(\theta^2 - 1\right)\beta w_{xxt} + \mathcal{O}(\alpha\beta, \beta^2) = 0. \tag{2.38}$$

Its dispersion relation is

$$\frac{\omega^2}{k^2} = gh_0\frac{1}{\left(1 + \left(\theta^2 - \frac{1}{3}\right)k^2h_0^2\right)\left(1 - \frac{1}{2}\left(\theta^2 - 1\right)k^2h_0^2\right)}. \tag{2.39}$$

From (2.39) we see that $1 - \frac{1}{2}\left(\theta^2 - 1\right)k^2h_0^2 \geq 1$ for all $\theta \in [0, 1]$, $k \in \mathbb{R}$, $h_0 > 0$, and that $1 + \left(\theta^2 - \frac{1}{3}\right)k^2h_0^2 \geq 1$ if $\theta^2 \in [\frac{1}{3}, 1]$, $k \in \mathbb{R}$, $h_0 > 0$. If $\theta^2 \in \left[0, \frac{1}{3}\right)$, then there always exists some $k \in \mathbb{R}$ such that $1 + \left(\theta^2 - \frac{1}{3}\right)k^2h_0^2 = 0$ and the dispersion relation (2.39) becomes singular for these values of θ. Hence the dispersion relation (2.39) is bounded above and positive for $\theta^2 \in \left[\frac{1}{3}, 1\right]$, $k \in \mathbb{R}$, $h_0 > 0$. This was also discussed in [10].

The linearized seventh order Boussinesq system (2.10), (2.12) with no terms/derivatives replaced has dispersion relation

$$\frac{\omega^2}{k^2} = gh_0\frac{f_4(k,\theta)}{f_2(k,\theta)} \tag{2.40}$$

where

$$\begin{aligned} f_4(k,\theta) =& 1-\frac{1}{2}\left(\theta^2-\frac{1}{3}\right)(kh_0)^2+\frac{5}{24}\left(\theta^2-\frac{1}{5}\right)^2(kh_0)^4-\frac{1}{5040}\left(7\theta^2\left(61\theta^4-25\theta^2+3\right)\right)-1\Big)(kh_0)^6 \\ =& 1-f_1(k,\theta)+f_0(k,\theta) \end{aligned}$$

and $f_2(k,\theta)$ is as defined in (2.15).
When $\theta = 11/25$ this becomes

$$\frac{\omega^2}{k^2} = gh_0\frac{6029083(kh_0)^6+656250(kh_0)^4+5373046875(kh_0)^2+76904296875}{63\left(84\left(9374(kh_0)^4+15625(kh_0)^2+5859375\right)(kh_0)^2+1220703125\right)}, \tag{2.41}$$

which is always positive, and the denominator obviously has no real roots.

Since the fifth order BBM-type system where only the w_{xxxxx} term is replaced by $-\eta_{xxxxt}$ has an unbounded dispersion relation for all $\theta^2 \neq 1/5$ (as discussed earlier), and the fifth order system reduces to a third order system that is not of BBM-type when the value $\theta^2 = 1/5$ is chosen, we only look at the fifth order system of pure BBM type instead. The fifth order system of pure BBM type can be obtained by neglecting terms of $\mathcal{O}(\alpha^2\beta, \alpha\beta^2, \beta^3)$ in the seventh order pure BBM system. The linearized fifth order system of pure BBM type is then obtained as

$$\eta_t + w_x - \frac{1}{2}\left(\theta^2-\frac{1}{3}\right)\beta\eta_{xxt} + \frac{1}{360}\left(15\theta^4-30\theta^2+7\right)\beta^2\eta_{xxxxt} + \mathcal{O}(\beta^3) = 0 \tag{2.42}$$

$$\eta_x + w_t + \frac{1}{2}\left(\theta^2-1\right)\beta w_{xxt} + \frac{5}{24}\left(\theta^2-1\right)\left(\theta^2-\frac{1}{5}\right)\beta^2 w_{xxxxt} + \mathcal{O}(\beta^3) = 0. \tag{2.43}$$

Its dispersion relation is

$$\frac{\omega^2}{k^2} = gh_0\frac{1}{g_1(k,\theta)g_2(k,\theta)} \tag{2.44}$$

Where

$$g_1(k,\theta) = 1+\frac{1}{2}\left(\theta^2-\frac{1}{3}\right)(kh_0)^2+\frac{1}{360}\left(15\theta^4-30\theta^2+7\right)(kh_0)^4$$

$$g_2(k,\theta) = 1-\frac{1}{2}(\theta^2-1)(kh_0)^2+\frac{5}{24}\left(\theta^2-1\right)\left(\theta^2-\frac{1}{5}\right)(kh_0)^4$$

It can be shown that this dispersion relation is bounded and positive for $\theta^2 \in [0, 1/5]$.

The choice of θ plays a large role in how the dispersion relations look. For instance, looking at the dispersion relation (2.24) for the seventh order pure BBM-type system, we see that the magnitude of the coefficient in front of the highest degree $k^{12}h_0^{12}$ in the

expanded denominator determines how rapidly the dispersion relation approaches zero as kh_0 becomes large. If the coeffient in front of the highest order term $k^{12}h_0^{12}$ in the dispersion relation is as small as possible, then the dispersion relation will remain closer to the dispersion relation for the full water wave problem as kh_0 gets larger. The dispersion relation (2.15) has a term in the numerator which balances out the denominator, and hence this dispersion relation will remain closer to the dispersion relation for the full water wave problem as kh_0 gets larger. For the dispersion relation (2.40) the situation appears to be even better, since unless $\theta = \sqrt{s_0}$ or $\theta = 1$, this dispersion relation has sixth degree polynomials in kh_0 in both the denominator and the numerator. Thus, this dispersion relation will remain much closer to $\frac{\tanh(kh_0)}{kh_0}$ than the other dispersion relations as kh_0 gets large. In some cases, these dispersion relations remain close to the full water wave dispersion relation for relatively large kh_0, but they approach zero too slowly (or never approach zero at all) as kh_0 grows larger and thus diverges from the curve for $\frac{\tanh(kh_0)}{kh_0}$ for such kh_0, which is not physically correct, and can cause problems numerically as there is no control over the phase velocity or the group velocity of the finer scale components, as was argued in [12]. The system (2.10), (2.12) is also not a BBM-type system, so it is more difficult to treat numerically. From the grid lines in Figures (2.1) and (2.2) it appears that values of θ chosen closer to the endpoints of the intervals in which the dispersion relation is bounded and positive yield a closer approximation to the dispersion relation for the full water wave problem, as the dispersion relations have larger magnitudes for values of θ close to the endpoints. It must be noted that if one of the endpoints is chosen as the value of θ, then one of the highest degree terms in the seventh order systems drop out. This is also true for the fifth and third order systems.

Plots of various dispersion relations for the different systems are shown in Figure (2.3). As expected, the dispersion relation (2.40) for the seventh order Boussinesq system (2.10), (2.12) with $\theta = 11/25$, indicated by a blue line, remains closest to $\frac{\tanh(kh_0)}{kh_0}$ (indicated by a black line) in the interval shown in the figure. However, since this dispersion relation does not approach zero as $kh_0 \to \pm\infty$ (it in fact approaches $6029083/49607208 \approx 0.12$), it eventually intersects the full dispersion relation at around $|kh_0| \approx 7.5$, and remains above the full dispersion relation $\frac{\tanh(kh_0)}{kh_0}$ (which approaches zero as $kh_0 \to \pm\infty$) for all $|kh_0|$ greater than ≈ 7.5. One might try other values of θ to find a dispersion relation that remains closer for a larger interval of kh_0, and gets closer to zero for large kh_0. All other dispersion relations shown in Figure (2.24) approach zero as $kh_0 \to \pm\infty$. In general, it appears that the dispersion relations for the seventh order BBM-type systems always stay closer to $\frac{\tanh(kh_0)}{kh_0}$ for small kh_0 than the lower order BBM-type systems, at least as long as similar values of θ are chosen for the different order systems. That is, if we compare the dispersion relation for the seventh order pure BBM-type system with the dispersion relation for the fifth order pure BBM-type system, and we choose a value of θ in the interval $\theta^2 \in [s_1, 1]$ that is close to the endpoints (such that the dispersion relation has the largest magnitude as kh_0 increases), and also choose a θ^2 close to the endpoints of the interval for which the fifth order pure BBM-type system has a bounded and positive dispersion relation (such that this dispersion relation has the largest magnitude as well), then the

dispersion relations for the seventh order system remains closer to $\frac{\tanh(kh_0)}{kh_0}$ than the fifth order dispersion relation does. This is indicated in Figure (2.24), where the dispersion relation (2.24) for the seventh order pure BBM-type system with $\theta = 0.52$ (indicated by a green line) is compared to the dispersion relation for the linearized fifth order pure BBM-type system (2.44) with $\theta = \sqrt{1/6}$ (indicated by a yellow line). The red line shows the dispersion relation (2.15) for the linearized seventh order BBM-type system with $\theta = 0.52$, and as expected, this dispersion relation remains closer to $\frac{\tanh(kh_0)}{kh_0}$ for all kh_0 due to the term $f_0(k,\theta)$ in the numerator balancing out the 12th degree polynomial $f_1(k,\theta)f_2(k,\theta)$ in the denominator. Finally, the purple line shows the dispersion relation (2.39) for the third order pure BBM-type system with $\theta = 0.95$. As can be seen from the figure, the fifth and seventh order BBM-type dispersion stay much closer to $\frac{\tanh(kh_0)}{kh_0}$ for small kh_0, but as $|kh_0| \to 4$, the seventh order and fifth order dispersion relations actually intersect the third order dispersion relation and remain (very) slightly below the third order dispersion relation for large kh_0. This is expected, due to the higher degree polynomials in the denominators of the seventh and fifth order pure BBM-type dispersion relations, which cause more rapid decay as kh_0 increases.

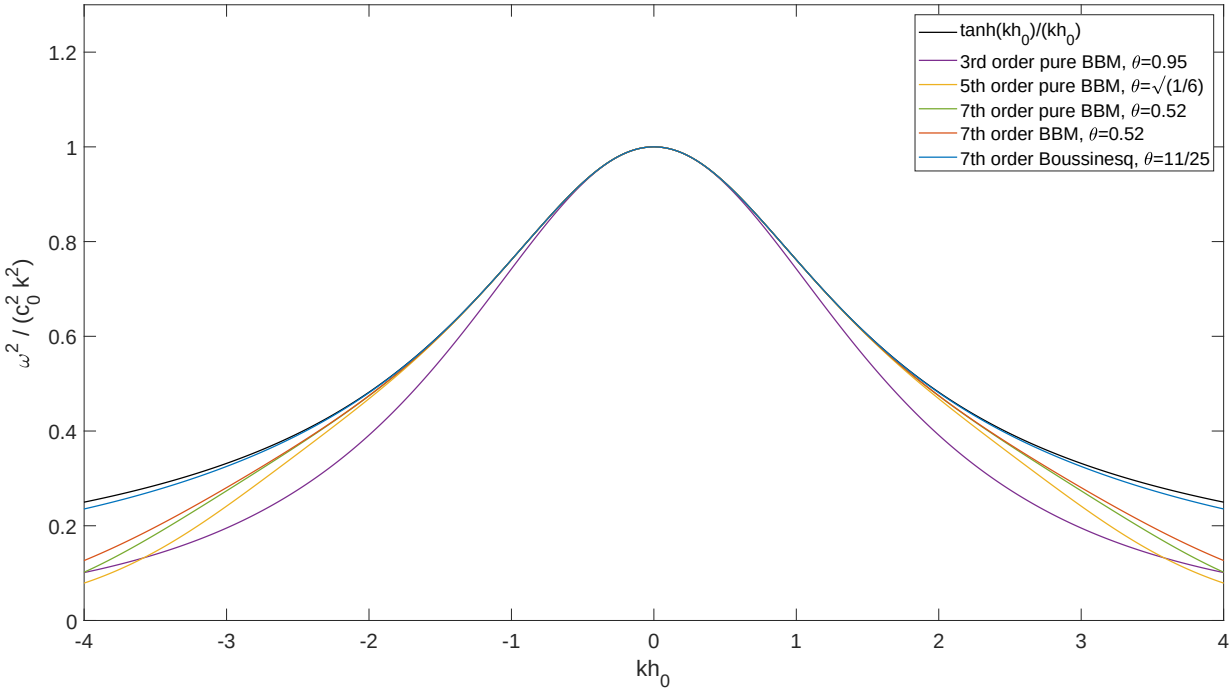

Figure 2.3: Comparison of the dispersion relation (2.24) for the linearized seventh order system of pure BBM-type with $\theta = 0.52$, the dispersion relation (2.15) for the linearized seventh order BBM system with $\theta = 0.52$, the dispersion relation (2.41) for the seventh order Boussinesq system (with no terms replaced) ($\theta = 11/25$), the dispersion relation for the linearized fifth order pure BBM system with $\theta = \sqrt{1/6}$, the dispersion relation for the linearized third order BBM system with $\theta = 0.95$, and the dispersion relation for the full water wave problem (2.34).

Chapter 3

Numerical experiments

In this chapter we solve the seventh order systems numerically, using various initial conditions, to illustrate the behaviour of the equations. To solve the equations numerically, we use Fourier collocation methods with periodic boundary conditions on the domain $[0, L]$. The equations are discretized using the discrete Fourier transform, and the resulting systems of ordinary differential equations are solved numerically using a fourth order Runge-Kutta method. The numerical scheme is implemented in MATLAB. A similar method was used in [7] for a single equation, here we will do the same for a system of two equations. This chapter is only meant as a brief illustration of the behaviour of the various BBM-type systems, for more in depth information on spectral collocation methods, refer to [9].

3.1 Third order pure BBM-type system, convergence tests

We begin by verifying that the numerical scheme converges for the third order pure BBM system, which has exact solitary wave solutions. The L^2 norm is used to measure the error between the numerical solution and the exact solution.

We use the discrete L^2 norm, as used in [7], defined as

$$||\mathbf{v}||_{L^2} = \sqrt{\frac{1}{N}\sum_{j=1}^{N} |v(x_j)|^2}$$

so that the relative L^2 error is

$$\frac{||\mathbf{v} - \mathbf{v}_N||_{L^2}}{||\mathbf{v}||_{L^2}}, \tag{3.1}$$

where $\mathbf{v}_N(x_j)$, $j = 1, 2, ..., N$, is the numerically approximated solution at a time t, and $\mathbf{v}(x_j)$ is the exact solution for $j = 1, 2, ..., N$ at a time t.

We test convergence with the third order pure BBM type system (2.37), (2.38) in dimensional variables, with $\theta = \sqrt{7/9}$.

This system features exact solitary wave solutions, originally derived in [8], given by

$$\begin{aligned} \eta(x,t) &= A_0 \operatorname{sech}^2\left(\lambda\left(x - x_0 - C_s t\right)\right) \\ w(x,t) &= W_0 \operatorname{sech}^2\left(\lambda\left(x - x_0 - C_s t\right)\right) \end{aligned} \tag{3.2}$$

where

$$W_0 = \sqrt{\frac{3g}{A_0 + 3h_0}} A_0, \quad C_s = \frac{3h_0 + 2A_0}{\sqrt{3h_0\left(A_0 + 3h_0\right)}}\sqrt{gh_0}, \quad \lambda = \frac{3}{2h_0}\sqrt{\frac{A_0}{2A_0 + 3h_0}},$$

h_0 is the undisturbed depth, g is the gravitational acceleration, and A_0 is the amplitude of the solitary wave (see also [10] or [5]).

The problem in dimensional variables is then

$$\eta_t + h_0 w_x + \left(\eta w\right)_x - \frac{1}{2}\left(\theta^2 - \tfrac{1}{3}\right) h_0^2 \eta_{xxt} = 0, \tag{3.3}$$

$$g\eta_x + w_t + \frac{1}{2}\left(w^2\right)_x + \frac{1}{2}\left(\theta^2 - 1\right) h_0^2 w_{xxt} = 0, \tag{3.4}$$

to $\mathcal{O}(\alpha\beta, \beta^2)$, where $x \in (0, L)$ and $t > 0$, and we use (3.2) as initial condition, $\theta = \sqrt{7/9}$.

Since we are assuming periodic boundary conditions on the domain $[0, L]$, we first translate the interval $[0, L]$ into $[0, 2\pi]$ before taking the Fourier transform of the equations. This is done by introducing the change of variables $x \mapsto ax$, where $a = \frac{L}{2\pi}$, and defining $\xi(x,t) = \eta(ax,t)$, $v(x,t) = w(ax,t)$. This implies from the chain rule that $\frac{\partial}{\partial x} \mapsto \frac{1}{a}\frac{\partial}{\partial x}$. With this change of variables the system (3.3), (3.4) becomes

$$a^2 \xi_t(x,t) + a h_0 v_x(x,t) + a\left(\xi(x,t) v(x,t)\right)_x - \frac{1}{2}\left(\theta^2 - \tfrac{1}{3}\right) h_0^2 \xi_{xxt}(x,t) = 0, \tag{3.5}$$

$$ag\xi_x(x,t) + a^2 v_t(x,t) + \frac{a}{2}\left(v^2(x,t)\right)_x + \frac{1}{2}\left(\theta^2 - 1\right) h_0^2 v_{xxt}(x,t) = 0, \tag{3.6}$$

for $x \in [0, 2\pi]$, $t \geq 0$.

Taking the Fourier transform in the spatial variable x of equations (3.5), (3.6) yields

$$a^2 \hat{\xi}_t(k,t) + a h_0 i k \hat{v}(k,t) + aik\widehat{(\xi v)}(k,t) + \frac{1}{2}\left(\theta^2 - \tfrac{1}{3}\right) h_0^2 k^2 \hat{\xi}_t(k,t) = 0, \tag{3.7}$$

for $t > 0$ with $\hat{\xi}(k, t=0) = \mathcal{F}(\xi(x,0))$, and

$$agik\hat{\xi}(k,t) + a^2 \hat{v}_t(k,t) + \frac{a}{2} ik\widehat{(v^2)}(k,t) - \frac{1}{2}\left(\theta^2 - 1\right) h_0^2 k^2 \hat{v}_t(k,t) = 0. \tag{3.8}$$

for $t > 0$ with $\hat{\xi}(k, t=0) = \mathcal{F}(\xi(x,0))$, and

These equations may be rewritten as

$$\hat{\xi}_t(k,t) = -\frac{ik}{a\left(1+\frac{1}{2}\left(\theta^2-\frac{1}{3}\right)h_0^2k^2/a^2\right)}\left(h_0\hat{v}(k,t)+\widehat{(\xi v)}(k,t)\right), \tag{3.9}$$

$$\hat{v}_t(k,t) = -\frac{ik}{a\left(1-\frac{1}{2}\left(\theta^2-1\right)h_0^2k^2/a^2\right)}\left(g\hat{\xi}(k,t)+\frac{1}{2}\widehat{(v^2)}(k,t)\right). \tag{3.10}$$

Note that the expressions $1+\frac{1}{2}\left(\theta^2-\frac{1}{3}\right)h_0^2k^2/a^2$ and $1-\frac{1}{2}\left(\theta^2-1\right)h_0^2k^2/a^2$ in the denominators of (3.9) and (3.10) are precisely the functions appearing in the dispersion relation (2.39), evaluated at k/a. Since $\theta=\sqrt{7/9}$ in this case, and the dispersion relation (2.39) is non-singular for $\theta^2\in[1/3,1]$, this ensures we are never dividing by zero.

We proceed by discretizing equations (3.9) and (3.10) in Fourier space, using the discrete Fourier transform, denoted here by $\mathscr{F}$. The discretized version of (3.9) is

$$\hat{\xi}_t(k,t) = -\frac{ik}{a\left(1+\frac{1}{2}\left(\theta^2-\frac{1}{3}\right)h_0^2k^2/a^2\right)}\left(h_0\hat{v}(k,t)+\mathscr{F}\left(\left(\mathscr{F}^{-1}(\hat{\xi})\right)\left(\mathscr{F}^{-1}(\hat{v})\right)\right)(k,t)\right), \tag{3.11}$$

for $k=-\frac{N}{2}+1,...,\frac{N}{2}$, $t>0$,

$\hat{\xi}_t(k,t)=0$ for $k=\frac{N}{2}$, $t>0$,

with initial condition $\hat{\xi}(k,0)=\mathscr{F}(\xi(x,0))=\frac{2\pi}{N}\sum_{j=1}^{N}e^{-ikx_j}\xi(x_j,0)$ for $k=-\frac{N}{2}+1,...,\frac{N}{2}$.

The discretized version of equation (3.10) is

$$\hat{v}_t(k,t) = -\frac{ik}{a\left(1-\frac{1}{2}\left(\theta^2-1\right)h_0^2k^2/a^2\right)}\left(g\hat{\xi}(k,t)+\frac{1}{2}\mathscr{F}\left(\left(\mathscr{F}^{-1}\hat{v}\right)^2\right)(k,t)\right), \tag{3.12}$$

for $k=-\frac{N}{2}+1,...,\frac{N}{2}$, $t>0$, $\hat{v}_t(k,t)=0$ for $k=\frac{N}{2}$, $t>0$, with initial condition $\hat{v}(k,0)=\mathscr{F}(v(x,0))=\frac{2\pi}{N}\sum_{j=1}^{N}e^{-ikx_j}v(x_j,0)$ for $k=-\frac{N}{2}+1,...,\frac{N}{2}$.

The discrete Fourier transform is implemented numerically using MATLAB's built in Fast Fourier Transform function `fft` and the Inverse Fast Fourier Transform function `ifft`.

Equations (3.11) and (3.12) are both systems of N ordinary differential equations for the discrete Fourier coefficients $\hat{\xi}(k,t)$ and $\hat{v}(k,t)$, for $k=-\frac{N}{2}+1,...,\frac{N}{2}$. The nonlinear terms ξv and v^2 appearing in these equations are treated pseudospectrally [9], in the sense that the products of the nonlinear terms are taken in the physical space before taking the Fourier transform.

We solve the coupled system of $2N$ ordinary differential equations using a fourth order Runge-Kutta method implemented in MATLAB.

The fourth order Runge Kutta method (RK4) for a system $\frac{d\mathbf{x}(t)}{dt}=\mathbf{f}(\mathbf{x}(t),t)$ of m ODE's is

$$\boldsymbol{x}_{n+1}=\boldsymbol{x}_n+\frac{\Delta t}{6}\left(\boldsymbol{k}_1+2\boldsymbol{k}_2+2\boldsymbol{k}_3+\boldsymbol{k}_4\right),$$

where

$\Delta t = 0.2 \times (0.5)^{p-1}$	L^2 error for η	R_η	L^2 error for w	R_w
$p = 1$	0.001084338954903		0.001121379001679	
$p = 2$	6.846446228660445e-05	15.8380	7.080110394023327e-05	15.8384
$p = 3$	4.284123005436054e-06	15.9810	4.430312328965367e-06	15.9811
$p = 4$	2.677412582051853e-07	16.0010	2.768763272647687e-07	16.0011
$p = 5$	1.673091451697128e-08	16.0028	1.730169955784558e-08	16.0028
$p = 6$	1.045553820488500e-09	16.0020	1.081224647945483e-09	16.0019
$p = 7$	6.545896835295415e-11	15.9727	6.772136813103757e-11	15.9658
$p = 8$	5.845947610408335e-12	11.1973	6.353704618024995e-12	10.6586
$p = 9$	4.236622994029508e-12	1.37990	4.797209561139811e-12	1.32450

Table 3.1: L^2 errors and convergence rate for the RK4 method. The convergence rate is the ratio of successive L^2-errors. R_η is the convergence rate for η and R_w is the convergence rate for w.

$$
\begin{aligned}
\boldsymbol{k}_1 &= \boldsymbol{f}(\boldsymbol{x}_n, t_n)\,, \\
\boldsymbol{k}_2 &= \boldsymbol{f}(\boldsymbol{x}_n + \tfrac{\Delta t}{2}\boldsymbol{k}_1, t_n + \tfrac{\Delta t}{2})\,, \\
\boldsymbol{k}_3 &= \boldsymbol{f}(\boldsymbol{x}_n + \tfrac{\Delta t}{2}\boldsymbol{k}_2, t_n + \tfrac{\Delta t}{2})\,, \\
\boldsymbol{k}_4 &= \boldsymbol{f}(\boldsymbol{x}_n + \Delta t\boldsymbol{k}_3, t_n + \Delta t)\,,
\end{aligned}
$$

and Δt is the time step.

To check that the method is correctly implemented in MATLAB, we run convergence tests from $t = 0$ to $t = T_{\max}$ with the initial conditions (3.2) at $t = 0$, $\theta = \sqrt{7/9}$, and compute the relative L^2 error (3.1) from the numerical solution obtained at $t = T_{\max}$ and the exact solution at the same time $T_{\max}$. We use $N = 1024$ grid points, $T_{\max} = 5$ s, $L = 200$ m, $h_0 = 2$ m, $x_0 = L/3$, and the amplitude of the solitary wave is $A_0 = 0.5$ m. We start with the time step $\Delta t = 0.2$ s, and in successive runs we halve the timestep while keeping all other parameters fixed, i.e., for simulation p the time step is $\Delta t = 0.2 \times (0.5)^{p-1}$. The results are given in Table (3.1). As can be seen from the table, the convergence rate is fourth order, since halving the time step results in a 16 times reduction of the error. A similar test was also run with the same parameters but with $N = 2048$ instead, which yielded similar results.

Spatial convergence is tested in Table (3.2). Here we keep the parameters $L = 100$, $A_0 = 0.5$ m, $h_0 = 1$ m, $x_0 = L/2$ and $\Delta_t = 0.0001$ s fixed, and we double the number of grid points N in each successive simulation. The convergence rate in Table (3.2) is exponential, which is called spectral accuracy. This shows that the numerical scheme is correctly implemented in MATLAB.

Plots of the numerically obtained solution $\eta(x, t)$ and $w(x, t)$ of the third order pure BBM-type system with initial condition (3.2) are shown in Figures (3.1) and (3.2). In these figures, the parameters $A_0 = 1$ m, $h_0 = 2$ m, $L = 100$, $\theta = \sqrt{7/9}$ and $T_{\max} = 10$ s were used.

Δt	N	L^2 error for η	R_η	L^2 error for w	R_w
0.0001	64	0.040054013348561		0.036178604449950	
0.0001	128	2.452905558521918e-04	0.0016e+05	2.565531063910353e-04	0.0014e+05
0.0001	256	2.796703973017485e-09	0.8771e+05	3.482178364372149e-09	0.7368e+05
0.0001	512	1.440649320748695e-14	1.9413e+05	1.625254052201758e-14	2.1425e+05
0.0001	1024	2.8002e-12	0.005145	2.9900e-12	0.005436

Table 3.2: L^2 errors and convergence rate due to spatial discretization. The convergence rate is the ratio of successive L^2-errors. R_η is the convergence rate for η and R_w is the convergence rate for w.

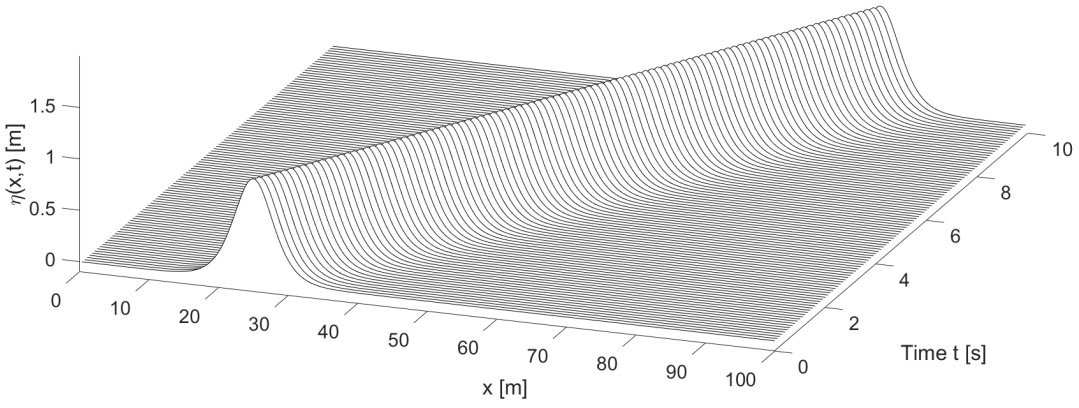

Figure 3.1: Space-time plot of the solitary wave solution $\eta(x,t)$ of the third order pure BBM system obtained numerically with the RK4 method, using initial condition (3.2). Here $h_0 = 2$ m, $A_0 = 1$ m.

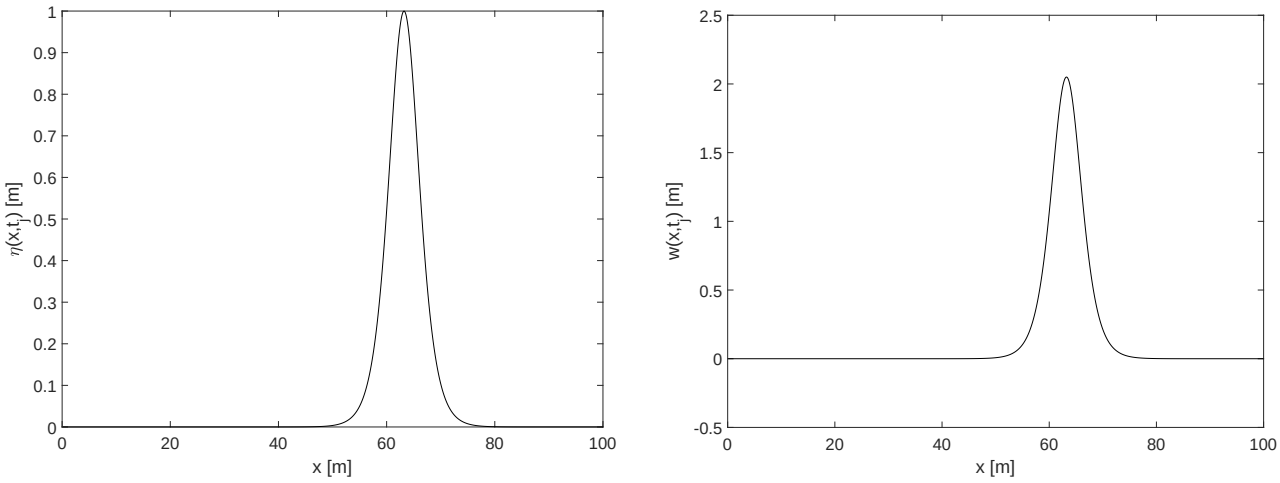

Figure 3.2: Plot of the numerical solution $\eta(x,t)$ (left panel) and $w(x,t)$ (right panel) of the third order pure BBM system at $t = 7$ s, obtained using (3.2) as initial condition. The parameters and initial conditions are the same as used in the space-time plot in Figure (3.1). The wave is right-moving.

3.2 Seventh order pure BBM-type system

We now turn to the seventh order equations. In many practical situations, α is generally smaller than β by a substantial amount. In such cases, it can be justified to make the assumption that $\alpha = \mathcal{O}(\beta^3)$. With this assumption, the pure BBM-type system (2.22), (2.12) reduces to

$$\begin{aligned}&\eta_t + w_x + \alpha\left(\eta w\right)_x - \frac{1}{2}\left(\theta^2 - \frac{1}{3}\right)\beta\eta_{xxt} + \frac{1}{360}\left(15\theta^4 - 30\theta^2 + 7\right)\beta^2\eta_{xxxxt}\\ &-\frac{1}{15120}\left(21\theta^6 - 105\theta^4 + 147\theta^2 - 31\right)\beta^3\eta_{xxxxxxt} + \mathcal{O}(\alpha\beta, \beta^4) = 0,\end{aligned} \tag{3.13}$$

$$\begin{aligned}&\eta_x + w_t + \alpha w w_x + \frac{1}{2}\left(\theta^2 - 1\right)\beta w_{xxt} + \frac{5}{24}\left(\theta^2 - \tfrac{1}{5}\right)\left(\theta^2 - 1\right)\beta^2 w_{xxxxt}\\ &+\frac{1}{720}\left(\theta^2 - 1\right)\left(61\theta^4 - 14\theta^2 + 1\right)\beta^3 w_{xxxxxxt} + \mathcal{O}(\alpha\beta, \beta^4) = 0.\end{aligned} \tag{3.14}$$

Note that the only non-linear terms in equations (3.13), (3.14) are $\alpha\left(\eta w\right)_x$ in (3.13) and $\alpha w w_x$ in (3.14).

Proceeding in exactly the same way as for the third order system, we first convert to dimensional variables, neglecting terms of $\mathcal{O}(\alpha\beta, \beta^4)$. Then we translate the problem onto the interval $[0, 2\pi]$ using the same scaling as for the third order system, and take the Fourier transform of the resulting equations. The equations are then discretized using the discrete Fourier transform.

The discretized version of (3.13) is

$$\hat{\xi}_t(k,t) = -\frac{1}{a^6}\frac{ik}{f_3(k/a,\theta)}\left(a^5 h_0 \hat{v}(k,t) + a^5\mathscr{F}\left(\left(\mathscr{F}^{-1}(\hat{\xi})\right)\left(\mathscr{F}^{-1}(\hat{v})\right)\right)(k,t)\right), \tag{3.15}$$

for $k = -\frac{N}{2} + 1, ..., \frac{N}{2}$, $t > 0$,
$\hat{\xi}_t(k,t) = 0$ for $k = \frac{N}{2}$, $t > 0$,
with initial condition $\hat{\xi}(k,0) = \mathscr{F}(\xi(x,0)) = \frac{2\pi}{N}\sum_{j=1}^{N} e^{-ikx_j}\xi(x_j,0)$ for $k = -\frac{N}{2} + 1, ..., \frac{N}{2}$.

Here

$$\begin{aligned}f_3(k/a,\theta) =& 1 + \frac{1}{2}\left(\theta^2 - \frac{1}{3}\right)h_0^2k^2/a^2 + \frac{1}{360}\left(15\theta^4 - 30\theta^2 + 7\right)h_0^4k^4/a^4\\ &+ \frac{1}{15120}\left(21\theta^6 - 105\theta^4 + 147\theta^2 - 31\right)h_0^6k^6/a^6\end{aligned}$$

is as defined in the dispersion relation (2.24), evaluated at k/a.

The discretized version of equation (3.14) is

$$\hat{v}_t(k,t) = -\frac{1}{a^6}\frac{ik}{f_2(k/a,\theta)}\left(a^5 g\hat{\xi}(k,t) + \frac{1}{2}a^5\mathscr{F}\left(\left(\mathscr{F}^{-1}\hat{v}\right)^2\right)(k,t)\right), \tag{3.16}$$

for $k = -\frac{N}{2}+1, ..., \frac{N}{2}$, $t > 0$, $\hat{v}_t(k,t) = 0$ for $k = \frac{N}{2}$, $t > 0$, with initial condition $\hat{v}(k,0) = \mathscr{F}(v(x,0)) = \frac{2\pi}{N}\sum_{j=1}^{N} e^{-ikx_j}v(x_j,0)$ for $k = -\frac{N}{2}+1, ..., \frac{N}{2}$.

Here

$$\begin{aligned} f_2(k/a,\theta) =& 1 - \frac{1}{2}\left(\theta^2-1\right)h_0^2k^2/a^2 + \frac{5}{24}\left(\theta^2 - \frac{1}{5}\right)\left(\theta^2-1\right)h_0^4k^4/a^4 \\ &- \frac{1}{720}\left(\theta^2-1\right)\left(61\theta^4 - 14\theta^2 + 1\right)h_0^6k^6/a^6 \end{aligned}$$

is as defined in the dispersion relation (2.15), evaluated at k/a.

Choosing a value of $\theta \in [\sqrt{s_1}, 1]$ ensures that we are never dividing by zero.

Plots of the solution obtained from the seventh order pure BBM system with $\alpha = \mathcal{O}(\beta^3)$ are shown in the figures below. Using the same initial condition as the exact solution (3.2), with $\theta = \sqrt{7/9}$, we get the result shown in Figure (3.3). The exact solution (3.2) of the third order equations obviously does not satisfy the seventh order equations, so we get components of left and right moving waves with low amplitudes. This can also be seen in the plot of the horizontal velocity $w(x,t)$ in Figure (3.3), where the velocity is negative for some values of x. The amplitude of the wave is also increasing slightly with time.

In figures (3.4) and (3.5) we use the initial conditions $\eta(x,0) = 0.5\,\mathrm{sech}(0.2(x-L/2))$, with $L = 200$ m, and $w(x,0) = 0.1$. Here $h_0 = 2$ m and $\theta = \sqrt{7/9}$ as before. As can be seen from the figures, the initial profile splits into a left-moving and right-moving solitary wave. This is expected of any BBM type system of equations, since these systems model waves propagating in two directions.

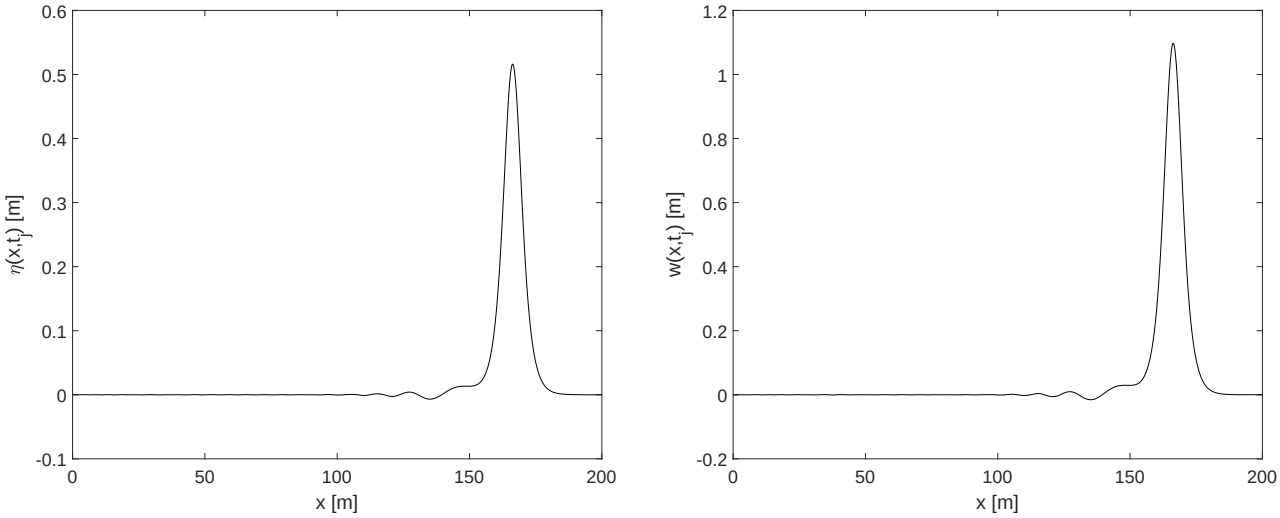

Figure 3.3: Plot of the numerical solution $\eta(x,t)$ (left panel) and $w(x,t)$ (right panel) of the seventh order pure BBM system, with $\alpha = \mathcal{O}(\beta^3)$ at $t = 20$ s. The initial condition (3.2) with $\theta = \sqrt{7/9}$, $A_0 = 0.5$ m, $h_0 = 2$ m was used. Since (3.2) is not an exact solution of the seventh order system, we get small amplitude waves emerging from the tallest wave. Since the velocity $w(x,t)$ is slightly negative for some values of x, some of the small-amplitude waves are moving to the left. The amplitude of the tallest wave also slightly increases with time from the initial maximum amplitude $A_0 = 0.5$.

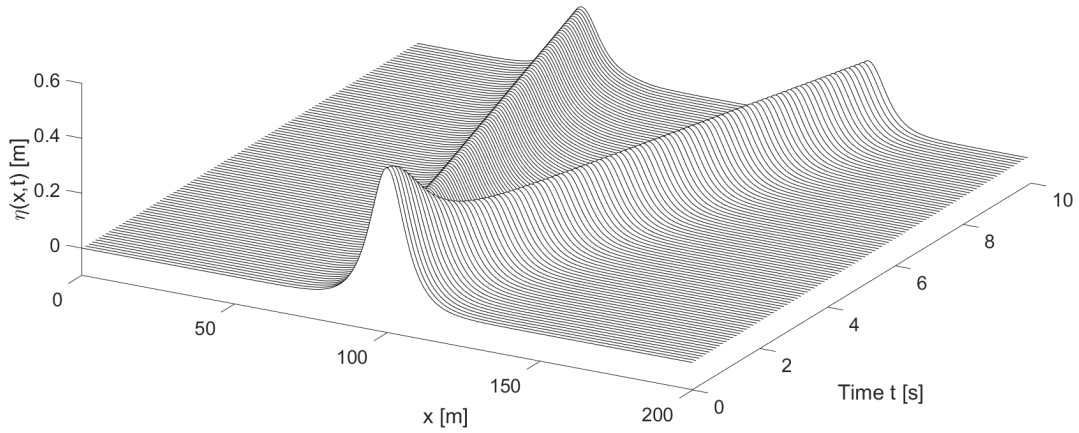

Figure 3.4: Space-time plot of the numerical solution $\eta(x,t)$ of the seventh order pure BBM system, with $\alpha = \mathcal{O}(\beta^3)$. The initial surface $\eta(x,0) = 0.5\,\mathrm{sech}(0.2(x - L/2))$, with $L = 200$ m, splits into a left and right moving wave. Here $h_0 = 2$ m, and the initial velocity was $w(x,0) = 0.1$ m/s.

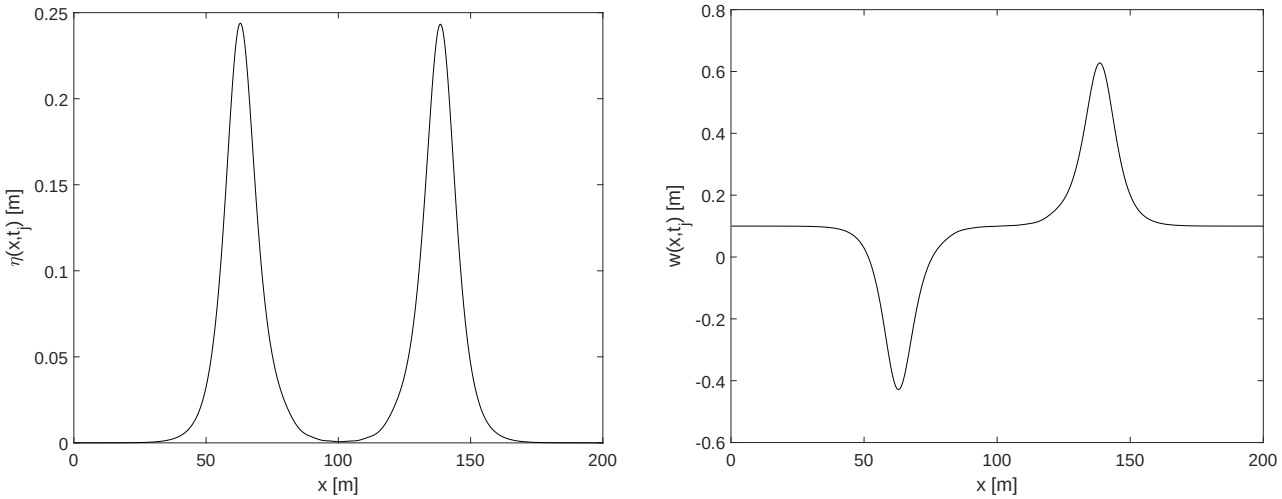

Figure 3.5: Plot of the numerical solution $\eta(x,t)$ (left panel) and $w(x,t)$ (right panel) of the seventh order pure BBM system, with $\alpha = \mathcal{O}(\beta^3)$ at $t = 8$ s. The parameters and initial conditions are the same as used in the space-time plot in Figure (3.4). Note how the velocity $w(x,t)$ is negative for the leftmost wave at $x \approx 60$ m, and the velocity is positive for the rightmost wave located at $x \approx 140$ m. The peak of the leftmost wave is travelling to the left with a slightly lower speed (≈ 0.43 m/s) than the peak of rightmost wave, which is travelling to the right with a speed ≈ 0.63 m/s. This is due to the small positive initial velocity $w(x,0) = 0.1$ m/s.

We shall now solve the full seventh order system of pure BBM-type (2.23), (2.12) numerically in a similar manner. Before we can proceed, we replace the nonlinear terms containing t-derivatives in (2.12) using relations (1.58) and (1.60), removing the nonlinear terms with t-derivatives, so that we can isolate the t - derivatives of η and w after taking the Fourier transform. Inserting these relations into (2.12) we obtain

$$\begin{aligned}
&\eta_x + w_t + \alpha w w_x + \frac{1}{2}\left(\theta^2-1\right)\beta w_{xxt} \\
&+\Big\{\alpha\beta\left(\eta\eta_{xx}\right)_x + \alpha^2\beta\left(\eta\left(ww_x\right)_x\right)_x - \tfrac{1}{2}\left(\theta^2-1\right)\alpha\beta^2\left(\eta\eta_{xxxx}\right)_x\Big\} \\
&+\frac{1}{2}\left(\theta^2-1\right)\alpha\beta w w_{xxx} + \frac{1}{2}\left(1+\theta^2\right)\alpha\beta w_x w_{xx} \\
&+\frac{5}{24}\left(\theta^2-\tfrac{1}{5}\right)\left(\theta^2-1\right)\beta^2 w_{xxxxt} + \Big\{\frac{1}{2}\alpha^2\beta\left(\eta^2\eta_{xx}\right)_x\Big\} - \alpha^2\beta w(\eta w_{xx})_x \\
&+\alpha^2\beta w_x(\eta w_x)_x + \Big\{\frac{1}{2}\left(\theta^2-\frac{1}{3}\right)\alpha\beta^2\left(\eta\eta_{xxxx}\right)_x\Big\} \\
&+\frac{5}{24}\left(\theta^2-\tfrac{1}{5}\right)\left(\theta^2-1\right)\alpha\beta^2 w w_{xxxxx} + \left(\frac{5}{24}\big(\theta^2+\tfrac{3}{5}\big)^2 - \frac{1}{5}\right)\alpha\beta^2 w_x w_{xxxx} \\
&+\frac{1}{4}\left(\theta^4+\tfrac{1}{3}\right)\alpha\beta^2 w_{xx}w_{xxx} + \frac{1}{720}\left(\theta^2-1\right)\left(61\theta^4-14\theta^2+1\right)\beta^3 w_{xxxxxxt} \\
&+\mathcal{O}(\alpha^3\beta,\alpha^2\beta^2,\alpha\beta^3,\beta^4) = 0.
\end{aligned} \tag{3.17}$$

after simplifying. The new terms are indicated by the curly brackets. The system we are solving numerically is then (2.23) and (3.17).

Note that the dispersion relation for the linearized system remains the same as before, and is given by eq. (2.24).

Proceeding as with the third order system above, we convert the equations to dimensional variables, neglect terms of $\mathcal{O}(\alpha^3\beta,\alpha^2\beta^2,\alpha\beta^3,\beta^4)$, then transform the interval $[0,L]$ into $[0,2\pi]$ using the same change of variables as was used for the third order system, and finally we take the Fourier transform $\mathcal{F}$ in the spatial variable x of the resulting equations.

Equation (2.23) then becomes

$$\begin{aligned}
\hat{\xi}_t(k,t) = -\frac{1}{a^6}\frac{1}{f_3(k/a,\theta)}\Big(&a^5 h_0 ik\hat{v} + a^5 ik\mathcal{F}\left(\xi v\right) \\
&+\tfrac{1}{2}a^3 ik^3\left(\theta^2-\tfrac{1}{3}\right)h_0^2\mathcal{F}\left(\xi v\right) + \tfrac{1}{4}aik^3\left(\theta^2-\tfrac{1}{3}\right)\left(\theta^2-1\right)h_0^4\mathcal{F}\left(\xi v_{xx}\right) \\
&+\tfrac{1}{360}aik^5\left(15\theta^4-30\theta^2+7\right)h_0^4\mathcal{F}\left(\xi v\right) + \tfrac{1}{2}a^3 ik\left(\theta^2-1\right)h_0^2\mathcal{F}\left(\xi v_{xx}\right) \\
&-\tfrac{1}{2}a^3 ikh_0\mathcal{F}\left(\xi^2 v_{xx}\right) + \tfrac{5}{24}aik\left(\theta^2-\tfrac{1}{5}\right)\left(\theta^2-1\right)h_0^4\mathcal{F}\left(\xi v_{xxxx}\right)\Big),
\end{aligned} \tag{3.18}$$

where

$$\begin{aligned}
f_3(k/a,\theta) =& 1 + \frac{1}{2}\left(\theta^2-\frac{1}{3}\right)h_0^2k^2/a^2 + \frac{1}{360}\left(15\theta^4-30\theta^2+7\right)h_0^4k^4/a^4 \\
&+\frac{1}{15120}\left(21\theta^6-105\theta^4+147\theta^2-31\right)h_0^6k^6/a^6
\end{aligned}$$

is as defined in the dispersion relation (2.24), evaluated at k/a.

Equation (3.17) becomes

$$\begin{aligned}
\hat{v}_t(k,t) = &-\frac{1}{a^6}\frac{1}{f_2(k/a,\theta)}\Big(a^5 gik\hat{\xi} + a^5\mathcal{F}\left(vv_x\right)\\
&+a^3 gh_0 ik\mathcal{F}\left(\xi\xi_{xx}\right) + a^3 h_0 ik\mathcal{F}\left(\xi\left(vv_x\right)_x\right) - \frac{1}{2}aik\left(\theta^2-1\right)gh_0^3\mathcal{F}\left(\xi\xi_{xxxx}\right) +\\
&+\tfrac{1}{2}a^3\left(\theta^2-1\right)h_0^2\mathcal{F}\left(vv_{xxx}\right) + \tfrac{1}{2}a^3\left(1+\theta^2\right)h_0^2\mathcal{F}\left(v_x v_{xx}\right)\\
&+\tfrac{1}{2}a^3 gik\mathcal{F}\left(\xi^2\xi_{xx}\right) - a^3 h_0\mathcal{F}\left(v\left(\xi v_{xx}\right)_x\right) + a^3 h_0\mathcal{F}\left(v_x\left(\xi v_x\right)_x\right)\\
&+\tfrac{1}{2}a\left(\theta^2-\tfrac{1}{3}\right)gh_0^3 ik\mathcal{F}\left(\xi\xi_{xxxx}\right) + \tfrac{5}{24}a\left(\theta^2-\tfrac{1}{5}\right)\left(\theta^2-1\right)h_0^4\mathcal{F}\left(vv_{xxxxx}\right)\\
&+a\left(\tfrac{5}{24}\left(\theta^2+\tfrac{3}{5}\right)^2 - \tfrac{1}{5}\right)h_0^4\mathcal{F}\left(v_x v_{xxxx}\right) + \tfrac{1}{4}a\left(\theta^4+\tfrac{1}{3}\right)h_0^4\mathcal{F}\left(v_{xx}v_{xxx}\right)\Big)
\end{aligned} \tag{3.19}$$

where

$$\begin{aligned}
f_2(k/a,\theta) =& 1 - \frac{1}{2}\left(\theta^2-1\right)h_0^2k^2/a^2 + \frac{5}{24}\left(\theta^2-\frac{1}{5}\right)\left(\theta^2-1\right)h_0^4k^4/a^4\\
&- \frac{1}{720}\left(\theta^2-1\right)\left(61\theta^4-14\theta^2+1\right)h_0^6k^6/a^6
\end{aligned}$$

is as defined in the dispersion relation (2.15), evaluated at k/a.

We discretize equations (3.18) and (3.19) in Fourier space using the discrete Fourier transform as for the third order system.

The discretized version of (3.18) is

$$\begin{aligned}
\hat{\xi}_t(k,t) = &-\frac{1}{a^6}\frac{1}{f_3(k/a,\theta)}\Big(a^5 h_0 ik\hat{v} + a^5 ik\mathscr{F}\left(\mathscr{F}^{-1}(\hat{\xi})\mathscr{F}^{-1}(\hat{v})\right)\\
&+\tfrac{1}{2}a^3 ik^3\left(\theta^2-\tfrac{1}{3}\right)h_0^2\mathscr{F}\left(\mathscr{F}^{-1}(\hat{\xi})\mathscr{F}^{-1}(\hat{v})\right)\\
&+\tfrac{1}{4}aik^3\left(\theta^2-\tfrac{1}{3}\right)\left(\theta^2-1\right)h_0^4\mathscr{F}\left(\mathscr{F}^{-1}(\hat{\xi})\mathscr{F}^{-1}\left(-k^2\hat{v}\right)\right)\\
&+\tfrac{1}{360}aik^5\left(15\theta^4-30\theta^2+7\right)h_0^4\mathscr{F}\left(\mathscr{F}^{-1}(\hat{\xi})\mathscr{F}^{-1}(\hat{v})\right)\\
&+\tfrac{1}{2}a^3 ik\left(\theta^2-1\right)h_0^2\mathscr{F}\left(\mathscr{F}^{-1}(\hat{\xi})\mathscr{F}^{-1}\left(-k^2\hat{v}\right)\right)\\
&-\tfrac{1}{2}a^3 ikh_0\mathscr{F}\left(\left(\mathscr{F}^{-1}(\hat{\xi})\right)^2\mathscr{F}^{-1}\left(-k^2\hat{v}\right)\right)\\
&+\tfrac{5}{24}aik\left(\theta^2-\tfrac{1}{5}\right)\left(\theta^2-1\right)h_0^4\mathscr{F}\left(\mathscr{F}^{-1}(\hat{\xi})\mathscr{F}^{-1}\left(k^4\hat{v}\right)\right)\Big),
\end{aligned} \tag{3.20}$$

for $k = -\frac{N}{2}+1, ..., \frac{N}{2}$, $t > 0$,

$\hat{\xi}_t(k,t) = 0$ for $k = \frac{N}{2}$, $t > 0$,

with initial condition $\hat{\xi}(k,0) = \mathscr{F}(\xi(x,0)) = \frac{2\pi}{N}\sum_{j=1}^{N} e^{-ikx_j}\xi(x_j,0)$ for $k = -\frac{N}{2}+1, ..., \frac{N}{2}$.

The discretized version of (3.19) is

$$
\begin{aligned}
&\hat{v}_t(k,t) = -\frac{1}{a^6}\frac{1}{f_2(k/a,\theta)}\Big(a^5 gik\hat{\xi} + a^5\mathscr{F}\left(\mathscr{F}^{-1}(\hat{v})\mathscr{F}^{-1}\left(ik\hat{v}\right)\right)\\
&+a^3 gh_0 ik\mathscr{F}\left(\mathscr{F}^{-1}(\hat{\xi})\mathscr{F}^{-1}\left(-k^2\hat{\xi}\right)\right)\\
&+a^3 h_0 ik\mathscr{F}\left(\mathscr{F}^{-1}(\hat{\xi})\mathscr{F}^{-1}\left(ik\mathscr{F}\left(\mathscr{F}^{-1}(\hat{v})\mathscr{F}^{-1}\left(ik\hat{v}\right)\right)\right)\right)\\
&-\frac{1}{2}aik\left(\theta^2-1\right)gh_0^3\mathscr{F}\left(\mathscr{F}^{-1}(\hat{\xi})\mathscr{F}^{-1}\left(k^4\hat{\xi}\right)\right)+\\
&+\tfrac{1}{2}a^3\left(\theta^2-1\right)h_0^2\mathscr{F}\left(\mathscr{F}^{-1}(\hat{v})\mathscr{F}^{-1}\left(-ik^3\hat{v}\right)\right)\\
&+\tfrac{1}{2}a^3\left(1+\theta^2\right)h_0^2\mathscr{F}\left(\mathscr{F}^{-1}\left(ik\hat{v}\right)\mathscr{F}^{-1}\left(-k^2\hat{v}\right)\right)\\
&+\tfrac{1}{2}a^3 gik\mathscr{F}\left(\left(\mathscr{F}^{-1}(\hat{\xi})\right)^2\mathscr{F}^{-1}\left(-k^2\hat{\xi}\right)\right)\\
&-a^3 h_0\mathscr{F}\left(\mathscr{F}^{-1}(\hat{v})\mathscr{F}^{-1}\left(ik\mathscr{F}\left(\mathscr{F}^{-1}(\hat{\xi})\mathscr{F}^{-1}\left(-k^2\hat{v}\right)\right)\right)\right)\\
&+a^3 h_0\mathscr{F}\left(\mathscr{F}^{-1}\left(ik\hat{v}\right)\mathscr{F}^{-1}\left(ik\mathscr{F}\left(\mathscr{F}^{-1}(\hat{\xi})\mathscr{F}^{-1}\left(ik\hat{v}\right)\right)\right)\right)\\
&+\tfrac{1}{2}a\left(\theta^2-\tfrac{1}{3}\right)gh_0^3 ik\mathscr{F}\left(\mathscr{F}^{-1}(\hat{\xi})\mathscr{F}^{-1}\left(k^4\hat{\xi}\right)\right)\\
&+\tfrac{5}{24}a\left(\theta^2-\tfrac{1}{5}\right)\left(\theta^2-1\right)h_0^4\mathscr{F}\left(\mathscr{F}^{-1}(\hat{v})\mathscr{F}^{-1}\left(ik^5\hat{v}\right)\right)\\
&+a\left(\tfrac{5}{24}\left(\theta^2+\tfrac{3}{5}\right)^2-\tfrac{1}{5}\right)h_0^4\mathscr{F}\left(\mathscr{F}^{-1}\left(ik\hat{v}\right)\mathscr{F}^{-1}\left(k^4\hat{v}\right)\right)\\
&+\tfrac{1}{4}a\left(\theta^4+\tfrac{1}{3}\right)h_0^4\mathscr{F}\left(\mathscr{F}^{-1}\left(-k^2\hat{v}\right)\mathscr{F}^{-1}\left(-ik^3\hat{v}\right)\right)\Big)
\end{aligned}
\tag{3.21}
$$

for $k = -\frac{N}{2}+1, ..., \frac{N}{2}$, $t > 0$, $\hat{v}_t(k,t) = 0$ for $k = \frac{N}{2}$, $t > 0$, with initial condition $\hat{v}(k,0) = \mathscr{F}(v(x,0)) = \frac{2\pi}{N}\sum_{j=1}^{N} e^{-ikx_j}v(x_j,0)$ for $k = -\frac{N}{2}+1, ..., \frac{N}{2}$.

In most of the simulations we ran, there was little observable difference between the solutions of the full seventh order pure BBM type system and the seventh order pure BBM type system with $\alpha = \mathcal{O}(\beta^3)$, except that the full seventh order pure BBM system appeared more sensitive to large amplitude, short wavelength initial conditions unless h_0 was large enough (at least twice the amplitude of the tallest wave), and was less stable in these cases over long time intervals. This is possibly due to aliasing errors from the pseudospectral treatment of the numerous nonlinear terms, accumulating over time. A possible fix for this could be to implement a de-aliasing filter by using, for instance, the standard two-thirds rule, which was not done in our experiments for the time being.

Chapter 4

Some further comments on our published article

Attached in the next chapter is our article which was published in Physics of Fluids. The article discusses applications of the Boussinesq systems discussed throughout this thesis, specifically how it is possible to determine whether a wave modeled by a BBM-type system starts breaking using a convective breaking criterion. Here we make a few comments on some details in the attached article.

The average flow depth behind the bore was calculated by locating each peak and trough in the wavetrain using MATLAB's built in `findpeaks` function, and averaging the result. We argue that, since the experiments were carried out by Wilkinson and Banner in 1977, when proper digitizing software was unavailable, it would be almost impossible to take the average of every single point on the free surface of the photographed undular bore from the physical experiments. Since Wilkinson and Banner did not define the mean depth behind the bore in [11] (outside of a sketch on a figure), we argue that they surely did something similar to calculate the mean depth behind the bore front.

We also numerically integrated the entire free surface η obtained from the numerical simulation, from the leftmost peak to the rightmost peak in the wavetrain, and calculated the true average of the function from this. Using this as the mean depth behind the bore front yielded similar results, our findings for the critical bore strength and Froude number were still within 5% of the values obtained by Wilkinson and Banner.

A few corrections regarding the published article must be made:

- On page 7, line 8, it should be $0 \leq \theta \leq 1$
- In Table II, simulation 2, the weir velocity U_w should be $U_w = 0.706$ m/s, and in Table II, simulation 3, the weir velocity U_w should be $U_w = 0.713$ m/s. The rest of the values in Table II are correct.

The figures from [11] were digitized using Engauge Digitizer, and thereafter imported into MATLAB.

Chapter 5

Published article

In this chapter, our article which was published online in Physics of Fluids on March 22., 2019 is presented.

Wave breaking in undular bores generated by a moving weir

Cite as: Phys. Fluids **31**, 033601 (2019); https://doi.org/10.1063/1.5085861
Submitted: 16 December 2018 . Accepted: 03 March 2019 . Published Online: 22 March 2019

Sondre Dahle Hatland, and Henrik Kalisch

Physics of Fluids ARTICLE scitation.org/journal/phf

Wave breaking in undular bores generated by a moving weir

Cite as: Phys. Fluids 31, 033601 (2019); doi: 10.1063/1.5085861
Submitted: 16 December 2018 • Accepted: 3 March 2019 •
Published Online: 22 March 2019

Sondre Dahle Hatland and Henrik Kalisch[a)]

AFFILIATIONS

Department of Mathematics, University of Bergen, P.O. Box 7800, 5020 Bergen, Norway

[a)]Author to whom correspondence should be addressed: henrik.kalisch@uib.no

ABSTRACT

If a weir is dragged through a wave flume, the upstream flow takes the form of an undular bore propagating ahead of the weir. It was found previously in the work of Wilkinson and Banner ("Undular bores," in 6th Australian Hydraulics and Fluid Mechanics Conference, Adelaide, Australia, 1977) that the leading wave of the undular bore will break if the bore strength given by the ratio of downstream to upstream flow depth exceeds a certain value. In the present work, a Boussinesq system is used to study the situation in a numerical wave tank. It is found that if a convective breaking criterion is used to indicate wave breaking, then the critical bore strength of the numerical model agrees with the experimental value of Wilkinson and Banner up to an error of less than 2%.

I. INTRODUCTION

A river bore is an upstream-propagating transition between two different flow depths usually caused by tidal forces. Similar flows can also be realized in controlled environments such as wave flumes, and a number of laboratory studies have been conducted in order to bring to light some of the main features of bores. One of the first in-depth investigations of undular bores in the laboratory was carried out by Favre in a dedicated wave flume,[1] and Favre's results have been examined theoretically from a number of angles. For example, the initial formation of the free-surface oscillations was under study in Refs. 2–4, and the energy balance at the bore front has been reviewed in Refs. 5–9. Dissipative effects were considered in Refs. 10 and 11, and the breaking of the leading oscillations in the bore was studied in Ref. 12.

Favre's experimental results highlighted in particular the transition between purely undular and partially turbulent bores in terms of the bore strength defined as the ratio of downstream to upstream flow depth, and the main purpose of the present work is to explore whether the critical bore strength can be found using standard wave models such as the classical Boussinesq system.

Favre himself used the shallow-water Saint-Venant system with frictional terms to describe the flow. One weakness of the shallow-water system is that it fails to describe the transition between undular and breaking bores because in the shallow-water theory, all waves eventually break (see Ref. 13, chap. 13.11, or, Ref. 14 chap. 11.3). On the other hand, the Boussinesq models incorporate dispersion, and small-amplitude waves do not feature the typical steepening observed in the shallow-water theory.[15] Therefore, wave breaking cannot be observed directly in the Boussinesq equations, but one may use a convective criterion comparing the crest speed of the leading wave to the fluid particle speed near the crest as a diagnostic for wave breaking. In these terms, a wave breaking criterion may be defined by saying that a wave starts to break when the horizontal component of the fluid velocity near the wavecrest exceeds the wavecrest velocity.

An initial study using this wave-breaking criterion in the context of Boussinesq modeling of Favre's experiments gave good qualitative results but was quantitatively inconclusive.[16] The relatively poor agreement with the experiments may be partially due to vorticity created by the discharge used to generate the undular bore. The existence of vorticity in a similar situation was also found in Refs. 17 and 18, and a mathematical inquiry into the Favre results also suggested that vorticity might be present in such flows.[19]

In the current work, we investigate the wave breaking onset in the leading wave in a bore created by moving a weir through a wave tank. Such experiments were carried out by Wilkinson and Banner,[20] and as shown in Fig. 1, this generating mechanism yields

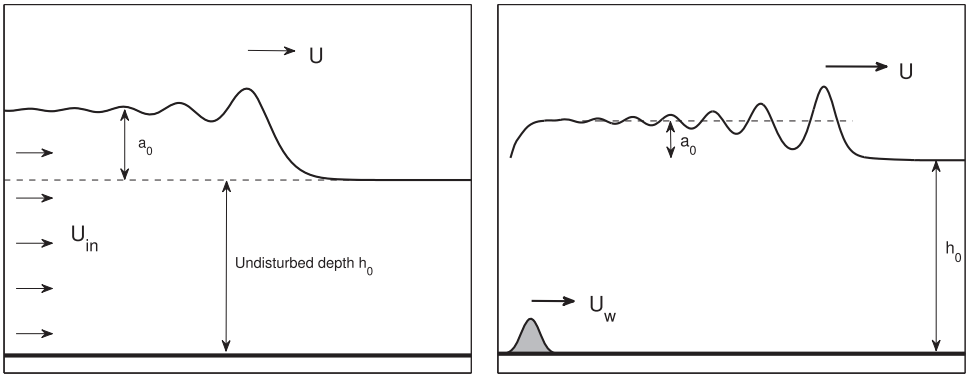

FIG. 1. Generating mechanisms for undular bores. Left panel: Undular bore created by a constant discharge imposed on the left-hand side of the wavetank. Right panel: Undular bore created by a moving weir through upstream influence. Note that the bore front propagates at a speed U which is generally larger than the speed U_w of the weir. The difference is exaggerated by the length of the arrows. The undisturbed depth is h_0, and the average flow depth behind the bore is $a_0 + h_0$.

bores that are markedly different from the ones created by a forced inflow. Favre found that wave breaking occurred when the bore strength was larger than 1.28. By contrast, in the experiments carried out by Wilkinson and Banner, the critical bore strength was found to be about 1.38. As will be shown in the body of the present paper, if the convective wave-breaking criterion is used in connection with a Boussinesq model in the case of a bore generated by a moving weir, then the critical bore strength may be found numerically to within an error of less than 2%. The plan of the paper is as follows. In Sec. II, the Boussinesq system used in the study of the undular bore is introduced. In Sec. III, the wave breaking criterion is explained in detail. The numerical experiments are described in Sec. IV, and the results are discussed in the Conclusion.

II. UNDULAR BORES AND BOUSSINESQ-TYPE SYSTEMS

In the experiments by Wilkinson and Banner, a moving weir is used to generate an undular bore (see Fig. 1 for an illustration of the geometric setup). The weir is placed at the bottom of a wave flume and dragged along the tank. As the weir is moving, it creates a mound of fluid propagating ahead of the weir itself. This phenomenon is well known to experimentalists and is sometimes called upstream influence.[23] The borefront develops oscillations (which in this case are often called undulations), and at first sight, the resulting undular bore seems similar to the bore featuring in the work of Favre.[1] However, as already mentioned, there are some important differences between these two flows. In particular, vorticity seems to be an important factor in the bores generated by a constant discharge, while as far as we can tell, vorticity is a minor effect in the bore generated by the moving weir. Some authors have pointed out the importance of bottom friction on the appearance of an undular bore.[10,7] Indeed, in a river bore, if the conditions are right, a nearly steady profile of undulations can be observed. However, in the present case, the main focus is on the onset of wave breaking which happens on relatively short time scales where dissipative effects do not have a major impact.

A bore may be characterized either by the bore strength already mentioned or using the Froude number. The Froude number is defined by $Fr = U/\sqrt{gh_0}$, where U is the velocity of the bore front, h_0 is the undisturbed (upstream) depth, and g is the gravitational acceleration.[24–26] While the Froude number seems to be more common in the literature, in the present case, since we are aiming for a favorable comparison with the experimental work in Ref. 20, it is expedient to use the same parameter as in that work to quantify the strength of the bore. Given the average downstream flow depth $a_0 + h_0$, the bore strength is defined as the ratio of flow depths by $r = \frac{a_0+h_0}{h_0}$.

As a side note, we should mention that recent work suggests that a single parameter such as the Froude number or bore strength may not be sufficient to classify bores and hydraulic jumps. For example, the authors of Ref. 27 proposed an additional parameter related to the vorticity of the flow. However, in the present case, such an extension is unnecessary.

Boussinesq systems are approximations of the full Euler equations valid for long waves of small amplitude if the fluid is incompressible and inviscid and the flow is irrotational.[28,15] Due to their relative simplicity, Boussinesq models are frequently used to model various surface wave phenomena. Since the undular bores described in Ref. 20 have small amplitudes and long wavelengths relative to the undisturbed depth, it is natural to use a Boussinesq model in the current situation.

Here, and in the rest of this article, a Cartesian coordinate system (x, z) is chosen such that $z = \eta(x, t)$ describes the free surface η, the undisturbed free surface is at $z = 0$, and the bottom of the wave tank is located at $z = -h_0$. Moreover, $u(x, t)$ is the horizontal fluid velocity at the fixed height $z = \left(\sqrt{7/9} - 1\right)h_0$. We use the Boussinesq system

$$\begin{aligned} \eta_t + h_0 u_x + (\eta u)_x - \tfrac{2}{9} h_0^2 \eta_{xxt} &= 0, \\ u_t + g\eta_x + u u_x - \tfrac{1}{9} h_0^2 u_{xxt} &= 0, \end{aligned} \tag{1}$$

to simulate an undular bore. The Boussinesq system (1) was introduced in Ref. 21. It is valid in the Boussinesq scaling regime, which applies when the parameters $\alpha = a/h_0$ and $\beta = h_0^2/\ell^2$ are small and of the same order of magnitude. Here a is a typical wave amplitude, ℓ is a typical wavelength, and h_0 is the undisturbed depth, and the parameters α and β describe the relative strength of nonlinear and dispersive effects in the flow.

System (1) is a coupled system of two regularized long-wave equations. Using the same rationale as the authors of Refs. 2 and 22 who introduced the Benjamin-Bona-Mahony (BBM) equation, it can be surmised that this system is more amenable to numerical methods than a number of other Boussinesq systems that were discussed in Ref. 21. In fact, the system can be solved efficiently using a Fourier-spectral collocation method.

As shown in Ref. 21, the system has exact solutions which can be used to test the convergence of numerical codes. The system can also be extended to accommodate time-dependent bathymetry. This was first done in Ref. 29, and in the present case, a time-dependent, spatially varying bottom topography $h(x,t)$ is included in these equations to model the weir moving along the bottom of the wave tank. The precise version of (1) to be used, including all parameter-values and some details on the numerical discretization, is given in the Appendix.

In Sec. III, it is shown how the full fluid velocity field is reconstructed from these variables, using an asymptotic expansion of the velocity potential. It will be shown that once a solution of (1) is available and the wave crest velocity is known, then a local convective criterion can be taken as an indication of whether the wave starts breaking or not. Denoting the crest speed by U and the horizontal component of the fluid particle velocity by $u(x,z,t)$, we say that the wave breaks if $u(x,\eta(x,t),t) > U$. This convective wave breaking criterion is standard in the study of breaking waves (see Ref. 30 and references therein) but has not been tested in the current situation.

III. WAVE BREAKING CRITERION FOR THE BOUSSINESQ SYSTEM

In order to understand the wavebreaking criterion, a look at the derivation of the Boussinesq system (1) is in order. Since this derivation is well known, we just summarize a few points of importance. For a more detailed discussion, the reader is referred to Refs. 16 and 13. As discussed above, since the bottom of the wave tank is constant away from the weir, and given by $z = -h_0$ near the leading wave crest behind the bore front, the following discussion is based on the Boussinesq system (1). It is assumed that α and β are small and of the same order so that Eq. (1) are valid and higher order terms in α and β can be neglected in the following derivation.

With the assumptions of irrotational flow of an inviscid and incompressible fluid, a velocity potential $\phi(x,z,t)$ can be introduced. The surface wave problem is then formulated in terms of the velocity potential as

$$\begin{aligned} \phi_{xx} + \phi_{zz} &= 0, \quad -h_0 < z < \eta(x,t), \\ \phi_z &= 0, \qquad\quad z = -h_0, \end{aligned}$$

with the free-surface boundary conditions

$$\left.\begin{aligned} \eta_t + \phi_x\eta_x &= \phi_z, \\ \phi_t + \tfrac{1}{2}\left(\phi_x^2 + \phi_z^2\right) + g\eta &= 0, \end{aligned}\right\} \quad z = \eta(x,t).$$

As discussed in Ref. 13, since the total depth is small, an ansatz of the form $\phi(x,z,t) = \sum_0^\infty (z+h_0)^n f_n(x,t)$ is suggested for the velocity potential. Inserting this into the Laplace equation and using the boundary condition on the bottom gives

$$\phi(x,z,t) = f - \frac{1}{2}(z+h_0)^2 f_{xx} \tag{2}$$

to second order in β. Note that $f = f_0$ is the velocity potential at the bottom $z = -h_0$ and that $\phi_x(x,z,t) = f_x(x,t) - \frac{1}{2}(z+h_0)^2 f_{xxx}(x,t)$ is the horizontal velocity at a height z in the fluid.

Using this relation, it is possible to derive systems of equations such as (1) where the horizontal velocity is modeled at a prescribed depth $z = (\sqrt{7/9} - 1)h_0$. Letting $u(x,t) = \phi_x(x,z,t)\big|_{z=(\sqrt{7/9}-1)h_0}$ be the horizontal velocity at $z = (\sqrt{7/9} - 1)h_0$, we obtain

$$f_x = u + \frac{7}{18}h_0^2 u_{xx} \tag{3}$$

to order β^2. Combining (3) and (2) gives

$$\phi_x(x,z,t) \approx u(x,t) + \frac{1}{2}\left(\frac{7}{9}h_0^2 - (z+h_0)^2\right)u_{xx}(x,t) \tag{4}$$

up to $\mathcal{O}(\beta^2)$.

Equation (4) can be used to approximate the horizontal fluid velocity field at any point (x,z) in the fluid domain. As discussed in Ref. 16, we assume that wave breaking commences when the horizontal fluid particle velocity at the leading wave crest exceeds the local phase velocity of the wave crest, denoted by U. Evaluating (4) at $z = \eta(x,t)$ yields the following breaking criterion:

A wave solution $\left(\eta(x,t), u(x,t)\right)$ *of system* (1) *starts breaking if*

$$u(x,t) + \frac{1}{2}\left(\frac{7}{9}h_0^2 - (\eta(x,t)+h_0)^2\right)u_{xx}(x,t) > U. \tag{5}$$

This criterion is illustrated in Fig. 2. From (5), it follows that once a solution $(\eta(x,t), u(x,t))$ of the BBM system (A2) is available,

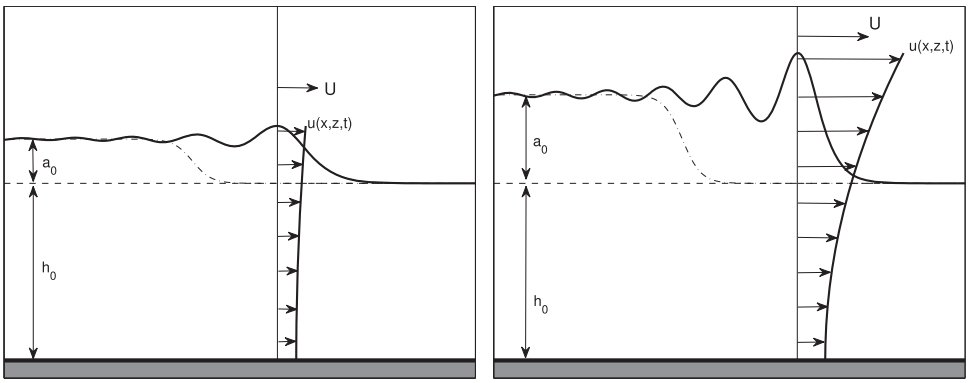

FIG. 2. Convective wave breaking criterion. The left panel shows a wave with horizontal particle velocity less than crest velocity. This wave is not breaking. The right panel shows a case where the horizontal particle velocity exceeds the crest velocity. This wave is breaking.

the onset of wave breaking can be predicted provided the wave propagation speed U is known.

IV. NUMERICAL EXPERIMENTS

We consider quasi-twodimensional fluid flow in a numerical wave tank of length L. The coordinate system (x, z) is as defined in Sec. II, with the positive z direction taken vertically upwards and the horizontal x-axis along the undisturbed free surface of the fluid. The bottom of the wave tank is located at $z = -h_0$, and the undisturbed free surface is located at $z = 0$, as shown in Fig. 3. The numerical domain is $x \in [0, L]$, and the fluid domain is then $(0, L) \times (-h(x,t), \eta(x,t))$, where $z = -h(x, t)$ describes the weir and the bottom of the tank, and $z = \eta(x, t)$ is the free surface as usual.

In the numerical simulation used in the present study, system (A2) is approximated using a spectral collocation method coupled with a 4-stage Runge-Kutta time integration scheme. At each time step, the resulting linear system is solved using a preconditioned conjugate gradient method. As the bore is generated by a weir moving along the bottom of the tank, we use initial values of zero surface displacement and zero initial velocity, i.e., $\eta(x, 0) = 0$ and $u(x, 0) = 0$.

Wilkinson and Banner conducted numerous experiments with varying undisturbed fluid depths and showed experimentally that undular bores may persist up to bore strength $r = 1.377$. Since the goal of this paper is to obtain favorable results in comparison with Wilkinson and Banner,[20] we used the same parameters as in that work. Accordingly, a weir of height 25 mm and length 150 mm was used in our simulation. As the value of h_0 is not consistently specified in Ref. 20 for a given Froude number, we have chosen to use the fluid depth $h_0 = 0.06$ m in all simulations shown, except the computations shown in Fig. 4. In this case, the undisturbed depth was specified in Ref. 20 to be $h_0 = 0.053$ m. We chose to run the simulations for $t = 15$ s as larger time intervals seemed to have little impact on the eventual bore strength r. The parameters used in our simulation are summarized in Table I. The function

$$z = -h(x,t) = \frac{A}{2}\left(1 + \tanh\left(\kappa t\sqrt{g/h_0} - m\right)\right) \times \exp\left(-\left(w(x/h_0 - \sigma - U_w t/h_0)\right)^2\right) - h_0 \quad (6)$$

with the parameters $A = 0.025$ m, $\kappa = 0.2$, $m = 2$, $w = 1.22$, $\sigma = 100$, and $h_0 = 0.06$ m is used to model the weir moving along the bottom of the tank. The speed U_w at which the weir is moving along the bottom of the tank is the only parameter which is varied, while the rest of the parameters in (6) are held fixed.

In order to test the validity of the numerical simulations, we first run a test with a purely undular bore. We choose the case shown in Fig. 3, page 372 from,[20] which features a Froude number $Fr = 1.24$, and is far from the breaking regime. In this case only, in order to obtain a good match with the experimental data, we have used the undisturbed depth $h_0 = 0.053$ m. Figure 3 from Ref. 20 is shown in Fig. 4 in digitalized form, alongside the numerical approximation of η obtained in our simulation. As can be seen, there is relatively good correspondence between the experimental data and numerical simulation. In particular, the wavelengths and amplitudes of the bores agree very well.

TABLE I. Parameters used in the numerical simulation.

Parameter	Symbol	Units	Value
Undisturbed depth	h_0	m	0.06
Tank length	L	m	50
Weir height	A	mm	25
Weir width		mm	150
Time interval length	T	s	15

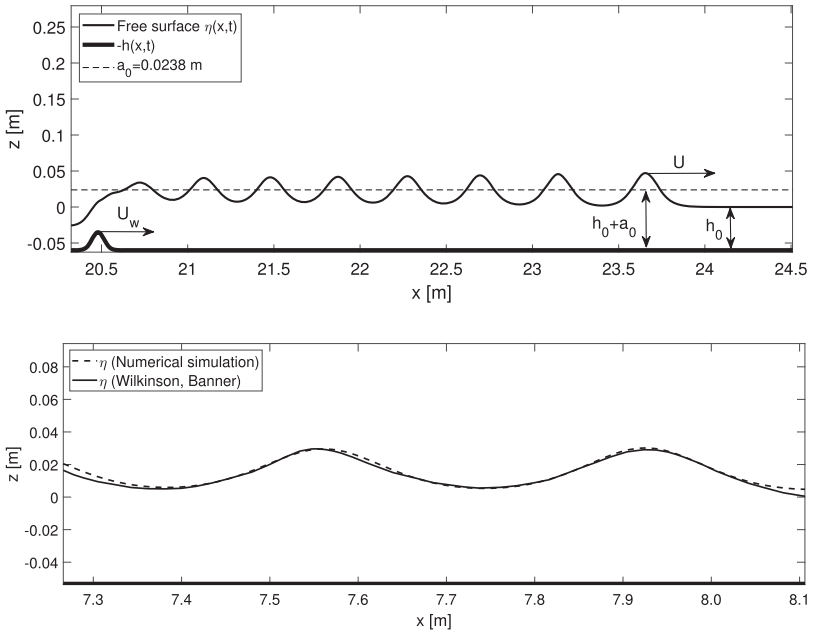

FIG. 3. Undular bore generated by a moving weir at the bottom of the tank $z = -h_0 = -0.06$ m.

FIG. 4. Digitized form of Fig. 3 in Ref. 20, $Fr = 1.24$ superimposed with a plot of η obtained from the numerical simulation with $Fr = 1.24$. The fluid depth is $h_0 = 0.053$ m, and the x-axis is aligned with the undisturbed water line. The bottom of the flume is indicated by a solid line at $z = -0.053$ m.

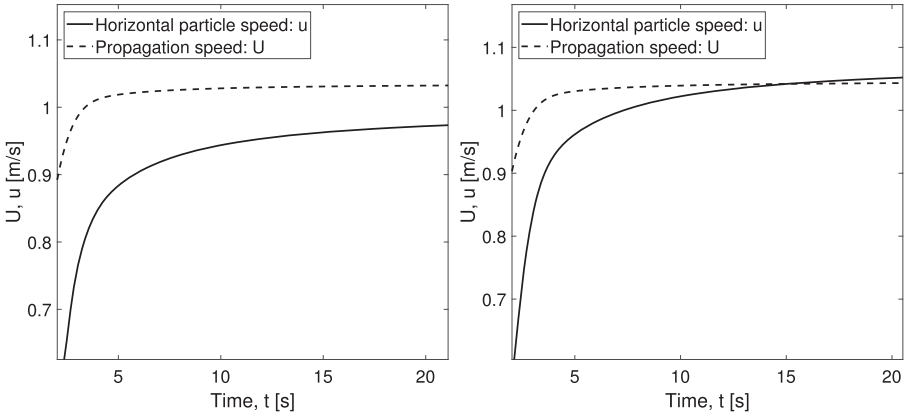

FIG. 5. Left panel: The horizontal particle speed does not exceed the phase speed, so the bore is purely undular. This corresponds to the bore strength $r = 1.38$. Right panel: The horizontal particle speed curve intersects the propagation speed curve at $t = 15$ s, and the leading wave starts breaking. This corresponds to the bore strength $r = 1.40$ as can be seen in the plot of the undular bore in Fig. 3.

Since the bottom is described by the constant function $z = -h_0$ near the leading wavecrest, Eq. (4) can be applied in approximating the particle velocity there. At each time step $t^n = n\Delta t$ in the simulation, the position x^n of the leading wave crest is located. From this sequence of values, the local phase velocity U^n of the wavecrest is estimated by a fourth-order, backwards finite-difference formula. The fluid particle velocity at the leading wavecrest behind the bore front is estimated from (4) with $z = \eta(x^n, t^n)$ at each time step.

As U_w is increased manually in each new run, the wave crest velocity and the horizontal fluid particle velocity also increase. Eventually the fluid particle velocity exceeds the phase velocity of the wave, and wave breaking commences. The process is illustrated in Fig. 5. In the left panel, the value of r is 1.38 and no intersection is taking place at times $t \le 15$ s. As shown in the right panel of Fig. 5, the particle velocity curve first intersects the phase velocity curve at $t = 15$ s for the value $r = 1.40$ which is therefore just above the critical bore strength for the current setup. The corresponding weir velocity is $U_w = 0.724$ m/s.

Table II tabulates whether the bore is breaking or not for different values of the bore strength r obtained numerically. Each row in Table II contains values of r and Fr_U obtained from a fixed value of U_w. We find the critical value of the bore strength in Table II to be

TABLE II. Wave breaking in the numerical model for different Froude numbers and bore strengths at $t = 15$ s. The critical bore strength is $r = 1.395$.

Simulation	$r = 1 + a_0/h_0$	$Fr_U = U/\sqrt{gh_0}$	U (m/s)	U_w (m/s)	Breaking/non-breaking
1	1.35	1.319	1.012	0.675	Not breaking
2	1.38	1.344	1.031	0.698	Not breaking
3	1.39	1.350	1.036	0.706	Not breaking
4	1.40	1.358	1.042	0.724	Breaking
5	1.41	1.375	1.055	0.744	Breaking
6	1.43	1.388	1.065	0.760	Breaking

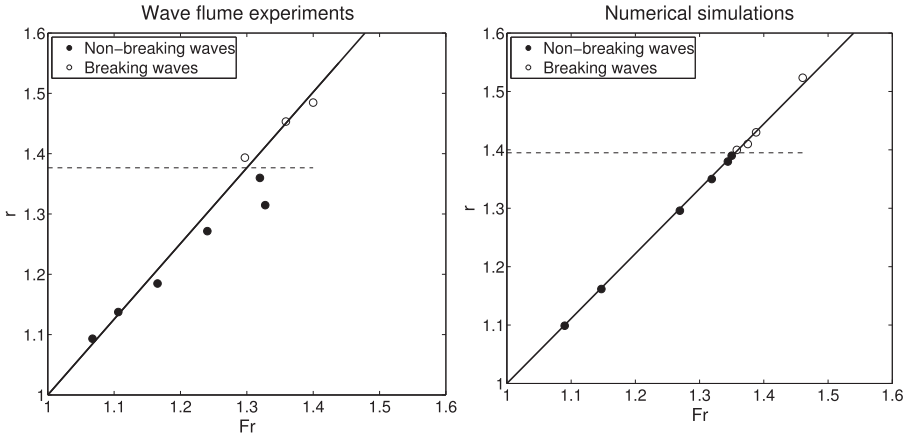

FIG. 6. Relation between the flow-depth ratio r and the Froude number Fr. The critical bore strength is indicated with a dashed horizontal line. Left panel: Experiments by Wilkinson and Banner.[20] The critical bore strength is $r = 1.377$. Right panel: Numerical simulations using Boussinesq system. The critical bore strength is $r = 1.395$.

$r = 1.395$, between the values 1.39 which does not feature breaking, and 1.40 which does lead to breaking. As an additional comparison, we also include the Froude numbers $Fr_U = U/\sqrt{gh_0}$, where U is the phase speed of the leading wave behind the borefront, approximated numerically at $t = 15$ s by the method described above.

Comparing the results in Table II with the ones in Ref. 20, we see that the numerical critical bore strength $r = 1.395$ is about 1.3% higher than the experimental value $r = 1.377$ in Ref. 20 and that $Fr_U = 1.358$ is about 4.5% larger than $Fr = 1.3$ in Ref. 20, so the results are relatively close in both cases. The data are also represented in Fig. 6, where the left panel shows data from the experiments in Ref. 20, and the right panel shows data based on our numerical simulations.

V. CONCLUSION

In this work, it has been shown that the transition from laminar to partially turbulent flow in an undular bore can be captured with a standard weakly nonlinear dispersive system of Boussinesq type. Reference is made to two experimental studies: the experiments of Favre[1] and the experiments of Wilkinson and Banner.[20] The particular quantity of interest is the bore strength r given by the ratio of downstream to upstream flow depths.

In previous work, it was shown that using a convective wave-breaking criterion leads to qualitative agreement with the experiments of Favre in the sense that the Boussinesq system features a critical ratio indicating the commencement of wave breaking.[16,31] However, the quantitative agreement between the numerical experiments in Refs. 16 and 31 was not very good. The discrepancy may possibly be ascribed to the appearance of vorticity in the undular bore, such as suggested in Refs. 17 and 19. Indeed, it was argued in Ref. 27 that a single parameter such as the bore strength r or the Froude number Fr may not be sufficient to classify bores, even in the case where the flow is quasi-two-dimensional. In the present case of a bore generated by a moving weir, it was found that the bore strength r can be used as an effective diagnostic parameter to predict whether a bore will break or not. The critical bore strength signaling the demarcation between laminar and turbulent flow was found experimentally to be about 1.377.[20] Our numerical simulations indicate that the leading wave breaks at a bore strength of 1.395. Thus, experiment and simulation coincide up to an error of less than 2%.

The separate comparison using the Froude number $Fr_U = U/\sqrt{gh_0}$ for the phase speed of the leading wave crest behind the bore front, which was found to be $Fr_U = 1.358$ when the bore started breaking, is also fairly close to the critical Froude number $Fr = 1.3$ in Ref. 20. Using this parameter as an indicator for the onset of breaking yields agreement between experiment and numerical simulation with an error of less than 5%. Additionally, Fig. 4 shows that the shape of the free surface of the bore obtained numerically for non-breaking bores is very similar to the free surface in Ref. 20. This further validates the results obtained from the model used in this work.

One may ask whether the bore strength r or the Froude number Fr is a better indicator for whether a bore features incipient breaking. While the Froude number is probably more commonly used than the bore strength, the present study found slightly better agreement between theory and experiment if the bore strength was used as a parameter. Indeed it can also be observed in the left panel of Fig. 6 that the relation between Fr and r is slightly nonlinear in the experimental measurements.

To put our findings into context, it should be mentioned that wave breaking in an undular bore is a special case of wave breaking on a planar beach, a phenomenon which has been studied widely. It is not immediately clear whether the convective breaking criterion can be used in this case as well. Recent work paints a complicated picture. The experiments described in Ref. 32 point to the convective criterion as being a good indicator for the commencement of wave breaking. On the other hand, if the wave breaking criterion is to be used in a numerical model in order to switch between a dispersive system and a hyperbolic system (in order to exploit the dissipative nature of numerical approximations to hyperbolic systems), then the convective breaking criterion should possibly be sharpened in order to give the waves time to adjust (see Refs. 36–38 and the references therein).

Indeed, the detection of wave breaking through various wave breaking criteria has been researched by a number of groups for many years. As explained in Ref. 33, there are essentially three classes of criteria. Geometric criteria are based on the shape and in particular the steepness of the waves close to breaking, while kinematic criteria such as used here are based on violation of the kinematic free surface boundary condition. As it generally seems to be understood that no dynamic insight or advance warning of imminent breaking is provided by geometric and kinematic criteria,[34] dynamic criteria based on evaluation of the energy flux such as proposed in Refs. 35 and 30 seem to be favored at the moment.

Recently a new parameter based on crest speed and local energy flux and density has been put forward as a diagnostic for the initiation of wave breaking. As shown in Ref. 30, using this parameter reduces to a sharpened convective criterion when evaluated at the free surface. However, it has been tested mainly in deep and intermediate water,[30,39] and it is not clear at this point whether this diagnostic will work in shallow water such as in the current situation.

It should also be noted that there have been extensive efforts to understand various aspects of wave breaking using numerical approximations of the full Euler equations. In particular, in the case of potential flow, we mention the work on overturning breakers reported in Refs. 40 and 41. On the other hand, some authors have advocated the use of conservative Boussinesq system[42] or indeed for the use of fully nonlinear long-wave systems, such as the Serre or Green-Naghdi equations[43,44] in order to study wave breaking on a slope (see Ref. 45 for example). However, in the present case, no such extension is needed.

ACKNOWLEDGMENTS

This research was supported by the Research Council of Norway under Grant No. 239033/F20. The numerical code used in this work was developed jointly by A. Senthilkumar, H. Kalisch, and H. Munthe-Kaas.

APPENDIX: BOUSSINESQ SYSTEMS WITH MOVING BATHYMETRY

In order to simulate an undular bore generated by a moving weir numerically, a BBM-BBM type system is used in this work. In Ref. 29, the following system describing unsteady fluid flow in

one horizontal dimension over a time dependent, spatially varying bottom topography is derived:

$$\begin{aligned}
&\eta_t + ((h+\eta)u)_x + \left\{Ah^2\left[(uh_x)_x + h_x u_x\right]\right.\\
&\quad \left. + ah^2(hu)_{xx} - bh^2\eta_{tx}\right\}_x + \tilde{A}\left(h^2 h_{tx}\right)_x + h_t = 0,\\
&u_t + g\eta_x + uu_x + \left\{Bgh\left[(h_x\eta_x)_x + h_x\eta_{xx}\right]\right.\\
&\quad \left. + cgh^2\eta_{xxx} - dh^2 u_{txx}\right\} - Bhh_{ttx} = 0.
\end{aligned} \tag{A1}$$

Here $u = u(x, t)$ is the horizontal fluid velocity at the height $z = (\theta - 1)h_0$, where $0 < \theta < 1$, $\eta(x, t)$ is the free surface, and $h(x, t)$ describes the bottom topography. The parameter θ is an arbitrary modeling parameter which has been chosen to be equal to $\sqrt{7/9}$ in the body of this paper. The definitions of the further parameters used in the system are as follows:

$$\begin{gathered}
\tilde{a} = \theta - 1/2, \quad \tilde{b} = -A, \quad \tilde{c} = -B,\\
A = \tfrac{1}{2}\left[\tfrac{1}{3} - (\theta-1)^2\right], \quad B = 1 - \theta, \quad \tilde{A} = \mu\tilde{a} - (1-\mu)\tilde{b},\\
a = \tfrac{1}{2}\left(\theta^2 - \tfrac{1}{3}\right)\mu, \quad b = \tfrac{1}{2}\left(\theta^2 - \tfrac{1}{3}\right)(1-\mu),\\
c = \tfrac{1}{2}\left(1-\theta^2\right)\nu, \quad d = \tfrac{1}{2}\left(1-\theta^2\right)(1-\nu),
\end{gathered}$$

where $\mu, \nu \in \mathbb{R}$. Taking $\mu = \nu = 0$ in (A1) gives

$$\begin{aligned}
&\eta_t - b(h^2\eta_{xt})_x + ((h+\eta)u)_x\\
&\quad + \left\{2Ah^2 h_x u_x + Ah^2 h_{xx} u\right\}_x - \tilde{b}(h^2 h_{xt})_x + h_t = 0,\\
&u_t + g\eta_x + uu_x + Bghh_{xx}\eta_x + 2Bgh h_x\eta_{xx}\\
&\quad - dh^2 u_{xxt} - Bhh_{xtt} = 0,
\end{aligned} \tag{A2}$$

where $b = \frac{1}{2}\left(\theta^2 - \frac{1}{3}\right)$, $d = \frac{1}{2}\left(1-\theta^2\right)$. The BBM-BBM type system (A2) with the boundary and initial conditions stated in Sec. IV is used to simulate an undular bore numerically in this work. Like system (1), this system is valid under the Boussinesq approximation. As discussed earlier, the time dependent bottom $h(x, t)$ is included in Eq. (A2) to model the weir moving along the bottom of the wave tank.

The numerical approximation of this system is effected by a pseudo-spectral collocation method based on a Fourier basis. This discretization entails the imposition of periodic boundary conditions. In the present one-dimensional case, this choice does not pose a serious problem since the numerical domain $[0, L]$ can be made large enough to prevent wave interactions at the far ends on either side. Rescaling the equations to the numerical interval $[0, 2\pi]$ introduces a scaling factor $\lambda = L/(2\pi)$. Using the standard collocation points $x_j = \frac{2\pi j}{N}$ for $j = 0, 1, \ldots, N-1$ yields the first-order collocation derivative matrix D_N and the corresponding second-order matrix $D_{N,2}$, such as detailed in Refs. 46 and 47. Defining the $N \times N$ identity matrix by I_N, and the discrete unknowns as Σ^N and U^N, the semi-discrete system is written as

$$\begin{aligned}
&\left[\lambda^3 I_N - \lambda b\, D_N \mathrm{diag}(h_N^2) D_N\right]\Sigma_t^N\\
&\quad = -D_N\left[2A\, h_N^2\, D_N h_N\, D_N(U^N) + A\, D_{N,2} h_N\, h_N^2\, U^N\right]\\
&\quad\quad - \lambda^2 D_N(h_N U^N) - \lambda A D_N(h_N^2 D_N(h_N)_t)\\
&\quad\quad - \lambda^2 D_N(\Sigma^N U^N) - \lambda^3 (h_N)_t,
\end{aligned}$$

$$\begin{aligned}
&\left[\lambda^3 I_N - \lambda d\, \mathrm{diag}(h_N^2) D_{N,2}\right] U_t^N\\
&\quad = -\lambda^2 g D_N \Sigma^N - \lambda^2 \frac{1}{2} D_N(U^N U^N) - 2Bgh_N\, D_N h_N\, D_{N,2}\Sigma^N\\
&\quad\quad - Bgh_N D_{N,2} h_N\, D_N \Sigma^N + \lambda^2 Bh_N D_N (h_N)_{tt},
\end{aligned}$$

where h_N is defined by $[h_N(t)]_j = h(x_j, t)$. This system of N ordinary differential equations is integrated using a 4-stage Runge-Kutta method. The most demanding operation is the inversion of the time-dependent matrices on the left-hand side of these equations which has to be performed at each time step. The inversion is performed using a preconditioned conjugate gradient (PCG) method (see Ref. 48). The scheme has been tested for convergence in Ref. 49. Alternative methods for the numerical discretization of these equations are finite-element methods[29] or finite-difference methods.[16] These methods would allow for straightforward incorporation of various boundary conditions, but in the present case, that is not necessary.

REFERENCES

[1] H. Favre, *Ondes de Translation* (Dunod, Paris, 1935).
[2] D. H. Peregrine, "Calculations of the development of an undular bore," J. Fluid Mech. **25**, 321–330 (1966).
[3] S. Soares Frazao and Y. Zech, "Undular bores and secondary waves-experiments and hybrid finite-volume modelling," J. Hydraul. Res. **40**, 33–43 (2002).
[4] G. A. El, V. V. Khodorovskii, and A. V. Tyurina, "Undular bore transition in bi-directional conservative wave dynamics," Physica D **206**, 232–251 (2005).
[5] R. Lemoine, "Sur les ondes positives de translation dans les canaux et sur le ressaut ondule de faible amplitude," La Houille Blanche **2**, 183–185 (1948).
[6] T. B. Benjamin and M. J. Lighthill, "On cnoidal waves and bores," Proc. R. Soc. London, Ser. A **224**, 448–460 (1954).
[7] B. Sturtevant, "Implications of experiments on the weak undular bore," Phys. Fluids **8**, 1052–1055 (1965).
[8] A. Ali and H. Kalisch, "Energy balance for undular bores," C. R. Mec. **338**, 67–70 (2010).
[9] A. Ali and H. Kalisch, "Mechanical balance laws for Boussinesq models of surface water waves," J. Nonlinear Sci. **22**, 371–398 (2012).
[10] J. G. B. Byatt-Smith, "The effect of laminar viscosity on the solution of the undular bore," J. Fluid Mech. **48**, 33–40 (1971).
[11] G. A. El, R. H. J. Grimshaw, and A. M. Kamchatnov, "Analytic model for a frictional shallow-water undular bore," Chaos **15**, 037102 (2005).
[12] S. L. Gavrilyuk, V. Y. Liapidevskii, and A. A. Chesnokov, "Spilling breakers in shallow water: Applications to Favre waves and to the shoaling and breaking of solitary waves," J. Fluid Mech. **808**, 441–468 (2016).
[13] G. B. Whitham, *Linear and Nonlinear Waves* (Wiley, New York, 1974).
[14] L. C. Evans, *Partial Differential Equations*, 1st ed., Graduate Studies in Mathematics, Vol. 19 (American Mathematical Society, Providence, RI, 1998).
[15] D. H. Peregrine, "Equations for water waves and the approximations behind them," *Waves on Beaches and Resulting Sediment Transport* (1972), pp. 95–121.
[16] M. Bjørkavåg and H. Kalisch, "Wave breaking in Boussinesq models for undular bores," Phys. Lett. A **375**, 1570–1578 (2011).
[17] H. G. Hornung, C. Willert, and S. Turner, "The flow field downstream of a hydraulic jump," J. Fluid Mech. **287**, 299–316 (1995).
[18] C. Koch and H. Chanson, "Unsteady turbulence characteristics in an undular bore," in *River Flow 2006* (Taylor & Francis Group, London, 2006).
[19] C. Kharif and M. Abid, "Whitham approach for the study of nonlinear waves on a vertically sheared current in shallow water," Eur. J. Mech. B: Fluids **72**, 12–22 (2018).
[20] D. L. Wilkinson and M. L. Banner, "Undular bores," in 6th Australian Hydraulics and Fluid Mechanics Conference, Adelaide, Australia, 1977.
[21] M. Chen, "Exact solutions of various Boussinesq systems," Appl. Math. Lett. **11**, 45–49 (1998).

[22]T. B. Benjamin, J. L. Bona, and J. J. Mahony, "Model equations for long waves in nonlinear dispersive systems," Philos. Trans. R. Soc., A **272**, 47–78 (1972).
[23]T. B. Benjamin, "Upstream influence," J. Fluid Mech. **40**, 49–79 (1970).
[24]F. M. Henderson, *Open Channel Flow* (Prentice Hall, 1996).
[25]H. Chanson, *The Hydraulics of Open Channel Flow* (Arnold, London, 1999).
[26]H. Chanson, "Current knowledge in hydraulic jumps and related phenomena. A survey of experimental results," Eur. J. Mech. B: Fluids **28**, 191–210 (2009).
[27]G. Richard and S. Gavrilyuk, "The classical hydraulic jump in a model of shear shallow-water flows," J. Fluid Mech. **725**, 492–521 (2013).
[28]D. Lannes, *The Water Wave Problem*, Mathematical Surveys and Monographs, Vol. 188 (American Mathematical Society, Providence, 2013).
[29]D. E. Mitsotakis, "Boussinesq systems in two space dimensions over a variable bottom for the generation and propagation of tsunami waves," Math. Comput. Simul. **80**, 860–873 (2009).
[30]X. Barthelemy, M. L. Banner, W. L. Peirson, F. Fedele, M. Allis, and F. Dias, "On a unified breaking onset threshold for gravity waves in deep and intermediate depth water," J. Fluid Mech. **841**, 463–488 (2018).
[31]M. K. Brun and H. Kalisch, "Convective wave breaking in the KdV equation," Anal. Math. Phys. **8**, 57–75 (2018).
[32]U. Itay and D. Liberzon, "Lagrangian kinematic criterion for the breaking of shoaling waves," J. Phys. Oceanogr. **47**, 827–833 (2017).
[33]M. Perlin, W. Choi, and Z. Tian, "Breaking waves in deep an intermediate waters," Annu. Rev. Fluid Mech. **45**, 115–145 (2013).
[34]Y. Pomeau, M. Le Berre, P. Guyenne, and S. Grilli, "Wave-breaking and generic singularities of nonlinear hyperbolic equations," Nonlinearity **21**, T61 (2008).
[35]J. B. Song and M. L. Banner, "On determining the onset and strength of breaking for deep water waves. Part I: Unforced irrotational wave groups," J. Phys. Oceanogr. **32**, 2541–2558 (2002).
[36]P. Bacigaluppi, M. Ricchiuto, and P. Bonneton, "A 1D stabilized finite element model for non-hydrostatic wave breaking and run-up," in *Finite Volumes for Complex Applications VII-Elliptic*, Parabolic and Hyperbolic Problems Springer Proceedings in Mathematics & Statistics Vol. 78 (Springer, 2014), pp. 779–790.
[37]P. Bacigaluppi, M. Ricchiuto, and P. Bonneton, "Upwind stabilized finite element modelling of non-hydrostatic wave breaking and run-up," hal-00990002, 2014.
[38]V. Roeber, K. F. Cheung, and M. H. Kobayashi, "Shock-capturing Boussinesq-type model for nearshore wave processes," Coastal Eng. **57**, 407–423 (2010).
[39]M. Derakhti, M. L. Banner, and J. T. Kirby, "Predicting the breaking strength of gravity water waves in deep and intermediate depth," J. Fluid Mech. **848**, R2 (2018).
[40]C. Fochesato and F. Dias, "A fast method for nonlinear three-dimensional free-surface waves," Proc. R. Soc. A **462**, 2715–2735 (2006).
[41]P. Guyenne and S. Grilli, "Numerical study of three-dimensional overturning waves in shallow water," J. Fluid Mech. **547**, 361–388 (2006).
[42]G. A. El, R. H. J. Grimshaw, and A. M. Kamchatnov, "Wave breaking and the generation of undular bores in an integrable shallow water system," Stud. Appl. Math. **114**, 395–411 (2005).
[43]G. A. El, R. H. J. Grimshaw, and N. F. Smyth, "Unsteady undular bores in fully nonlinear shallow-water theory," Phys. Fluids **18**, 027104 (2006).
[44]D. Lannes and P. Bonneton, "Derivation of asymptotic two-dimensional time-dependent equations for surface water wave propagation," Phys. Fluids **21**, 016601 (2009).
[45]G. Wei, J. T. Kirby, S. T. Grilli, and R. Subramanya, "A fully nonlinear Boussinesq model for surface waves. Part 1. Highly nonlinear unsteady waves," J. Fluid Mech. **294**, 71–92 (1995).
[46]C. Canuto, M. Y. Hussaini, A. Quarteroni, and T. A. Zang, *Spectral Methods in Fluid Dynamics* (Springer, New York, 1988).
[47]R. Peyret, *Introduction to Spectral Methods with Application to Fluid Mechanics*, in Von Karman Inst. for Fluid Dynamics Computational Fluid Dynamics, Volume 1 (Rhode-Saint Genese, Belgium, 1986).
[48]G. H. Golub and C. F. Van Loan, *Matrix Computations* (JHU Press, Baltimore, 2012), Vol. 3.
[49]A. Senthilkumar, "On the relation between surface profiles and internal flow properties in long-wave models," Ph.D. thesis, University of Bergen, 2017.

Bibliography

[1] J.L. Bona, M. Chen and J.-C. Saut *Boussinesq Equations and Other Systems for Small-Amplitude Long Waves in Nonlinear Dispersive Media. I: Derivation and Linear Theory* J. Nonlinear Sci. **12** (2002), 283–318.

[2] P. K. Kundu, I. M. Cohen, and D. R. Dowling *Fluid Mechanics, sixth edition*, (Academic Press, 2014).

[3] P. K. Kundu and I. M. Cohen *Fluid Mechanics, fourth edition*, (Academic Press, 2008).

[4] G. B. Whitham, *Linear and Nonlinear Waves*, (Wiley, New York, 1974).

[5] A. Ali and H. Kalisch, *Mechanical balance laws for Boussinesq models of surface water waves*, J. Nonlinear Sci. **22** (2012), 371–398.

[6] A. Ali and H. Kalisch, *A dispersive model for undular bores*, Anal. Math. Phys. **2** (2012), 347–366.

[7] N. T. Nguyen and H. Kalisch, *Orbital stability of negative solitary waves*, Elsevier, J. Mathematics and Computers in Simulation, **80** (2009), 139–150

[8] M. Chen, *Exact solutions of various Boussinesq systems*, Appl. Math. Lett., **11** (1998), 45–49

[9] L.N. Trefethen, *Spectral Methods in Matlab*, (Siam, 2000).

[10] M. Bjørkavåg and H. Kalisch, *Wave breaking in Boussinesq models for undular bores*, Phys. Lett. A **375** (2011), 1570–1578.

[11] D.L. Wilkinson and M.L. Banner, *Undular bores*, 6th Australian Hydraulics and Fluid Mechanics Conference, Adelaide, Australia, 1977.

[12] T. B. Benjamin, J. L. Bona, and J. J. Mahony, *Model equations for long waves in nonlinear dispersive systems*, Philos. Trans. R. Soc., A **272** (1972), 47–78.

[13] G.A. Korn and T.M. Korn, *Mathematical Handbook for Scientists and Engineers: Definitions Theorems and Formulas for Reference and Review, 2nd. ed.*, Dover Publications, Inc., New York (2000) (Reprinted from McGraw-Hill Inc., New York (1968)).

[14] N. Cutland, *Computability: An Introduction to Recursive Function Theory*, Cambridge University Press (1980).

[15] B.L. van der Waerden, *Modern Algebra, vol. 1 (F. Blum, Trans.)*, Ungar, New York (1949).

[16] S. Basu, R. Pollack, M. Roy, *Algorithms in Real Algebraic Geometry*, Algorithms and Computation in Mathematics, vol. 10, 2nd ed., Springer-Verlag (2006).